ASSESSMENT OF THE POTENTIAL HEAT STORED IN THE DEEP AQUIFERS OF THE WILLISTON BASIN FOR GEOTHERMAL ENERGY PRODUCTION

A Thesis Submitted to the

College of Graduate and Postdoctoral Studies

in Partial Fulfillment of the Requirements for the

Degree of Master of Science in the

Department of Civil, Geological and Environmental Engineering

University of Saskatchewan

By

Lotanna Somadina Ufondu

PERMISSION TO USE STATEMENT AND DISCLAIMER

In presenting this thesis/dissertation in partial fulfillment of the requirement for a Postgraduate degree from the University of Saskatchewan, I agree that the Libraries of this University may make it freely available for inspection. I further agree that permission for copying of this thesis/dissertation in any manner, in whole or in part, for scholarly purposes may be granted by the professor or professors who supervised my thesis/dissertation work or, in their absence, by the Head of the Department or the Dean of the College in which my thesis work was done. It is understood that any copying or publication or use of this thesis/dissertation or parts thereof for financial gain shall not be allowed without my written permission. It is also understood that due recognition shall be given to me and to the University of Saskatchewan in any scholarly use which may be made of any material in my thesis/dissertation.

Requests for permission to copy or to make other uses of materials in this thesis/dissertation in whole or part should be addressed to:

Head of the Department of Civil, Geological and Environmental Engineering
3B48.3 Engineering Building, 57 Campus Drive
University of Saskatchewan
Saskatoon, Saskatchewan S7N 5A9 Canada

ABSTRACT

As the world shifts from fossil based energy generation towards renewable energy, it is important to consider the role geothermal energy can play in Saskatchewan. The deep reservoirs of the Williston Basin possess some geothermal qualities that can be harnessed for direct purpose (heating and cooling of buildings) and for electrical power generation. Previous studies have looked at this potential at a large scale, however, this research focused on the moderate temperature geothermal resources (80-150^{o}C) within two deep reservoirs, one formed by the Deadwood and Winnipeg formations of the upper Cambrian to Mid-Ordovician age and another consisting of the Red River and its stratigraphic equivalent, the Yeoman Formation of the Upper Ordovician age. This thesis uses the production and injection data acquired from the numerous hydrocarbon and waste disposal wells within Saskatchewan to quantify the probable heat and thermal power associated with hot waters historically produced at the basin scale. The research quantified electrical geothermal power within the reservoirs using three different techniques: 1) observed production rates; 2) maximum production rates (using well hydraulics); and 3) rock thermal volume.

For the first technique, the production or injection rate for each well within the reservoirs of Deadwood-Winnipeg and Red River-Yeoman was extracted from well production or injection history data. A simple thermal equation was used to estimate the thermal power that could be generated from each well. The results show that, on average, each well within the Deadwood-Winnipeg reservoir and Red River-Yeoman reservoirs can generate thermal power valued at 0.4 MWt and 10 MWt respectively. The second technique used the well hydraulics, core analysis data and literature values to calculate the maximum possible values for production rates using the Cooper-Jacob empirical equation. The Gringarten and Sauty model was used in conjunction with these results to determine the required well spacing. The results show that the average well within Deadwood-Winnipeg and Red River-Yeoman reservoirs can generate thermal power of about 101 and 105 MWt respectively. The final method estimated the geothermal power by calculating the volumetric heat capacity of the geothermal reservoir with respect to the area of the reservoir between the production and injection wells, thermal properties and the thickness of the reservoir. The results show that, on average, the entire reservoir based on the Gringarten and Sauty estimate for well spacing has the capability of generating geothermal power of about 170 MWt for sandstone (Deadwood-Winnipeg) and 286 MWt for the carbonate (Red River-Yeoman)

reservoirs. This method overestimated the geothermal power that can be generated from the entire volume of the reservoir based on well spacing. However, when a recovery factor is added into the equation, it gives values that are reasonable and comparable to those estimated from theoretical production.

ACKNOWLEDGMENTS

I would like to express my profound gratitude to my supervisor, Dr. Grant Ferguson for the NSERC funding, guide and support he gave me during this research. Also, gratitude and thanks to Dr. Chris Hawkes for consistent support and funding assistance.

Special thanks to my committee members, Dr. Chris Hawkes, and Dr. Doug Milne for the enthusiasm they showed towards my research and their brainstorming questions and discussions which helped focus this research towards a better direction.

Many thanks to my friends and colleagues, Ouafi, Mostafa, Randy, Shahid, and my church community (Church of Christ Saskatoon) for their support and encouragement during this research.

Finally, my deepest gratitude goes to my beautiful wife Doris and lovely children Joyce, Daniella and Victoria for their prayers, patience, understanding and consistent support throughout this long tortuous journey.

TABLE OF CONTENTS

LIST OF FIGURES

LIST OF TABLES

LIST OF SYMBOLS AND MEANING

Symbols	Meaning	Units (SI)
A	cross sectional area	m^2
C_p	Heat Capacity at constant pressure	J/K
C_R, C_w, C_m	Heat capacity of rock, water and matrix	J/kg^oC
D	Distance between production and injection well	m
Gp	Electrical geothermal power (electric watt)	W_e
g	Acceleration due to gravity	m^2/s
H	hydraulic head	m
H_G	Reservoir thermal energy	J
h	Reservoir thickness	m
K	Hydraulic conductivity	m/s
K_R	Caprock/bedrock/rock thermal conductivity	W/m.K
k	Permeability	m^2
n_e	Effective porosity	-
n_G	Geothermal energy-electricity conversion factor	%
P, P_{wf}	formation pressure or in situ pore pressure, wellbore flowing pressure or bottom hole pressure	Pa
P_E	Electrical Geothermal Power	MWe
P_T	Thermal power	MWt
Q	Production/injection rate	m^3/s
q	Flow rate	m^3/s
r	Radial distance from pumping well to observation well	m
r_w	Well radius	m

S	Storativity	-
s	Drawdown	m
T	Transmissivity	m^2/s
T_A	Aquifer temperature	^oC
T_h	Characteristic average reservoir temperature	^oC
T_R	T_R is temperature of the overlying /underlying rock	^oC
T_0	Assumed temperature when the reservoir block is cooled down	^oC
t	Time since the start of pumping/production/injection (seconds)	s
t_E	Period of commercial exploitation of the reservoirs	s
u	Variable that mathematically describes the cone of depression	-
V_B	Volume of the reservoir block	m^3
v	Darcy velocity	m/s
$W(u)$	Theis well function	-
x	Vertical depth of well	m
α	Aquifer compressibility	Pa^{-1}
β	Compressibility of water	Pa^{-1}
ΔT	Change in input and output temperature	^oC
$đp$	difference in pressure	pa
$đx$	length of flow	m
μ	dynamic Fluid viscosity	Pa.s
ρ	Density of water	kg/m^3
$\rho_{R,}\rho_w\rho_m$	Grain density of rock, density of water and matrix	kg/m^3
$Ø$	Rock porosity	-

1 INTRODUCTION

1.1 Background and overview

This research assesses the capability of the Saskatchewan portion of the Williston Basin to generate geothermal energy for direct use and/or electrical power production, using the thermal and petro-physical properties of the deep reservoirs within the basin.

Geothermal energy is a clean and renewable energy source which utilizes the thermal properties of the earth's crust to generate energy which can be used for the heating and cooling of buildings, and generation of electricity. The primary sources of this energy are radioactive decay and primordial heat generated billions of years ago. It is categorized into high temperature resources ($> 150^{o}C$), found in areas of high tectonic activity, and moderate to low temperature resources ($< 150^{o}C$) which are usually found in the shallow subsurface or deep sedimentary rocks (Dickson et al., 2004). High temperature resources have gained an extensive application in electricity power generation in many countries of the world including Iceland, United States, Indonesia, and the Philippines (Fridleifsson et al., 2008). Grasby et al. (2012) has identified British Columbia as having potential for high temperature geothermal energy. Moderate to low temperature geothermal resources are mainly used for direct application (heating and cooling of buildings, aquaculture, recreation, agricultural drying), and for the generation of low wattage electricity in some places. There are about six active geothermal pilot projects for electricity production in Canada including; Saskatchewan (water from sedimentary aquifer/reservoir), British Colombia, Northwest Territories and Alberta (CanGEA Report, 2013). Canada is not currently producing electrical energy from this source. The potential for geothermal energy in Canada is yet untapped, especially in terms of electricity production. This study will focus on the assessment of moderate temperature geothermal resources within the Williston Basin of the Western Canada Sedimentary Basin (WCSB).

The Western Canada Sedimentary Basin (WCSB) is a sedimentary basin that is bounded by the Canadian Cordillera to the west and the Precambrian Shield to the east. It covers 1,400,000 square kilometres of western Canada and runs across southern Saskatchewan, Alberta and northeastern British Columbia. It is made up of two major sedimentary basins: the Alberta Basin and the northern part of the Williston Basin (Wright et al., 1994), as shown in Figure 1.1. The Alberta

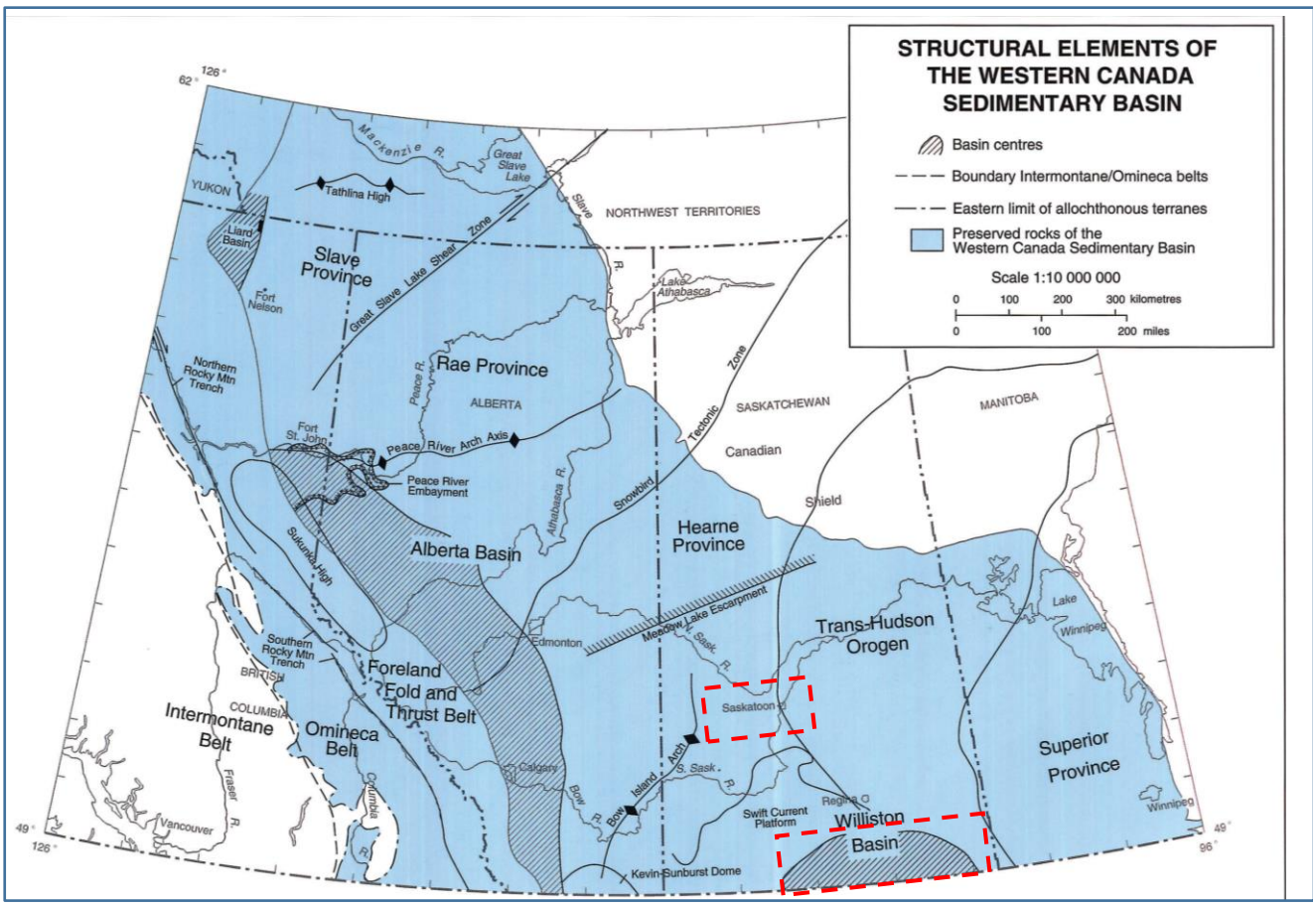

Figure 1.1 Structural map of the WCSB showing sample locations marked in red line (modified from Wright et al., 1994)

Basin is a foreland basin located along the eastern part of the Rocky Mountains in western Canada. The Williston Basin is a cratonic basin, which lies within Saskatchewan, and extends to eastern Montana, South and North Dakota in the USA. These sub-basins contain sedimentary rocks of Cambrian to Tertiary age with a total thickness reaching about 3.5 km for the Williston Basin (Kent and Christopher, 1994) and greater than 4 km for the Alberta Basin (Bekele et al., 2002).

The WCSB has high geothermal potential due to its geothermal gradient and deep permeable aquifers which produce hydrocarbons and hot water (Gosnold et al., 2010). Some studies have generally assessed the geothermal potential of the WCSB in terms of enhanced geothermal systems (EGS), coproduced water, and areas of high to low geothermal potential have been identified within the basin (Grasby et al., 2012, Gosnold et al., 2010, Ferguson and Grasby, 2014). Previous work within this basin is explored in Chapter 2. However, this study will focus

specifically on quantifying the geothermal energy within the Saskatchewan portion of the Williston Basin. The potential to produce geothermal power from heat stored in the different reservoirs of the basin will be assessed using three different techniques. Chapter 3 of this research discusses these techniques in detail.

Data from 221 production wells completed in the Deadwood-Winnipeg and Red River-Yeoman reservoirs and 20 injection wells data from Deadwood Formation were used to quantify the potential heat and power within the Williston Basin. The results of this study are presented and discussed in Chapters 4 and 5 respectively. In Chapter 6 conclusions are made on the capability of the basin to support geothermal energy for direct use and/or electricity generation.

1.2 Hot water and binary system (Organic Rankine Cycle – ORC)

The development of geothermal power is possible with binary power plants using the Organic Rankine cycle (ORC) and Kalina cycle technology to generate electricity from moderate temperature resources between 80-150^{o}C (DiPippo, 2014). Hot water from aquifers within the Williston Basin falls into this category. Figure 1.2 shows the ORC set up as designed by Kaplan (2007), in which hot geothermal fluid extracted from the production well is passed through a pipe to the heat exchanger, where it heats and vaporizes a working fluid (a preheated organic fluid with a low boiling point – Isobutene). The organic vapours then drive the turbine which rotates the generator, to produce electricity. The organic vapours are then condensed and cooled by either air or water and recycled back into the heat exchanger, completing the cycle. Then the waste water is reinjected into the geothermal reservoir without much cooling.

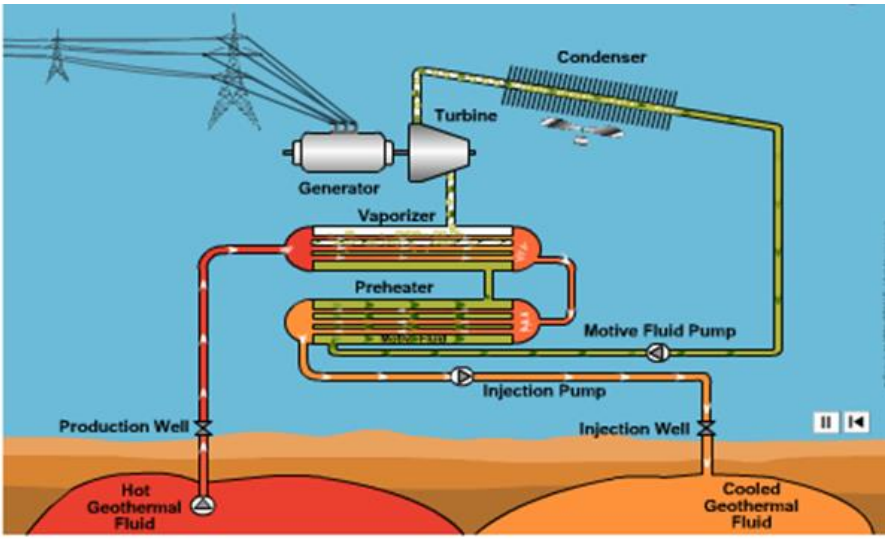

Figure 1.2 Air-Cooled Binary Geothermal Power Plant (Kaplan, 2007)

1.3 Objectives

The objectives of this research are:

- To estimate power production rates and the total quantity of heat and thermal power associated with the hot waters based on historical and existing records at the basin scale.
- To examine the effect of hydraulic parameters on production rates and the difference between the theoretical and the actual or observed production rates obtained from oil and gas wells, injection wells, and waste disposal wells within the basin.
- To assess the probable heat and geothermal electric power to be produced from the same block of rock using the Bundschuh & Suárez-Arriaga (2010) equation with respect to rock thermal properties and the effect of fluid production on this assessment.

These objectives will help answer the question of the capability of this basin to generate thermal power for direct use purposes and/or electricity generation. The focus will be on the Cambrian-Ordovician reservoirs within the Williston Basin. These are deep sedimentary reservoirs that possess some qualities of a good geothermal reservoir, such as; medium to high porosity and permeability, moderate temperature (80-150^{o}C) and high fluid content.

1.4 Significance

The reservoir rocks of the Williston Basin, within the depth range of 2-3 km, appear to have thermal and hydraulic properties appropriate to support future geothermal power generation. The extensive database from hydrocarbon exploitation within the basin presents an opportunity to assess these properties and achieve the above stated objectives. This study develops a database that can be used for future geothermal projects in the Williston Basin. It will also create opportunities for further research within the Williston Basin and other deep sedimentary basins.

2 LITERATURE REVIEW

This section summarizes the concept underlying geothermal power production from hot aquifers and estimates the potential power that can be produced based on previous studies. To effectively study the potential of a geothermal reservoir, it is important to know its depositional and thermal history. The quality of a good geothermal reservoir is characterized by its petrophysical, hydraulic and thermal properties. Therefore, this section will also consider the regional geology, hydrogeology and the geothermal regime of the reservoirs of interest with respect to these properties.

2.1 Geothermal power production

Geothermal power uses the thermal energy stored underground to generate electricity. There are three types of geothermal power generation plants; Flash steam (hot water), dry steam (vapor-dominated) and binary cycle (moderate temperature) (Duffield and Sass, 2003). The flash steam system (Figure 2.1 a) pulls high pressure hot water of about 180^{o}C or more from great depth into a low-pressure separator, the resulting steam drives the turbine to generate electricity and the waste water from the separator and the condenser is reinjected through an injection well back to the ground. In the dry steam system (Figure 2.1 b) high pressure steam above 235^{o}C stored in a porous reservoir is extracted through production wells and used to turn the turbine to generate electricity. The waste fluids are returned to the reservoir through injection wells to sustain the system's pressure and lifespan. The binary cycle system discussed earlier in section 1.2 (Figure 1.2 and Figure 2.1 c) generates electricity from hot water of a moderate temperature reservoir. The hot fluid is passed through a heat exchanger where a second working fluid with a low boiling point is vaporized to generate electricity. The geothermal powered binary cycle system has the potential to generate electricity if the recoverable fluid has a temperature range between 80^{o}C and 150^{o}C. This range of temperature can be found within the WCSB (Bachu and Burwash, 1994, Grasby et al., 2009, Majorowicz and Grasby, 2010).

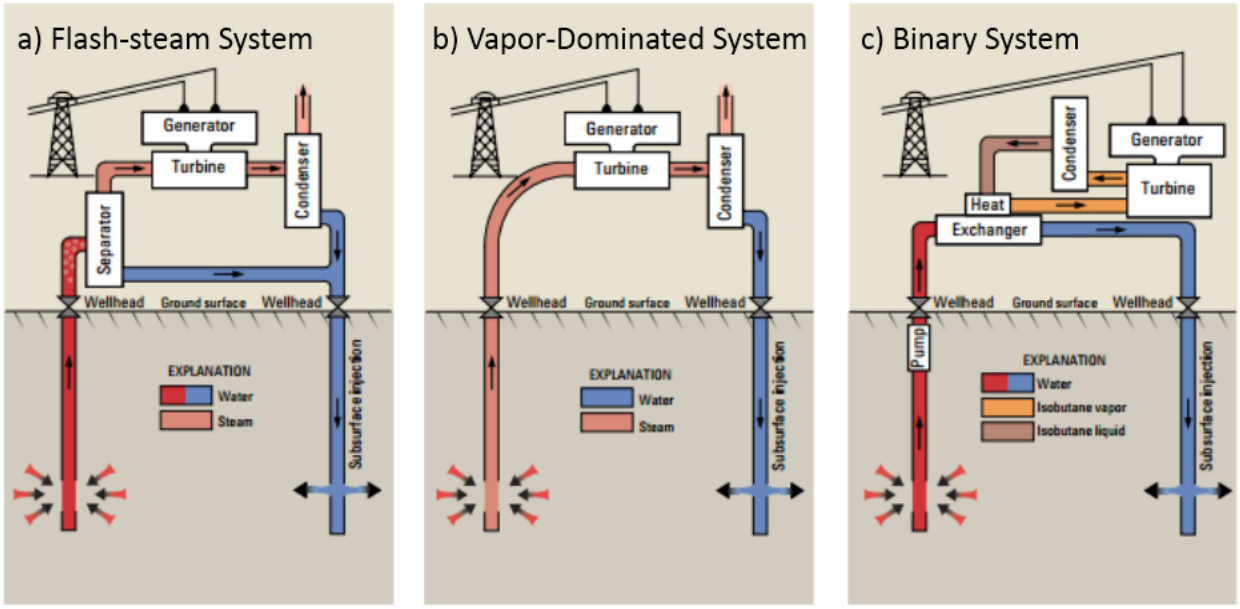

Figure 2.1 Geothermal power plant systems: a) Hot water (Flash steam) system b) Vapor-dominate system c) Binary system (Duffield and Sass, 2003)

The produced water temperature is always higher than the injected water temperature. According to Gong et al. (2011) and Bedre and Anderson (2012) higher injection fluid temperature at a constant production rate increases the reservoir life. Though this might lead to a lower ΔT (change in production and injection temperature) and lower heat extraction from the reservoir, it will increase the reservoir life. Another factor considered by Gong et al. (2011) is the injection rates. They concluded that higher injection temperature requires lower injection rate to reduce reservoir temperature drop and increase productivity. This study will assume sustained production and longer reservoir lifetime by using a lower ΔT as shown in Chapter 3.

2.1.1 Hot sedimentary aquifer source for geothermal power production

Hot sedimentary aquifer sources are typically porous sandstones or carbonates containing hot water heated as a result of crustal heat flow or their proximity to hot rocks. The Deadwood and Winnipeg formations within the Williston Basin contain hot brines sourced from the heat of the Precambrian Basement rock (Majorowicz et al., 1986; Vigrass et al., 2007; and Ferguson and Grasby, 2014). See section 2.5 for a more detailed discussion on this source.

2.1.2 Geothermal doublet system for geothermal production

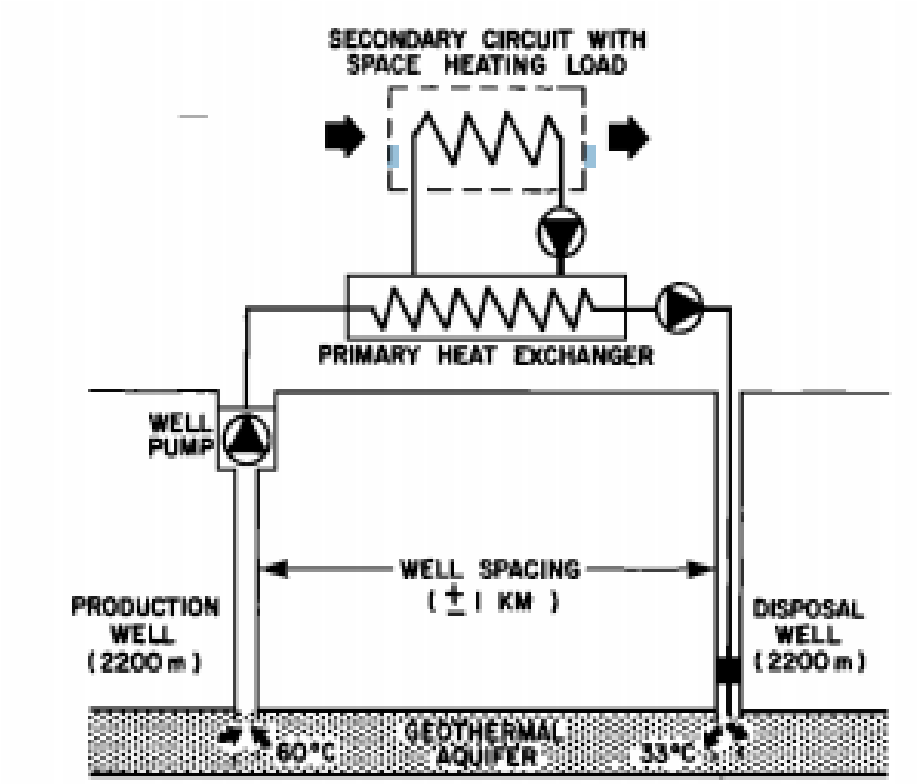

Figure 2.2 Geothermal doublet system (Hutchence et al. 1986)

A geothermal doublet system comprises a pair of production and an injection wells located within a hot horizontal sedimentary reservoir and connected to a heat exchanger as shown in Figure 2.2. In a doublet geothermal system, the water used to generate electricity is re-injected into the reservoir at a temperature lower than the initial reservoir temperature. The travel time for the thermal cold front through the reservoir from the injection well to the producing well depends mainly on the separation distance between the wells, thickness of aquifer, porosity, thermal conductivity, injection/production rate, etc. The equation developed by Gringarten and Sauty (1975), also applied by some studies (Lippmann and Tsang, 1980; Chevalier and Banton, 1999; Wellmann et al., 2010; and Ferguson and Grasby, 2014) can be used to determine the separation distance between injection and production wells. This equation was developed by solving fluid flow and heat transport equations for one-dimensional mass flow and two-dimensional heat flows (vertical heat flow through the confining rocks by conduction and horizontal heat flow by advection); see Equations 2.1, 2.2 and 2.3. This can be used to determine the spacing between two wells (Equation 2.4) that would maintain a constant temperature at the production well over a

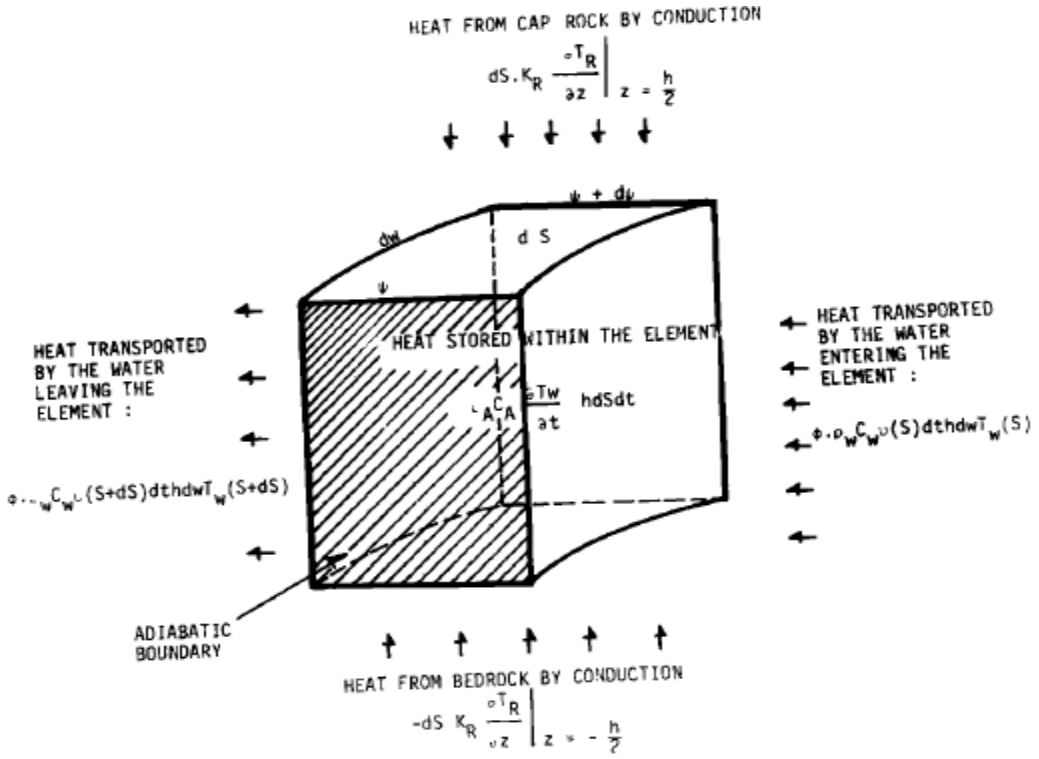

Figure 2.3 Doublet geothermal model block (Gringarten and Sauty 1975)

given reservoir life time (e.g., 30 years). This model is based on some assumptions outlined by Gringarten and Sauty (1975) as shown in Figure 2.3.

The reservoir is assumed to be:

- Horizontal, homogenous and isotropic with a constant thickness,
- bounded by cap-rock and bedrock, with constant production/injection rate,
- injection and production wells are the source and sink respectively,
- uniform thermal and petrophysical properties,
- the lateral boundary condition is an infinite boundary with a no-heat-flow condition,
- 1D fluid flow in the reservoir. Heat transfer is dominated by advective flow.

Darcy's Law determines fluid flow rate in the reservoir (Figure 2.3) is shown by

$$v = \frac{q}{A} = -\frac{k}{\mu}\frac{\partial p}{\partial x} \tag{2.1}$$

The differential equation describing heat transport from the overlying and underlying rocks as shown in Figure 2.3 is given by:

$$K_R \frac{\partial^2 T_R(S,z,t)}{\partial z^2} = \rho_R C_R \frac{\partial T_R(S,z,t)}{\partial t} \qquad S > 0,\ z \geq h/2,\ t > 0 \tag{2.2}$$

Equation 2.3 is a simplified energy conservation equation for fluid flow in the reservoir involving heat conduction, advection and heat transport through the confining rock layers based on the assumption that all parameters are constant.

$$\frac{h}{2}\rho_A C_A \left(\frac{\partial T_A}{\partial t}\right) + \frac{q}{2}\rho_w C_w \left(\frac{\partial T_A}{\partial S}\right) = K_R \left(\frac{\partial T_A}{\partial z}\right) = 0 \quad S > 0,\ z = h/2,\ t = 0 \tag{2.3}$$

Where,

v is Darcy velocity (m/s),

q is flow rate (m^3/s)

A cross sectional area (m^2),

q is the rate of flow (m^3/s),

k is permeability (m^2),

μ - dynamic viscosity (Pa.s),

$đp$ – difference in pressure (pa),

$đx$ – length of flow (m)

K_R is caprock/bedrock thermal conductivity W/(m-k).

T_R is temperature of the overlying /underlying rock

T_A is reservoir temperature

S is distance in longitudinal direction parallel to the reservoir

$p_w C_w$ is the water heat capacity.

$\rho_A C_A = \emptyset \rho_w C_w + (1-\emptyset)\, p_m C_m$

$\rho_A C_A$ is the aquifer heat capacity,

$p_m C_m$ is heat capacity of the matrix,

$$D = \left\{ 2.Q.\Delta t \Big/ \left[\left(\emptyset + (1-\emptyset)\frac{\rho_R C_R}{\rho_w C_w}\right) h + \left(\left(\emptyset + (1-\emptyset)\frac{\rho_R C_R}{\rho_w C_w}\right)^2 h^2 + 2\frac{K_R \rho_R C_R}{(\rho_w C_w)^2}\Delta t \right)^{1/2} \right] \right\}^{1/2} \tag{2.4}$$

Where,

D is the distance between production and injection well (m),

Q is the Injection/Production rate (m^3/s),

$Ø$ is the rock porosity, h is the reservoir thickness (m),

$\rho_{w,}$ is the density of water (kg/m^3),

ρ_R is the grain density of rock(kg/m^3),

Δt is the time before thermal breakthrough (s).

The success of this geothermal doublet system depends on some reservoir parameters identified by Hutchence et al. (1986) which include: well separation distance, pumping rates, porosity, and aquifer thickness. Hydraulic conductivity and storativity were considered less influential. However, the sensitivity studies carried out by Bedre and Anderson (2012) ranked reservoir temperature, injection rate and injection fluid temperatures as the parameters with the strongest influence on heat extraction. While water loss, rock thermal conductivity, well spacing and porosity were ranked less influential on heat extraction, they noted that large well spacing leads to larger reservoir size; therefore well spacing should be optimized for maximum production. However, larger well spacing can result in more influence from geologic factors (porosity, permeability and fractures), pressure drop and decrease in production and will require very high pressure difference to sustain production. A reasonable well spacing should be used to optimize geologic factors and reservoir size (Bedre and Anderson, 2012). Ferguson and Grasby (2014) applied Equation 2.4 (Gringarten and Sauty 1975) to their data and concluded that a reservoir lifetime of more than 30 years could be expected with an aquifer thickness of 100 m, a well spacing of 1 km or more, and a production/injection rate of 270 m^3/h.

2.2 Analytical background for potential power calculations

This section discusses existing equations used to quantify potential geothermal power.

2.2.1 The quantification of thermal power

The thermal power produced from a geothermal doublet system can be used for direct application such as space heating and cooling, providing hot water for houses and industrial purposes, snow and ice melting, etc. (Bundschuh and Suárez-Arriaga 2010). Majorowicz and Grasby (2010) and Ferguson and Grasby (2014) have identified southern Saskatchewan portion of the Williston Basin as an area of relatively high fluid temperature which could be favorable for direct

application purposes. The thermal power that can be produced by a geothermal doublet system is defined by Ferguson and Grasby (2014) as follows:

$$P_T = Q * \rho * C_w * \Delta T \quad (2.5)$$

Where,

P_T is thermal Power in megawatts thermal output (MWt),
Q is the production/injection rate (m^3/s),
ρ is density of water (kg/m^3),
C_w *i*s the heat capacity of water in (J/kg^oC) and
ΔT is the temperature difference between production and injection well (^oC).

Temperature differences of 20^oC and 33^oC were considered by Ferguson and Grasby (2014) with average production/injection rates of 270 m^3/h and 36 m^3/h respectively. The thermal power that could be produced for with the two temperature differences are 12 MWt and 1.4 MWt respectively.

In accordance with Bundschuh and Suárez-Arriaga (2010), Equation 2.6 can be used to estimate the electrical geothermal power within a geothermal reservoir.

$$P_E = n_g P_T = n_G * Q * \rho * C_w * \Delta T \quad (2.6)$$

Where,

P_E is the electrical geothermal power measure in megawatt electrical output (MW_e), and

n_g is the conversion efficiency factor from thermal power to electrical power which has a value between 7-12% for moderate temperature resources (80 to 150 ^oC) and 12-20% for higher temperature resources (above 150 ^oC), Bundschuh & Suárez-Arriaga (2010). Ferguson and Grasby (2014) assumed a 10% conversion factor.

2.2.2 Cooper-Jacob's equation for calculating hydraulic properties

The Cooper and Jacob (1946) equation approximates the Theis (1935) equation and is equivalent to the equation which Horner (1951) used to analyse Drill Stem Tests (DSTs). Theis developed the following equations to analyse data obtained during pumping tests with transient conditions.

$$s = \frac{Q}{4\pi T} W(u) \quad (2.7)$$

$$u = \frac{r^2 S}{4Tt} \quad (2.8)$$

Where:

Q is pumping rate (m^3/s),
r is the radial distance from pumping well to observation well (m),
s is drawdown (m),
S is storativity (-),
t is time since start of pumping (s),
T is transmissivity (m^2/s),
u is a dimensionless variable that mathematically describes the cone of depression.

Theis (1935) solution is based on the following assumptions:

- Aquifer is horizontal, confined, homogeneous, and isotropic, of infinite extent and constant thickness with constant hydraulic properties (transmissivity and storativity).
- Well storage is negligible since the well diameter is small; and
- The well is pumping at a constant discharge rate

The values for the Theis well function, $W(u)$ can be found in tables and can be used for the Theis type curve.

$$W(u) = -0.5772 - \ln(u) + u - \frac{u^2}{2.2!} + \frac{u^3}{3.3!} - \frac{u^4}{4.4!} + \cdots \quad (2.9)$$

Cooper and Jacob (1946) show that for small values of u the solution of Theis well function can be simplified without producing significant errors. Small values of u result from large values of time and/or small values of radial distance (Equation 2.8). Therefore, they used an approximate form of Equation 2.9 which retained only the first two terms to get Equation 2.10. This approximation allows plotting of drawdown vs time, or vs distance on a linear scale of semi-log plot (Figure 2.4).

$$s = \frac{2.3Q}{4\pi T} log \frac{2.25Tt}{r^2 2S} \quad (2.10)$$

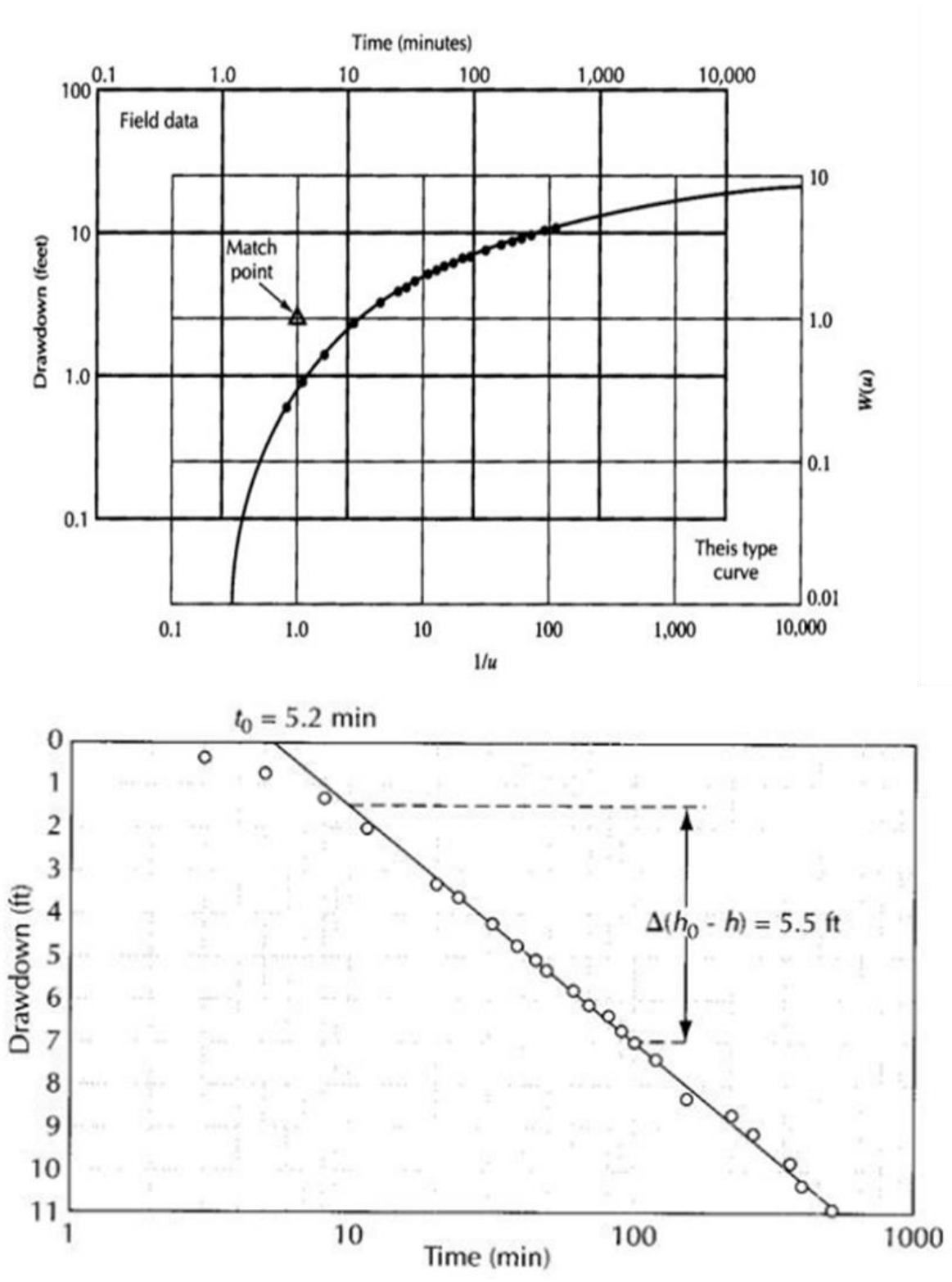

Figure 2.4 Theis type curve and Cooper-Jacob straight-line time-drawdown method for confined aquifer (Fetter, 2001)

The transmissivity, T (m^2/s) is obtained using Equation 2.11 (Bear 1972):

$$T = Kh = \left(\frac{k\rho g}{\mu}\right) h \tag{2.11}$$

Where,

K is hydraulic conductivity in (m/s),

ρ is density (kg/m^3),

μ is fluid viscosity (Pa.s),

h is reservoir thickness (m),

g is acceleration due to gravity (m/s^2), and

k is average permeability (m^2).

Fluid viscosity is affected in general by pressure, temperature and salinity. For the hot brines within the Williston Basin (discussed later in section 2.4.2) the dominant factors that affect viscosity are temperature and salinity. This study estimates viscosity using table generated by Kestin et al. (1981) and concentration which correlates to that of brine within the Williston Basin (Bachu and Hitchton, 1996).

According to Singhal and Gupta (2010), the storativity of a geothermal reservoir can be calculated using the following equation:

$$S = \rho g(\alpha + n_e\beta)h \tag{2.12}$$

Where,

ρ is density of water (kg/m^3),
g is gravitational acceleration m/s^2,
α is aquifer compressibility (Pa^{-1}),
n_e is effective porosity,
β is the compressibility of water (Pa^{-1}), and
h is reservoir thickness (m).

2.2.3 Geothermal electrical power using rock volume

The heat energy content of a geothermal reservoir (H_G) can be estimated "especially if the total volume of the reservoir is unknown" Bundschuh & Suárez-Arriaga (2010). The total volume, V_B is defined as the product of length, width, and thickness (*xyz*) as shown by Figure 2.5. They estimated the reservoir thermal energy, H_G (J) using Equation 2.13:

$$H_G = \rho_s c_p V_B (T_A - T_0) \quad (2.13)$$

Where,

$\rho_s c_p$ is the volumetric specific heat of the reservoir (J/m^{3O}C),
T_A is the average reservoir temperature (^{o}C),
T_0 is a reference value close to the average ground surface temperature (^{o}C), and
V_B is the volume of the reservoir (m^3).

In a situation where the volume is unknown the volumetric geothermal energy can be estimated using Equation 2.14:

$$\frac{H_G}{V_B} = \rho_s c_p (T_A - T_0)\ in\ \left[\frac{MJ}{m^3}\right] \quad (2.14)$$

Equation 2.15 can be used to estimate the electric geothermal power, P_E (electric watt, W_e) contained in the reservoir

$$P_E = n_G \frac{H_G}{t_E} = n_G \frac{\rho_s c_p V_B (T_A - T_0)}{t_E} \quad (2.15)$$

Where t_E represents the period of commercial exploitation of a reservoir, typically up to 30 years (in seconds).

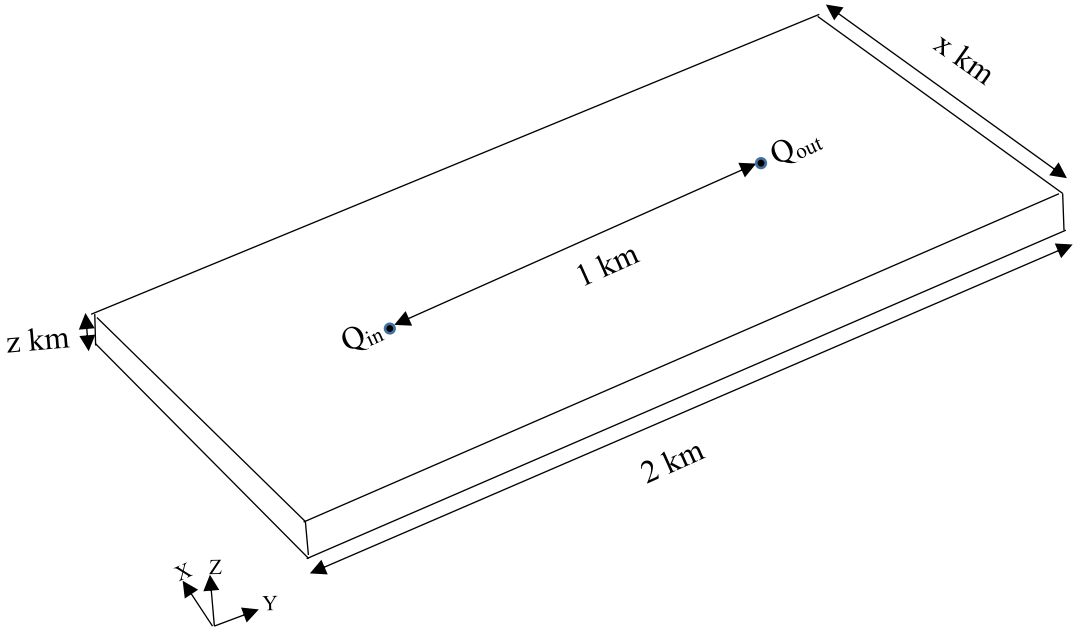

Figure 2.5 Geothermal Reservoir Block

This study uses similar equations to estimate the energy content of a geothermal block (Figure 2.5) with an assumed width of influence (x km) to estimate both the reservoir thermal energy and electrical thermal energy.

2.2.4 Hydraulic head distribution within the reservoirs of the Williston Basin

In order to operate a geothermal injection well, there is need to estimate the wellbore flowing pressure (bottom hole pressure) required in the injection well. This pressure is a function of thickness, hydraulic properties of the reservoir, injection rates and the formation pressure (i.e., in situ pore pressure). The general steady state equation (Equation 2.16) derived from Darcy's law for the radial flow of single phase as indicated by Dake (2001) can be used to estimate wellbore flowing pressure.

$$P_{wf} = P - \frac{Q\mu}{2\pi kh} \ln\frac{r}{r_w} \tag{2.16}$$

Where,

P is formation pressure (Pa),

P_{wf}, is wellbore flowing pressure (Pa),

r is the one-half the radial distance between injection and production wells (m),

r_w, wellbore radius.

μ = fluid viscosity (Pa.s),

h is reservoir thickness (m),

Q is injection rate (m^3/s).

If P is known P_{wf} can be calculated.

The hydraulic head distribution map of the Basal aquifer within the Williston Basin was presented by Bachu and Hitchon (1996), Figure 2.6. The map shows a wide range of head distribution from less than 300 meters in the northeast to about 900 meters in the southwest within the Williston, a reflection of the north-eastward flow from southern Saskatchewan. The Yeoman aquifer head distribution map from Palombi (2010) in Figure 2.7 also follow the same pattern with hydraulic head ranging between 270 to 850 meters from northeast to southwest. These head distribution maps are very important because they can be converted to formation pressure, which can be used

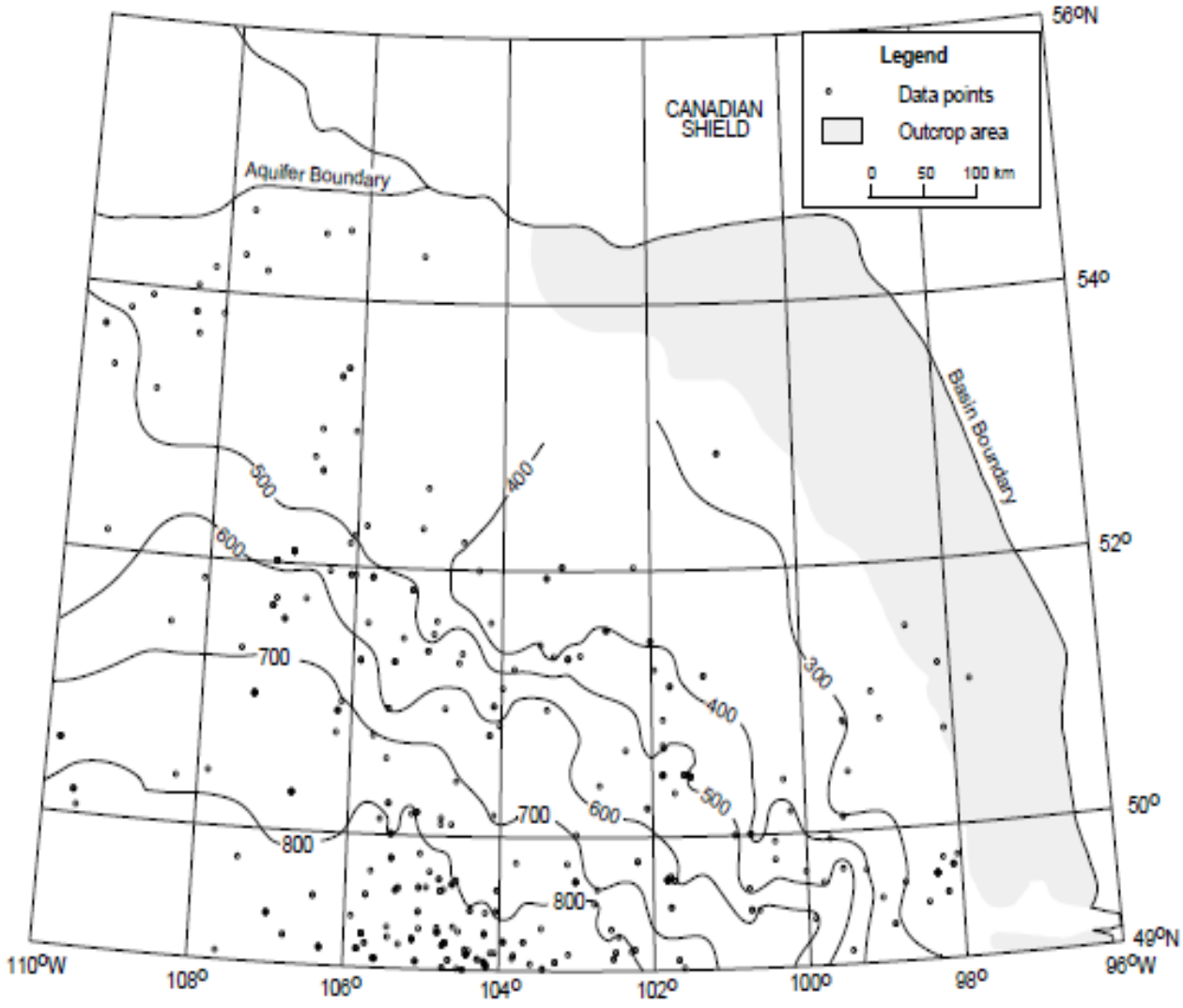

Figure 2.6 Hydraulic head (in meters above sea-level) distribution map for the basal clastics of the Williston Basin (Bachu and Hitchon, 1996)

in equation 2.16, as shown by equation 2.17.

$$P = \rho g H \tag{2.17}$$

Where:

P is formation pressure (Pa),

ρ is the fluid density (kg/m^3),

g is gravitational acceleration (m/s^2), and

H is the hydraulic head above ground level (m). H = Total depth (x) + (hydraulic head above sea-level – Ground surface elevation (GL)).

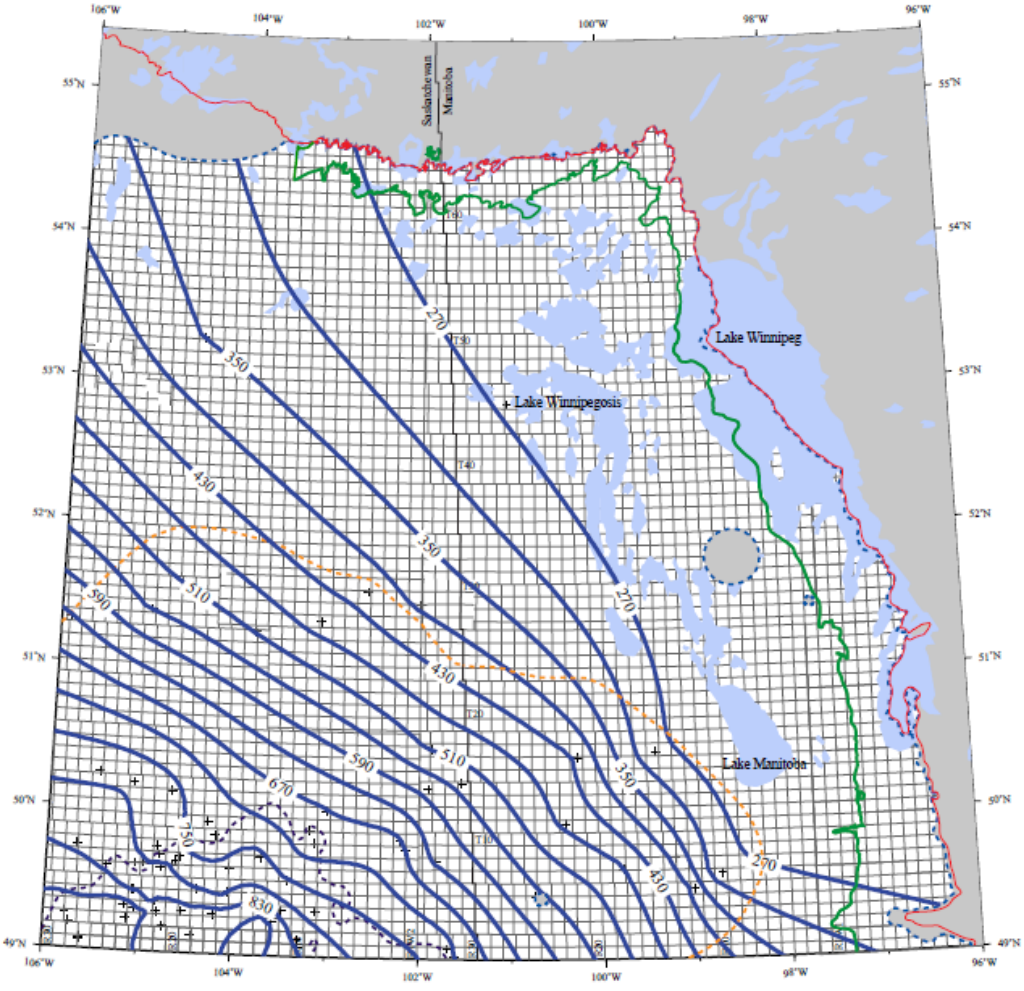

Figure 2.7 Yeoman aquifer head (in meters above sea-level) distribution map from (Palombi, 2010)

2.3 Geology of the Western Canada Sedimentary Basin

Lithology and thickness play a very important role in assessing the potential of a conventional geothermal reservoir because it helps to estimate the reservoir volume and the net thickness of the reservoirs of interest. Also, lithology helps to understand the petrophysical properties of a rock unit (see 2.4.3). Therefore, this section gives a general overview of the geology of the WCSB and a summary of the lithology, depositional history and stratigraphy of the Williston Basin.

The Western Canada Sedimentary Basin (WCSB) is a sedimentary basin that is bounded by the Canadian Cordillera to the west and the Precambrian Shield to the east. It is made up of two major sedimentary basins: the Alberta Basin and the northern part of the Williston Basin (Wright et al., 1994). The Alberta Basin is a foreland basin located along the eastern part of the Rocky Mountains in western Canada. The Williston Basin is a cratonic basin, which lies within Saskatchewan, and extends to eastern Montana, South and North Dakota in the USA. These sub-basins contain sedimentary rocks of Cambrian to Tertiary age with a total thickness reaching about 3.5 km for the Williston Basin (Kent and Christopher, 1994) and greater than 4 km for the Alberta Basin (Bekele et al., 2002).

This research focuses on the deepest reservoir rocks within the formations of the Williston Basin; i.e., the Deadwood, Winnipeg, Red River, and Yeoman formations. The stratigraphic and hydrostratigraphic positions of the formations are shown in Figure 2.8 and 2.9.

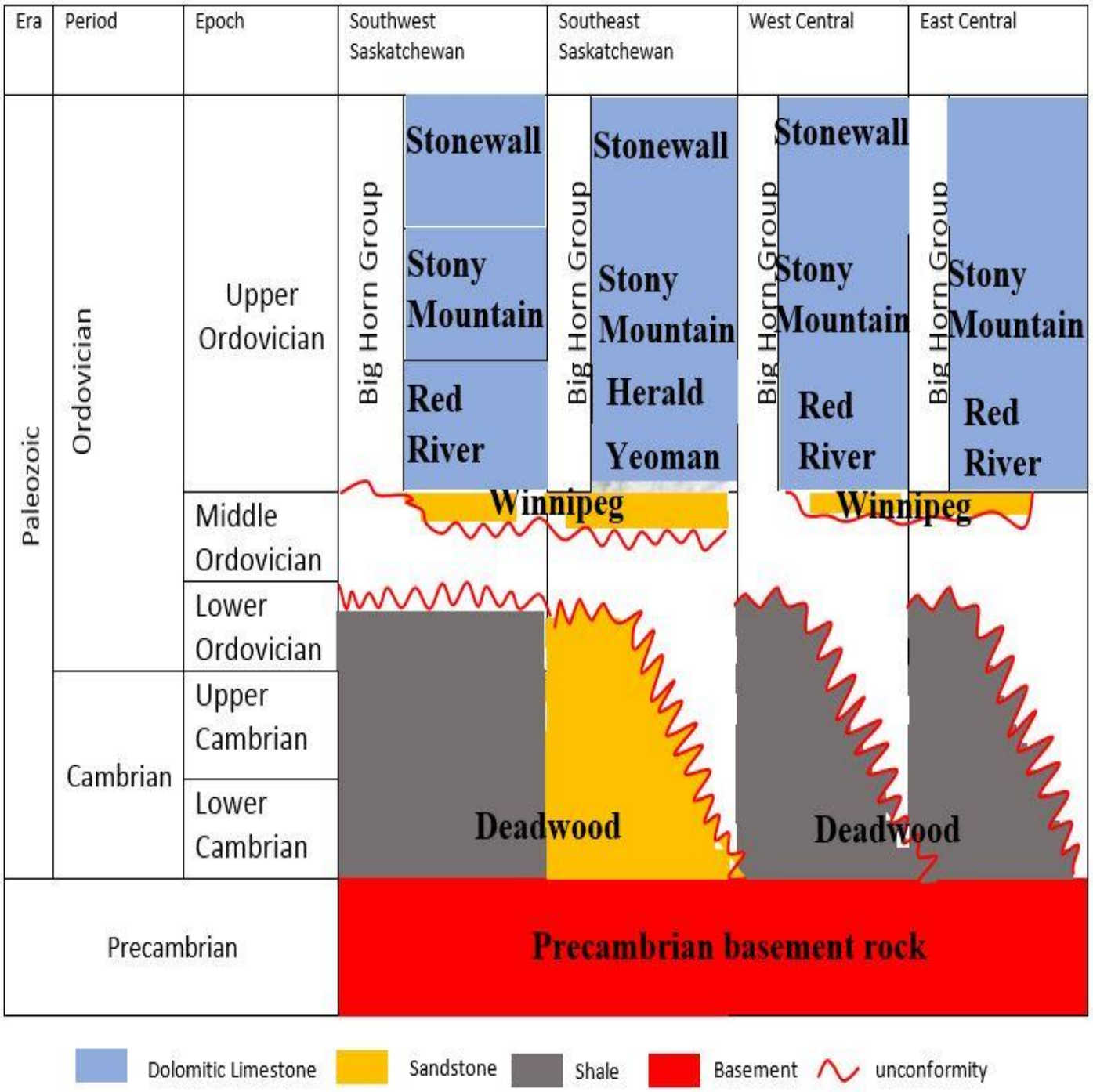

Figure 2.8 The stratigraphic chart of the reservoirs of interest in Williston Basin (modified from Okulitch, 2004)

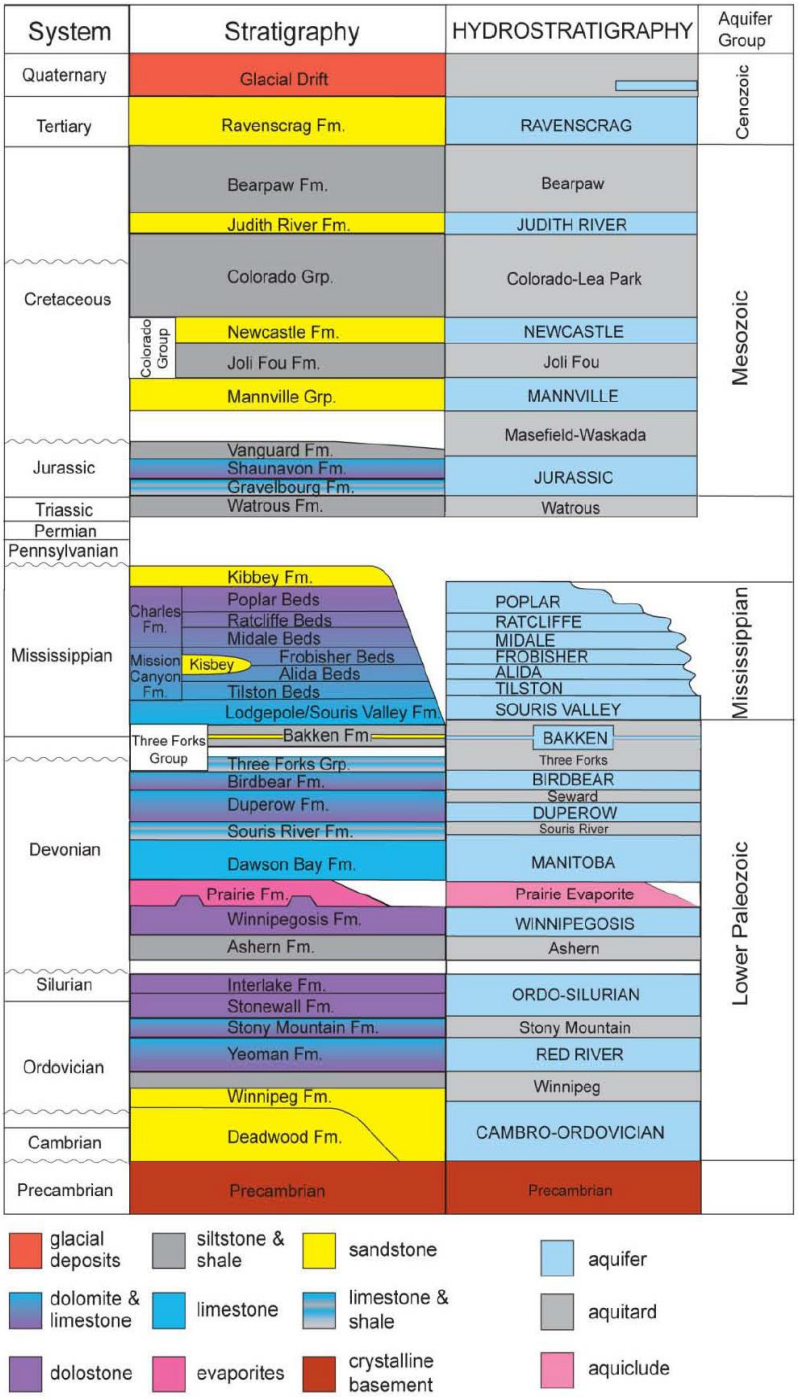

Figure 2.9 The hydrostratigraphy of the Williston Basin (Palombi and Rostron, 2010)

2.3.1 The Cambrian-Ordovician geology of the Williston Basin

There are five major transgressive-regressive sequences within the Williston Basin from Cambrian to Tertiary; all of which are bounded by unconformities (Kent and Christopher, 1994). The first transgressive event occurred during the Cambrian period and resulted in the deposition

of the Deadwood Formation (Kent and Christopher, 1994; Kreis et al., 2004). The mid-Ordovician regression led to the erosion of the Cambrian rocks (Peterson and MacCary, 1987).

The second transgressive-regressive sequence occurred during the Ordovician and Silurian periods. The early part of this sequence deposited the Winnipeg Formation which is primarily composed of siltstone, sandstone and shale, with the remaining part of the sequence being dominantly composed of carbonate rocks. These were overlain by evaporites from the Ordovician-Silurian period (Peterson and MacCary, 1987; Kent and Christopher, 1994).

The Cambrian rocks of the basin can be divided into lower, middle and upper Cambrian. The upper Cambrian to Lower Ordovician is represented by the Deadwood Formation, which overlies the Pika Marker. Where this marker is absent the Deadwood directly overlies the Earlie Formation of the middle Cambrian age within the Williston Basin. Given that sub Devonian erosion removed the lower and middle Cambrian rocks in Saskatchewan, the Deadwood unconformably overlies weathered Precambrian basement rock in this location. Its thickness ranges from 187 m in the southwest to 507 m in the northwest of Saskatchewan with a maximum thickness of about 514 m (Vigrass, 1971, Paterson, 1988, Kent and Christopher, 1994, and Kreis, 2004). For this study a constant thickness is assumed because there might be less variation in thickness between injection and production wells.

The Deadwood and Winnipeg formations are basal clastic rocks of the upper Cambrian to Mid-Ordovician periods. Both formations are composed mainly of siltstone, sandstone and interbedded shale with little carbonate rocks (Slind et al., 1994; Kreis et al., 2004; Ferguson and Grasby, 2014). They are bounded by shaly cap-rocks and crystalline basement rocks and are overpressured at some locations. According to Paterson (1988), the maximum thickness of the Winnipeg Formation within Saskatchewan is about 70 m.

The Upper Ordovician period are represented by the Big Horn Group which is subdivided into Red River, Stony Mountain and Stonewall formations (Figure 2.8). Red River Formation underlies the Stony Mountain Formation and overlies the Winnipeg Formation in western and east central Saskatchewan; it has a maximum thickness of 215 m in the centre of the Williston Basin. It is composed of crystalline and micritic dolomite and fossiliferous dolomitic limestone (Norford et al., 1994). Within southeast Saskatchewan, the Red River Formation is elevated to the group level and consists of the Yeoman and Herald formations (Figure 2.8). The Yeoman Formation

overlies the Winnipeg Formation and underlies the Herald Formation; it is composed of fossiliferous dolomite and dolomitized sandstone in its upper part (Norford et al., 1994). The Herald Formation overlies the Yeoman Formation and underlies the Stony Mountain Formation with a maximum thickness of 38 m; it has more argillaceous beds and contains anhydrite (Norford et al., 1994). The Stony Mountain Formation is between 25 and 45 m thick and underlies the Stonewall Formation and overlies the Red River (Yeoman) Formation. It is composed of argillaceous and fossiliferous limestone, calcareous shale and anhydrite at the top (Norford et al., 1994). The Stonewall Formation underlies the Interlake Group and overlies the Stony Mountain Formation. It is dominantly composed of dolomite, and calcareous dolomite with anhydrite at the base. It is less argillaceous and has a maximum thickness of 34 m (Norford, 1994).

2.4 The hydrogeology of the Williston Basin

Having discussed the lithologies and thicknesses of Cambrian to Ordovician aged strata of the Williston basins, this research considers the major basal reservoir units in pairs of Deadwood-Winnipeg and Red River-Yeoman reservoir units. Understanding the hydrogeology of the study area, including regional groundwater flow patterns, hydrostratigraphy, water chemistry, hydrogeological properties and pressure regime allows for a better assessment the geothermal potential of the basin. For example, the water chemistry will help in estimating the viscosity of brine as discussed earlier and in section 2.4.2.

2.4.1 Regional hydrogeology and hydrostratigraphy

Thermal conditions, as well as hydrogeology and flow conditions, are important to the economics of geothermal energy. Regional groundwater flow in the Paleozoic strata of the WCSB is driven by gravity and flow from the southwest towards the low-lying northeast direction. It is recharged from the Rocky Mountain and Black Hills and discharged into west-central Manitoba through Devonian age carbonates (Bachu, 1993; Bachu and Hitchon 1996; Grasby and Betcher, 2002; Grasby and Chen, 2005).

Previous studies from Bachu (1995), Bachu and Hitchon (1996) and Grasby and Chen (2005) identified seven major aquifer systems within the Williston Basin divided by a sequence of regional aquitards. These aquifer systems include: the Basal aquifer (Cambrian-Ordovician), Winnipegosis and Devonian aquifers (Devonian), the Mississippian aquifer (Mississippian),

Mannville and Viking aquifers (Cretaceous) and the upper aquifer system of the Tertiary period. A recent study by Palombi and Rostron (2010) divided the aquifer of the Williston Basin into four major aquifer groups comprised of a total of roughly twenty aquifer units (Figure 2.9). However, this research focuses more on Cambrian-Ordovician siliciclastics (Deadwood-Winnipeg) and the Ordovician carbonates (Red River-Yeoman) of the Williston Basin.

2.4.2 Water chemistry

To further understand the previous and the current water movement within the Williston Basin many studies (e.g., Hitchon and Friedman, 1969; Bachu and Hitchton, 1996; Benn and Rostron, 1998) have considered the effect of rock-water interaction on solute transport and regional groundwater flow. Bachu and Hitchon (1996) developed a salinity distribution map for formation waters of the basal aquifers within the Williston Basin (Figure 2.10). Areas within southeast and central Saskatchewan show salinity in the 200,000 to 300,000 mg/L range, while the southwest

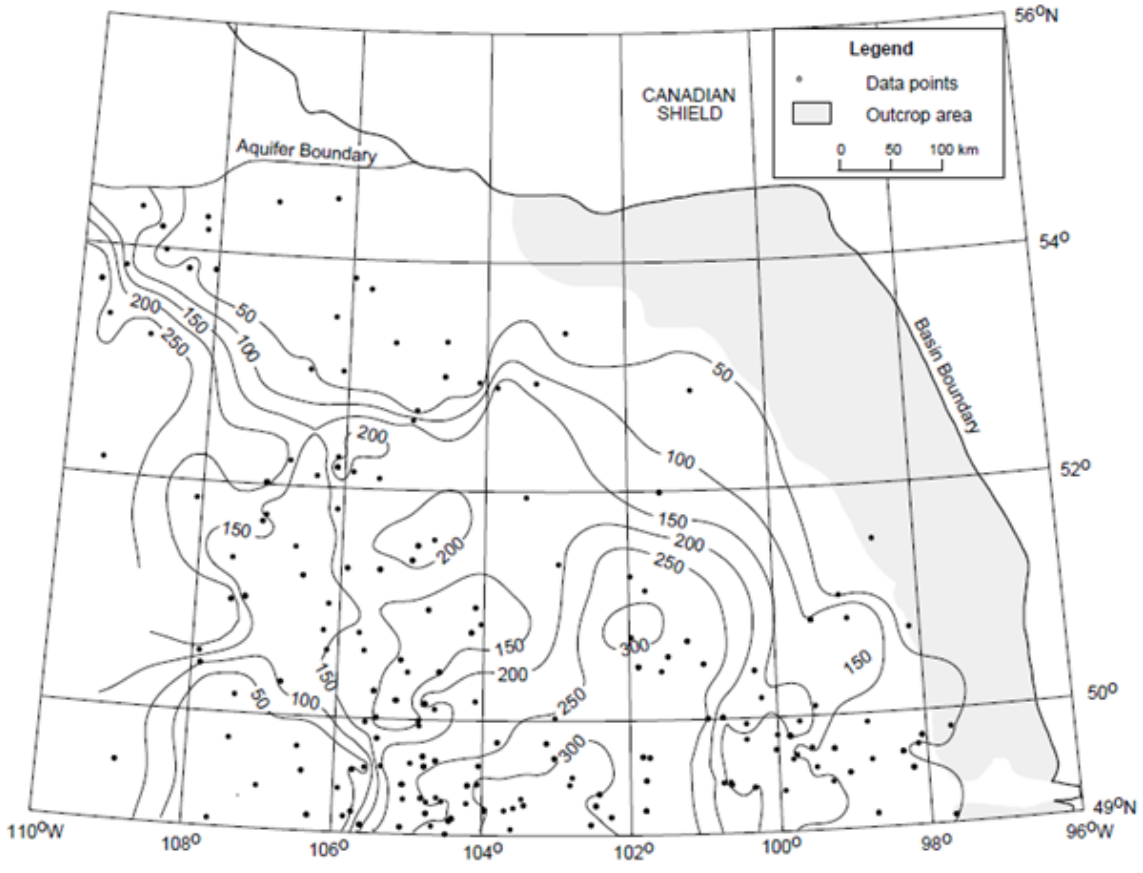

Figure 2.10 Salinity distribution map for formation waters of the basal aquifers of the Williston Basin (10^3 mg/L) (Bachu and Hitchon 1996)

portion has lower salinity (less than 50,000 mg/L). These concentration values help determine the viscosity values assigned to the different well data used for this study.

Iampen and Rostron (2000) identified three distinct pre-Mississippian brine waters within the Williston Basin using drill stem test (DST) data from hydrocarbon wells. These waters are:

1. Brackish-Ca-SO_4 (TDS<30,000mg/l) mainly in southwestern Saskatchewan,
2. Na-Cl (100,000-200,000 mg/l) within the central Saskatchewan and northern part of the basin; and
3. Na-Ca-Cl (>300,000mg/l) located in the central part of the basin.

Iampen and Rostron (2000) also observed that a mixture of evaporated seawater and dissolved halite is responsible for the high salinity of the Williston Basin, contrary to the model that claims dissolution of Prairie Evaporite Formation alone accounts for the high salinity of the Williston Basin. Further studies made recently by Palombi and Rostron (2010) identified four types of formation waters within the Williston Basin using the distribution of salinity range (2,000-470,000 mg/l) within the Cambrian to upper Cretaceous aquifers: (1) Brines (Na-Cl), (2) brackish water (Na-SO_4) (3) Freshwater (Ca-SO_4) and (4) freshwater (Na-HCO_3). The Na-Cl brines were predominantly found within the deepest aquifers of the Williston Basin. Palombi and Rostron (2010) also observed vertical flow and mixing where weak aquitards exist in the basin. Finally, in support of the previous studies, Palombi and Rostron (2010) used hydraulic head distributions to show that flow within the Lower Paleozoic aquifers is dominantly from the southwest to northeast and within the central portion of the Williston Basin flow is generally lateral and parallel to the confining aquitard contacts.

2.4.3 Petrophysical and hydraulic properties of the sandstone and carbonate aquifers

Petrophysical and hydraulic properties affect the performance of geothermal reservoirs by dictating fluid storage and flow capacity. Therefore, it is important to account for these properties when estimating geothermal potential. Table 2.1 shows a summary of the petrophysical studies reported by different authors within the Saskatchewan portion of the Williston Basin.

Early geothermal studies were carried out by Jessop and Vigrass (1989) on a geothermal well drilled in Regina. Based on core and drill log analyses, the petrophysical properties of five aquifer units from the Basal clastic rocks (Deadwood and Winnipeg formations) were estimated.

Table 2.1 Petrophysical properties of Deadwood and Winnipeg formation aquifers as reported from different studies within the Williston Basin

Reservoir Properties	Hutchence et al. 1986	Jessop and Vigrass, 1989	Betcher et al. 1995
Average Porosity (%)	13 - 17	11.2 - 17	
Permeability (md)	111 - 223	70 – 223	
Hydraulic conductivity (m/s)	1.0×10^{-6} - 3.0×10^{-6}		1.1×10^{-3} to 3.6×10^{-6}
Transmissivity (m^2/s)	1.0×10^{-4} to 3.0×10^{-3}		2.9×10^{-2} m^2 /s to 1.16×10^{-3}

The average porosity values range from 11.2% to 17% and the average permeability values ranged from 6.9 x 10^{-14} to 2.2 × 10^{-13} m^2 (70 – 223 md) with a storativity value of 0.5 × 10^{-3} determined from DST data.

From the Regina, geothermal project (Jessop and Vigrass, 1989), the mean porosities for the Basal Deadwood and Winnipeg aquifer units were 17% and 13% respectively with intrinsic permeability values of 1.1 × 10^{-13} and 2.2 × 10^{-13} m^2 (111 and 223 md) (Hutchence et al., 1986).

Hydraulic conductivities ranging from 1.1 × 10^{-3} to 3.6 × 10^{-6} m/s for 20 wells within the Winnipeg Formation aquifer in Manitoba were calculated from pumping test results. Transmissivity values ranged from 5.2 × 10^{-5} m^2 /s to 3.6 × 10^{-2} m^2 /s (Betcher et al., 1995, Betcher, 1986 and Ferguson et al., 2007).

The hydraulic conductivity of the Deadwood and Winnipeg formations near Regina, Saskatchewan range from 1.0×10^{-6} and 3.0×10^{-6} m/s (Hutchence et al., 1986 and Vigrass et al., 2007) and transmissivity values range from 1.0 x 10^{-4} to 3.0×10^{-3} m^2/s (Hutchence et al., 1986).

Transmissivity values reported for the Red River Formation in Manitoba are 2.9 × 10^{-2} m^2 /s to 1.16 × 10^{-3} m^2 /s (Betcher et al., 1995). The values may not be representative of the entire formation, and by extension may not represent the values within the Saskatchewan portion of the Williston Basin, but it does provide some indication of what range might be reasonable.

There is limited literature on the porosity and permeability of the Red River Formation within the Canadian portion of the Williston Basin. However, there are extensive studies of the petrophysical

properties of the Red River Formation in the USA. Tanguay and Friedman (2001) analysed core samples of Red River Formation from the depth range of 2683 – 4144 m and divided them into limestone, mixed lithology, and dolostone units. The limestone consists of mainly calcite with minor amounts of dolostone, and the dolostone units are predominantly dolomite with minor amount of calcite. Tanguay and Friedman's (2001) measurements show that the limestone units have a very low porosity range of 1-3.3%, the mixed lithology units have a porosity range of the 1-4.7% and the dolostone units have higher porosity (3-19%), making them good reservoirs. They concluded that the lithology and pore-throat size sorting of the Red River Formation have a strong effect on its permeability. For instance the dolostone units analysed by Tanguay and Friedman (2001) have permeability as high as 1.40×10^{-13} m^2 (140 md), whereas the mixed lithology and limestone have permeability values no higher than 1.2×10^{-14} m^2 (12 md) and 1.2×10^{-14} m^2 (11 md), respectively.

2.4.4 Production and injection rates

Historical production and injection rates are useful for this study because they give an idea of how prolific the reservoirs are and help in quantifying potential fluids produced over time. Ferguson and Grasby (2013) noted that there are no Saskatchewan production wells within the Deadwood or Winnipeg formations currently operating. However, several wells with injection rates ranging from 30 to 140 L/s (108 to 504 m^3/h) are in operation within central Saskatchewan (Ferguson and Grasby 2014).

2.5 Coproduced fluid, thermal properties and geothermal energy of WCSB

2.5.1 Coproduced fluids

Coproduced fluid or brine has been defined as "hot aqueous fluids produced during oil and gas production" (Tester et al., 2006). The idea that a geothermal potential is embedded within coproduced fluid came from the studies carried out by McKenna and Blackwell (2005) and McKenna et al. (2005). They estimated that about 1000 to 5000 MW of electricity can be produced by seven USA states near the Gulf coast depending on the temperature and the water production rate. According to Ferguson (2015) about 700,000 drilled hydrocarbon wells and up to 25 billion cubic meters of fluids (including coproduced fluid) have been produced in WCSB and millions of cubic meters of fluids have been injected into wells for enhanced recovery and

disposal. The energy stored within these fluids has not been completely quantified. Few studies have been carried out with respect to coproduced water within the WCSB.

The annual coproduced water from about eight states in the USA is about 6.5 billion cubic meters (Curtice and Dalrymple 2004), as per the Massachusetts Institute of Technology (MIT; MIT 2006) up to 11,000 MWe of electricity can be generated from coproduced hot waters with temperatures ranging from 100^{o}C to 180^{o}C using organic binary power plants. They also estimated that coproduced water of about 82 ^{o}C and 93 ^{o}C would require a flow rate of about 570 and 370 m^3/h respectively to achieve a 1 MW (net) power plant, which is the total power that can be achieved from a power plant using 100^{o}C fluid at the rate of about 300 m^3/h.

2.5.2 Geothermics in Canada

Previous studies (Jessop et al., 1991, Majorowicz et al., 1999, Majorowicz. and Grasby,, 2010, and Grasby et al., 2012) have identified areas of high geothermal potential in Canada, mainly in western and northern Canada. High geothermal potential is based on temperature, geothermal gradient, heat flow, thermal conductivity and petrophysical properties. These studies focused mainly on the potential for Enhanced or Engineered Geothermal Systems (EGS).

2.5.3 Heat generation, flow and temperature

The heat flow map of the Precambrian surface at the base of WCSB is shown in Figure 2.11. Bachu (1994) noted that the basement heat flow within the Alberta Basin ranges between 30 – 40 mW/m^2 in the southern part and 80 – 100 mW/m^2 in the northern part. Majorowicz et al. (1986) stated that, in the Williston basin, the geothermal gradient below the Paleozoic formations ranges from 15 ^{o}C/km to greater than 25^{o}C/km with a heat flow 40 – 80 mW/m^2 in central Saskatchewan and up to 100 mW/m^2 in the southern part of Saskatchewan near Weyburn and Estevan. The temperature map in Figure 2.12, generated by Bachu (1994), shows the temperature of the upper Precambrian contact measured from DST's of wells within the WCSB. Temperatures range from 20-50^{o}C in the shallowest areas (north and central Saskatchewan) to just over 100^{o}C in the deeper areas (southern part of Saskatchewan), in agreement with Ferguson and Grasby (2014). The average annual ground surface temperature within the Williston Basin is 2^{o}C (Beltrami et al., 2003).

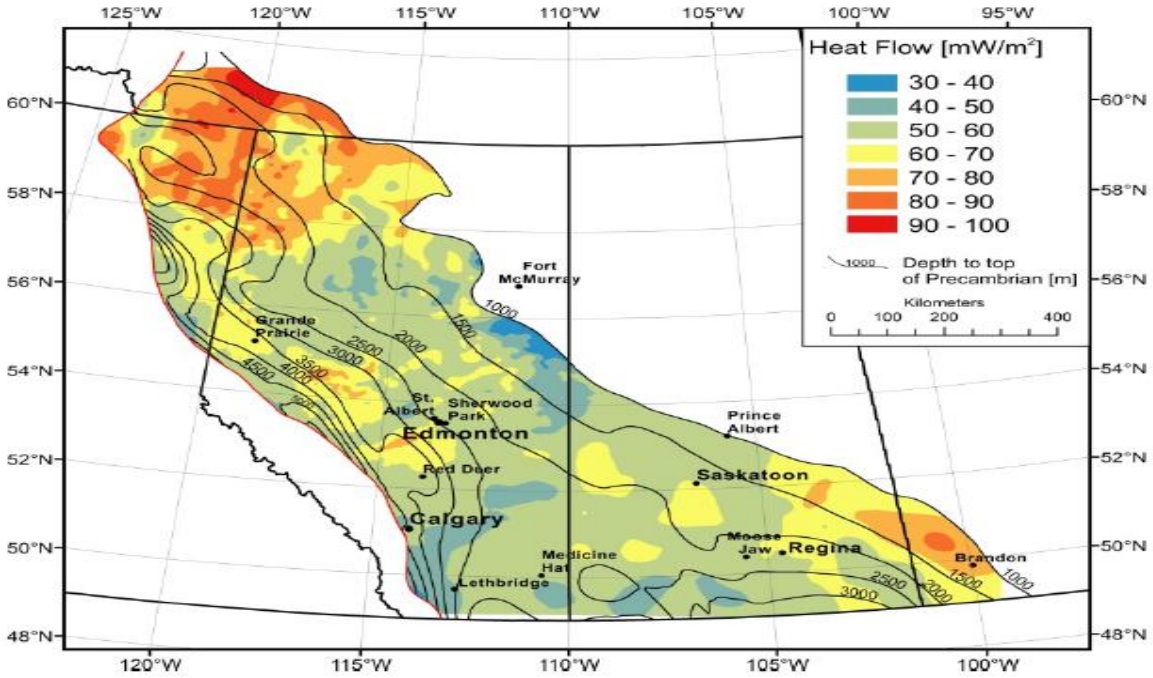

Figure 2.11 Heat flow map of WCSB (Weides and Majorowicz, 2014)

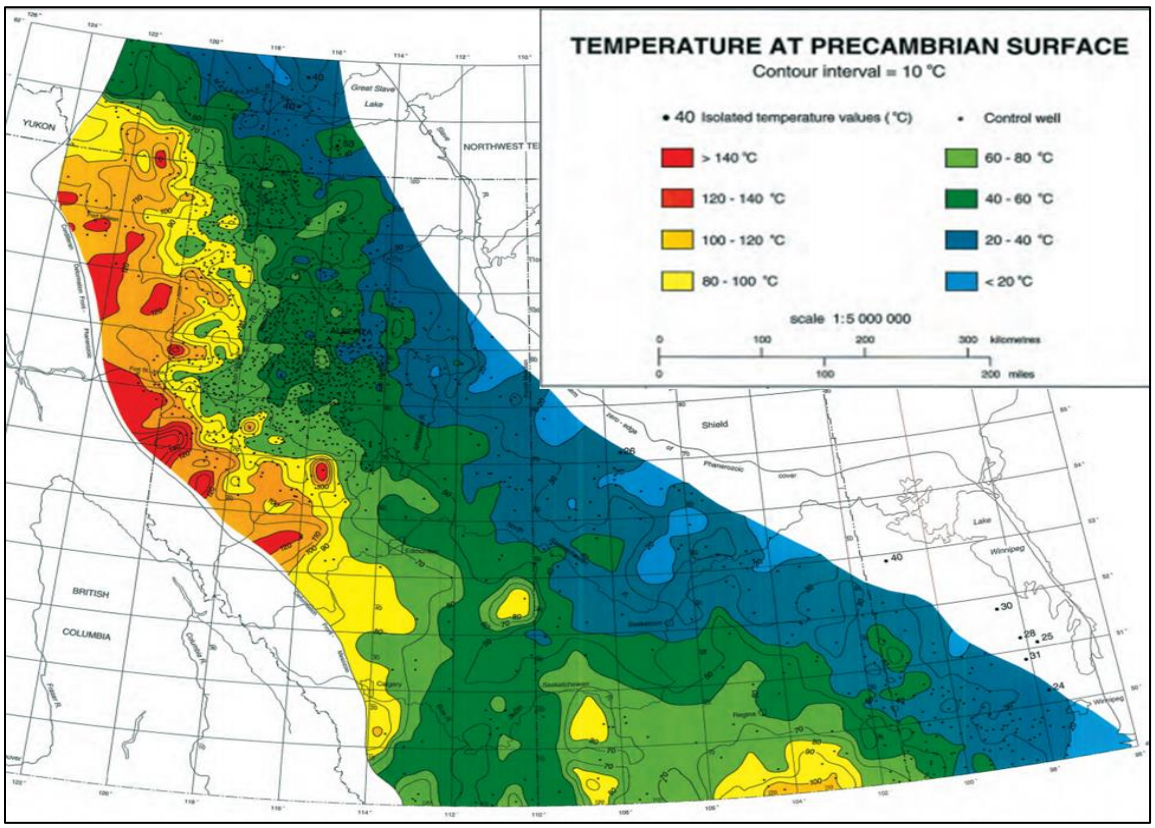

Figure 2.12 Temperature distribution at the top of the Precambrian within WCSB (Bachu 1994)

The heat retained because of the thick sedimentary cover and the heat from the Precambrian rocks contributes to the relatively high temperature (40 to 110^{o}C) and high heat flow (40-60 mW/m^{2}) within the basin (Majorowicz et al., 1986, Vigrass et al., 2007, Majorowicz and Grasby, 2010, Jones, 1991, and Ferguson and Grasby, 2014). Figure 2.12 shows southeast and southwest Saskatchewan as a potential zone for geothermal electricity production based only on temperature and central Saskatchewan has a potential for direct application (Ferguson and Grasby, 2014). Further research is required to clearly assess these zones.

2.5.4 Thermal conductivity

Thermal conductivity is one of the major factors controlling the geothermal gradient, and is therefore important for estimating geothermal energy potential. Some general studies on thermal conductivity have been conducted within the WCSB. Jessop and Vigrass (1989) documented thermal conductivity values measured from a well in Regina. Their results include average thermal conductivity values measured from basal clastic units (2.09 – 2.41 W/m.K) and carbonate units (2.63 – 3.71 W/m.K). Bachu (1993) presented a WCSB map with effective thermal conductivity ranging between 1.20 and 3.30 W/m.K) and a dominant westward decrease throughout the entire sedimentary basin. These estimates are based on measurements from core and drill log. However, the study carried out by Lengyel (2013) generated specific values for thermal conductivities of the formations within the Saskatchewan portion of the Williston Basin (Table 2.2).

Table 2.2 Thermal conductivities of the deeper rock formations of the Williston Basin in Saskatchewan and North Dakota

Rock units	(Lengyel, 2013) K_R (W/m.K)	(Gosnold *et al.*, 2012) K_R (W/m.K)
Shale	1.10	1.10
Red River	2.82	3.28
Winnipeg	2.28	4.07
Deadwood	2.23	3.46

More comprehensive studies on thermal conductivity have been carried within the USA portion of the Williston Basin. Gosnold et al. (2010 and 2012) measured the thermal conductivities of multiple strata of the Williston Basin. Table 2.2 compares the results for the deeper rock formations (Deadwood, Winnipeg and Red River) reported by Lengyel (2013) with those of Gosnold et al. (2010 and 2012). Even though the values fall within the range reported by several authors (Jessop and Vigrass, 1989; Bachu (1993); and Majorowicz et al. 1999) there is a significant difference between the values. This could be because of the depth and lithological variation, as suggested by Lengyel (2013). The formations are deeper in the USA portion and this can play an important role in influencing the thermal properties of the rocks. Furthermore, the Saskatchewan portion of the Winnipeg Formation comprises sandstone and shale whereas the USA portion it is composed of dolomite and sandstone. Grasby et al. (2012) noted that the generally low thermal conductivity rocks within the basal units of the WCSB overlying the high thermal conductivity crystalline basement, generates a thermal blanketing effect. This leads to the high temperature, high geothermal gradient and makes it a strong candidate for geothermal energy production.

3 RESEARCH METHODOLOGY

3.1 Research questions and overview

Quantifying and evaluating the hot fluids produced from the Williston Basin is one of the major steps to understanding the geothermal potential of the basin. To assess the capability of the Williston Basin in generating sufficient thermal power for direct use and/or electricity generation, this research estimates the heat and power stored in the basal reservoirs/aquifers of the Williston basins (Deadwood-Winnipeg and Red River-Yeoman), using three different techniques:

1) Observed production/injection rates (fluid thermal properties),
2) Theoretical production rates (hydraulic properties), and
3) Rock thermal volume.

Temperatures, production/injection rates, and core analysis data from both injection and production wells were used to achieve these objectives.

Furthermore, this section considers the effect of different parameters on the geothermal doublet system with respect to the study carried out by Gringarten and Sauty (1975) and compares their findings with the parameters associated with this study. This will give an idea of the size of reservoir block to use for estimating the rock thermal volume.

3.2 Research Procedure

3.2.1 Quantification of thermal power using observed production/injection rates

Production and injection data compiled using the AccuMap and Geoscout databases included the cumulative volume of water produced and injected, total production/injection hours, density, and bottom-hole temperature (BHT). These data were used to estimate the geothermal power and heat energy produced. The simple power formula shown in Equation 2.5 was used to quantify heat and calculate potential electrical power to be produced per well in the Deadwood-Winnipeg and Red River-Yeoman reservoirs. This calculation was done using Equation 2.5 from section 2.2.1, using the production rates (m^3/s) of 238 wells. The production rate for each of these wells within the Deadwood-Winnipeg and Red River-Yeoman was estimated using the total production hours and cumulative water produced as recorded in AccuMap. For this research, ΔT of 20^oC was used to estimate the potential thermal power. The lower temperature difference allows for a more

conservative estimate, especially if electricity production is to be considered at low in situ temperatures. As mentioned earlier the temperature difference of 20^{o}C and 33^{o}C were used by Ferguson and Grasby (2014). Also, the heat losses that could result from piping and heat exchangers are ignored, assuming that insulators would be used to keep the heat and improve efficiency.

Furthermore, Equation 2.6 was used to estimate the electrical geothermal power within the reservoirs. This research used 10% conversion factor as suggested by Ferguson and Grasby (2014). See Appendices A and B for sample calculation and results.

3.2.2 Estimating maximum production rates using hydraulic properties (Core permeability and Cooper-Jacob's Equation)

This section used the hydraulic properties of individual wells to estimate the maximum production/injection rates that are obtainable from each well within the Deadwood-Winnipeg and Red River-Yeoman reservoirs by using the Cooper-Jacob (1946) equation discussed in section 2.2.2.

In this study the Cooper-Jacob's equation (Equation 2.10) was rearranged and used to determine the production/injection rate, *Q* (Equation 3.1) necessary to bring hydraulic head to a point where the well bore goes dry (an upper bound estimation).

$$Q = \frac{\Delta s T}{0.183 \log\left(\frac{2.25 T t}{r^2 S}\right)} \tag{3.1}$$

Where,

Q is Production/injection rate (m^3/s),

T is transmissivity (m^2/s),

t is time (s),

Δs is drawdown; distance to the surface of water level (m),

S is Storativity,

r is the radial distance between the production and injection well (m).

This was achieved by using the depth to the top of formation as the drawdown and a total of 1050 and 5385 core permeability data for Deadwood-Winnipeg and red River-Yeoman respectively from AccuMap were used to calculate transmissivity. The core analysis summary data for each

well has the following information; well Id, sample depth and thickness, sample formation, horizontal permeability (kmax), vertical permeability (kvert), porosity, grain density, and lithology (see Appendices C and D). Average of horizontal permeability (kmax) was used for the calculation and a dominant horizontal flow is assumed because at a separation distance of 1 km variation of thickness is less also this corresponds to the assumption made by Gringarten and Sauty (1975) model.

A time *t* of 30 years was used because it is the useful lifetime of a doublet geothermal system (Gringarten and Sauty, 1975, Lippmann and Tsang, 1980 and Wellmann et al., 2010). In this study the total depth to the top of formation was used as drawdown to simulate a situation where the borehole is dry (this is an upper bound assumption; it might not be practically obtainable). A radial distance of 1 km was used – similar to that proposed by many studies including Lippmann and Tsang, 1980 and Wellmann et al., 2010 and Ferguson and Grasby (2014).

Equation 2.11 was used to obtain the transmissivity of each well. The concentrations of brines in the Williston Basin (200,000 to 300,000 mg/l (about 3.5-5.0 Mol/kg) as discussed in section 2.4.2) were used in conjunction with the Table 10 of Kestin et al. (1981) to determine the appropriate viscosity values for the basin. The viscosity values used for Deadwood-Winnipeg and Red River-Yeoman reservoirs are 5.67×10^{-4} to 7.82×10^{-4} and 4.82×10^{-4} to 7.28×10^{-4} respectively (See Appendices C and D).

The storativity was calculated using Equation 2.12 and the effective porosity was obtained from core data. The aquifer compressibility, α, and compressibility of water, β used for this calculation are 1.0×10^{-08} Pa^{-1} and 4.4×10^{-10} Pa^{-1} respectively (Freeze & Cherry, 1979).

The pumping rate calculated from the hydraulic properties was entered into Equation 2.5 and used to quantify thermal power production that can be produced from the reservoirs of interest.

3.2.3 Effect of different parameters on a geothermal doublet system

The properties of the Deadwood and Winnipeg formations are variable, therefore the effect of these variations on the relationship between well separation distance and the time at which breakthrough of the cold front occurs at the production well were tested using the Gringarten and Sauty (1975) model discussed in Chapter 2.1.2 (Equation 2.4). Table 3.1 shows the parameters used

Table 3.1 Parameters used for the Gringarten and Sauty (1975) model

Parameters	Values	Sources
Q - Production/Injection rates	100, 150, 200[c], 250, 300 (m^3/h)	Accumap data
Ø - Rock porosity	15, 20, 25[c], 30, 35 (%)	Accumap data
h - Reservoir thickness	150 [c], 200, 250, 300, 350 (m)	Kreis (2004), Ferguson and Grasby (2014)
ρ_R - Grain density of rock	Sandstone 2727 (kg/m^3)	Mean value from AccuMap
	Carbonate 2794 (kg/m^3)	
ρ_w - Density of water	1065 (kg/m^3)	Hutchence et al. (1986)
C_R - Heat capacity of rock	Sandstone 920 (J/kg^{o}C) Carbonate 840 (J/kg^{o}C),	ETB (2011)
C_w - Heat capacity of water	3770 (J/kg^{o}C)	Hutchence et al. (1986)
λ_R - Caprock/bedrock thermal conductivity	2.5 (W/m-K)	Clark (1966)
Δt - time before thermal breakthrough	30 years	Gringarten and Sauty (1975)

[c] denotes the value kept constant while varying the other parameters

for this model. Three different scenarios were considered by varying; Injection/production rate, reservoir thickness, porosity while other parameters were kept constant.

3.2.4 Estimating geothermal electrical power using rock volume

In this section the thermal energy and power of each reservoir block were estimated based on well spacing using the method outlined by Bundschuh & Suárez-Arriaga (2010) as discussed in section 2.2.3 using Equation 2.13. The volume of the reservoir block, V_B (m^3) was estimated using the product of well spacing, average reservoir thickness, and width of influence. A well spacing of 1 km was used as recommended by Gringarten and Sauty (1975). Equation 2.15 was used to estimate the average electrical geothermal power that can be generated from each geothermal reservoir. This geothermal block was used to conduct a sensitivity analysis to see how the width of influence affects the estimated reservoir thermal and electrical energy for each reservoir while thickness and separation distance (length) were kept constant.

3.2.5 Production/Injection Pressure Estimation

The general steady state equation (Equation 2.16) was used to estimate wellbore flowing pressure (P_{wf}), due to injection using the thickness, hydraulic properties of the reservoir, observed production/injection rates and the formation pressure (see Table 3.2,).

The scenarios were for a thin reservoir and low permeability, and another for a thick reservoir and high permeability, in order to assess upper and lower bounds on pressure. Equation 2.17 was used to estimate the formation pressure, P for the selected wells and then entered into Equation 2.16 to get the injection pressure of the wells.

3.2.6 Data acquisition and processing

The data used for this research were generally obtained from the IHS AccuMap (AccuLogs) and geoLOGIC geoSCOUT databases software, which store large quantity of hydrocarbon well logs, core data, well completion reports etc. Most of the borehole temperature data used for this research were obtained from Geoscout. The well coordinates were used to generate well location maps using ArcGIS as shown in Appendices E and F.

The index map of wells within Saskatchewan was created and queried based on criteria of interest for example core availability, well production data, DSTs, formation tops, coordinates, etc. These wells were saved and exported through MS Excel. In Excel format the data were sorted based on different geological formation (Deadwood, Winnipeg, Red River, and Yeoman). In Appendices A and B the water production information (cumulative production and production hours) were used to estimate production rates for each well within the different reservoirs and this was in turn used to estimate geothermal energy and power.

Table 3.2 Table of Parameters used to estimate (P_{wf}), r and r_w are 1000 and 0.15 meters respectively

Well ID	**Reservoir**	**h (m)**	**k (m^2)**	Q (m3/s)	**μ (Pa.s)**	**H (m)**
131/08-16-006-11W2/0	Deadwood-Winnipeg	49	8.12E-15	0.0018	6.81E-04	850
02/01-09-017-14W3/0	Deadwood-Winnipeg	173	1.00E-13	0.0037	5.66E-04	800
141/08-22-008-13W2/0	Red River-Yeoman	18	6.35E-16	0.0171	5.66E-04	790
101/03-20-002-16W2/0	Red River-Yeoman	381	8.78E-14	0.0025	5.67E-04	870

The data used to generate the results in Appendices C & D were extracted from core summary reports. Data such as porosity and permeability were entered into equations 2.11, 2.12 and 2.17 to obtain transmissivity, storativity, and production rates as aforementioned in section 3.2.2.

4 PRESENTATION OF RESULTS

The locations of the production and injection wells used for this study are shown in Fig. 4.1 (see Appendices A and E for detailed data and maps). The production wells are mainly located within the Williston Basin in the south-eastern part of Saskatchewan and the injection wells are dominantly located within the central portion of Saskatchewan close to Saskatoon. The injections wells are mainly disposal wells. Table 4.1 shows the summary of the data used in estimating injection/production rates and the potential power that can be generated from the Williston Basin

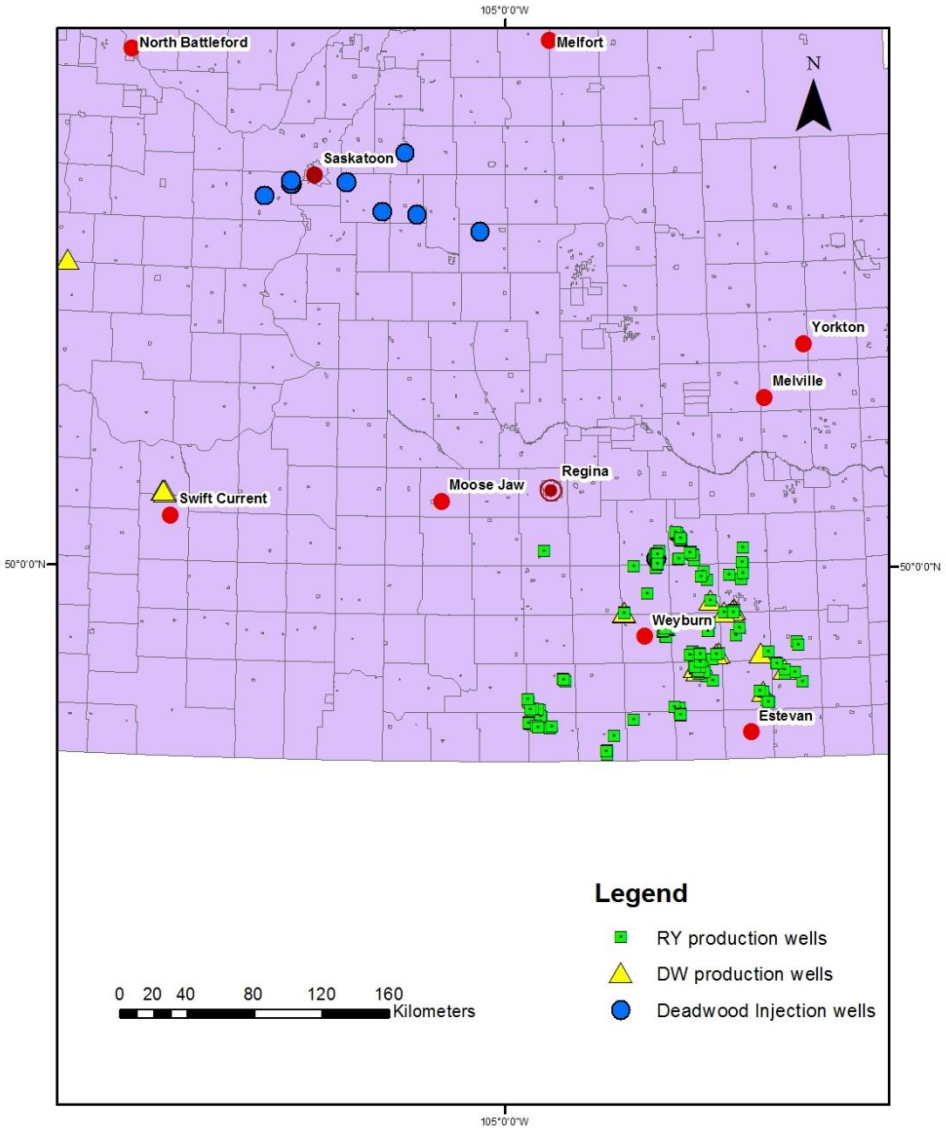

Figure 4.1 Map of Southern Saskatchewan showing the locations of the wells used for this study (RY denotes Red River and Yeoman, DW denotes Deadwood and Winnipeg formations).

Table 4.1 Summary of data used for the estimation of production/injection rates and potential thermal power within the reservoirs of interest

Reservoir	No. of wells	Vertical depth (m)	Average Thickness (m)	Borehole Temperature (^oC)	Cumulative water Prod/Inj. (m^3)	Mean Injection and Production Rates per well (m^3/h)
Deadwood (Injection wells)	20	1200 to 2137	268	NA	112,923,024	80
Deadwood-Winnipeg (Production wells)	23	2000 to 2850	107	60 - 87	2,149,663	21
Red River-Yeoman (Production wells)	198	1400 to 3975	108	65 - 100	27,372,345	480

NA – Not available

with respect to the reservoirs of interest (see Appendix A-D for the full dataset used for this study). Numerous wells were drilled within the Deadwood-Winnipeg and Red River-Yeoman formations, however only 20 injection wells and 221 production wells respectively have the data that is needed for this research (Table 4.1).

The bottom hole temperature (BHT) (Figure 4.2) was extracted from AccuMap and Geoscout database software. The depth of the production wells analysed falls between 2000 and 3000 m within the Deadwood-Winnipeg reservoir and between 1400 and 4000 m within the Red River-Yeoman reservoir with BHTs ranging from 60 to 120 ^oC (Figure 4.2). The depth of the injection

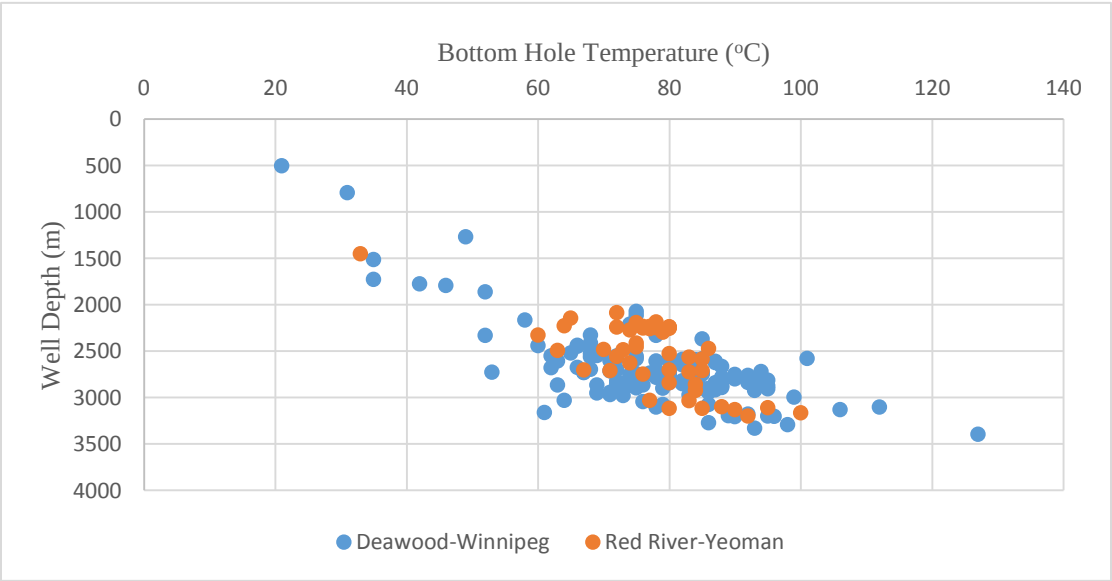

Figure 4.2 A plot showing well depths vs temperature within the reservoirs of interest

wells within the Deadwood Formation is much less than those of the production wells (see Table 4.1), because they are present in the central part of Saskatchewan where the Deadwood Formation lies at a shallower depth.

4.1 Historical injection and production rates

Based on the data compiled for this research a significant amount of water (about 30 million cubic metres in total) has been co-produced from Deadwood-Winnipeg and Red River-Yeoman hydrocarbon reservoirs, and over 100 million cubic metres of water have been injected into the Deadwood Formation with average rates shown in Table 4.1.

4.1.1 Deadwood-Winnipeg reservoirs

60% of the injection rates are above 40 m^3/h in the Deadwood-Winnipeg reservoirs, with the average rate at 80 m^3/h and maximum rate just above 500 m^3/h (Figure 4.3). Though the locations of the injection wells are not situated around the area of interest, these rates can be used for inference and extrapolation purpose (if the hydraulic properties and thicknesses are similar).

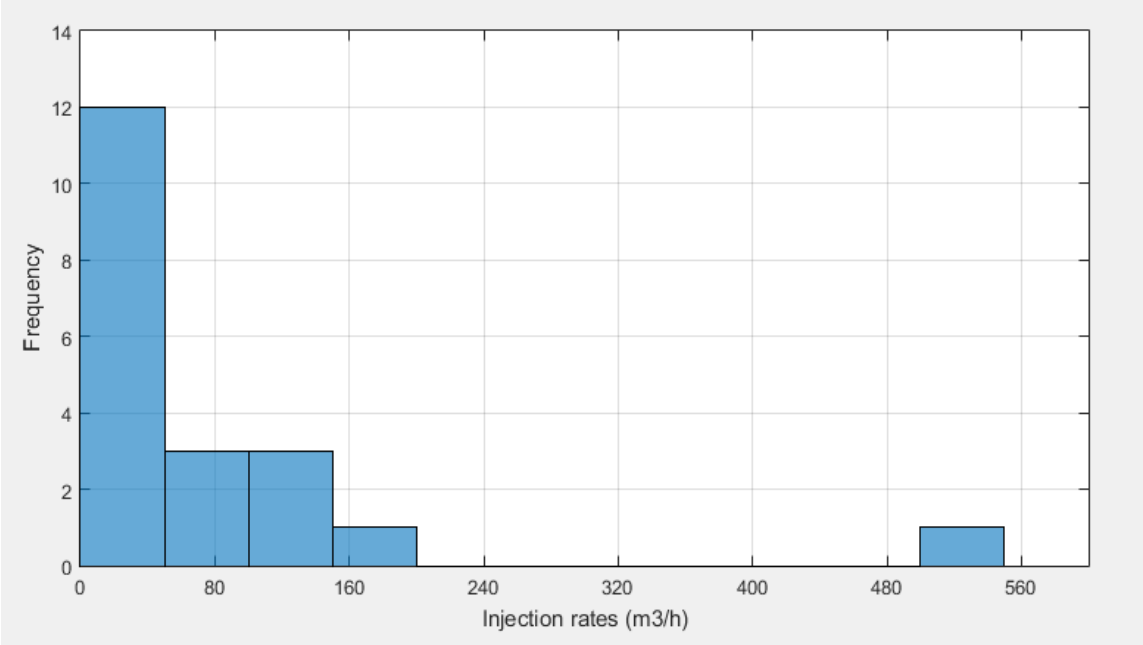

Figure 4.3 Histogram showing injection rates within Deadwood-Winnipeg wells

The observed production rates from Deadwood-Winnipeg wells (Figure 4.4) show more than 80% of the wells have pumping rates below 40 m^3/h (See Appendix A for the full results).

4.1.2 Production Rates within Red River-Yeoman reservoirs

The observed production rates from the Red River-Yeoman reservoirs are significantly greater than those of the Deadwood-Winnipeg reservoirs, with about 20% of the wells studied having rates above 500 m^3/h and with an average production rate of about 480 m^3/h as shown in Figure 4.5 and Table 4.1, respectively (See Appendix C for full results).

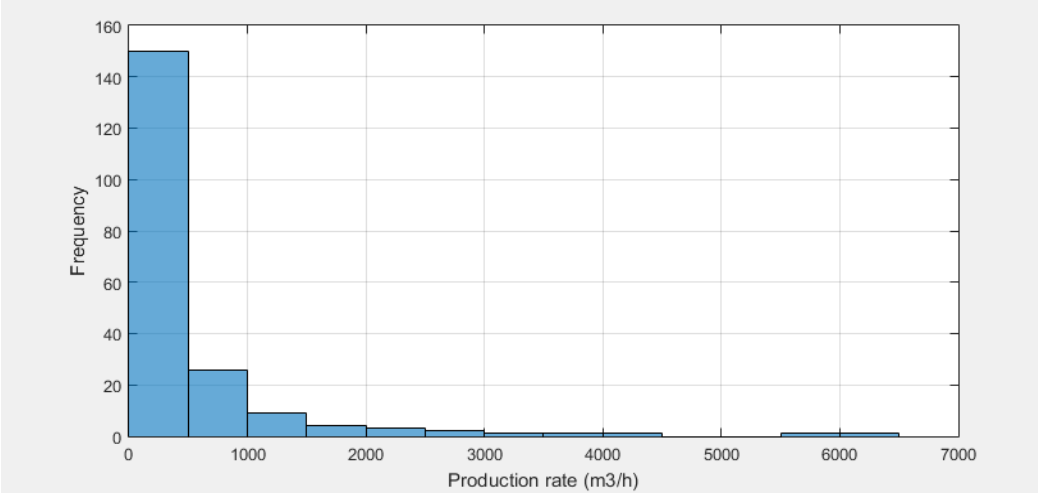

Figure 4.5 Histogram showing observed pumping rates from Deadwood-Winnipeg wells

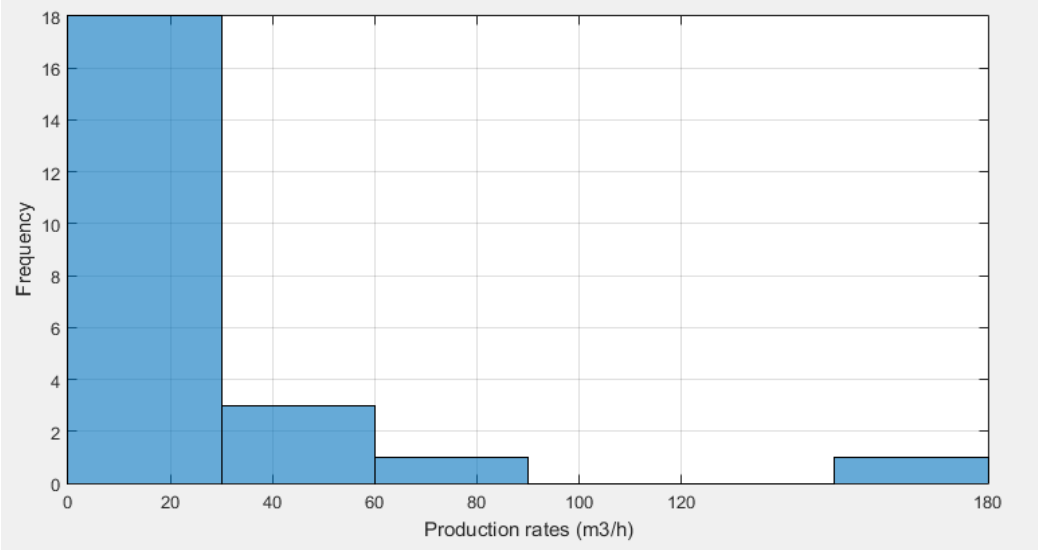

Figure 4.4 Histogram showing the observed pumping rates Red River-Yeoman wells

4.2 Potential thermal power production

4.2.1 Potentials based on temperature data

A temperature distribution map of Saskatchewan produced from the BHT data of the wells within the Deadwood-Winnipeg and Red River-Yeoman reservoirs (Figure 4.6) shows relatively high

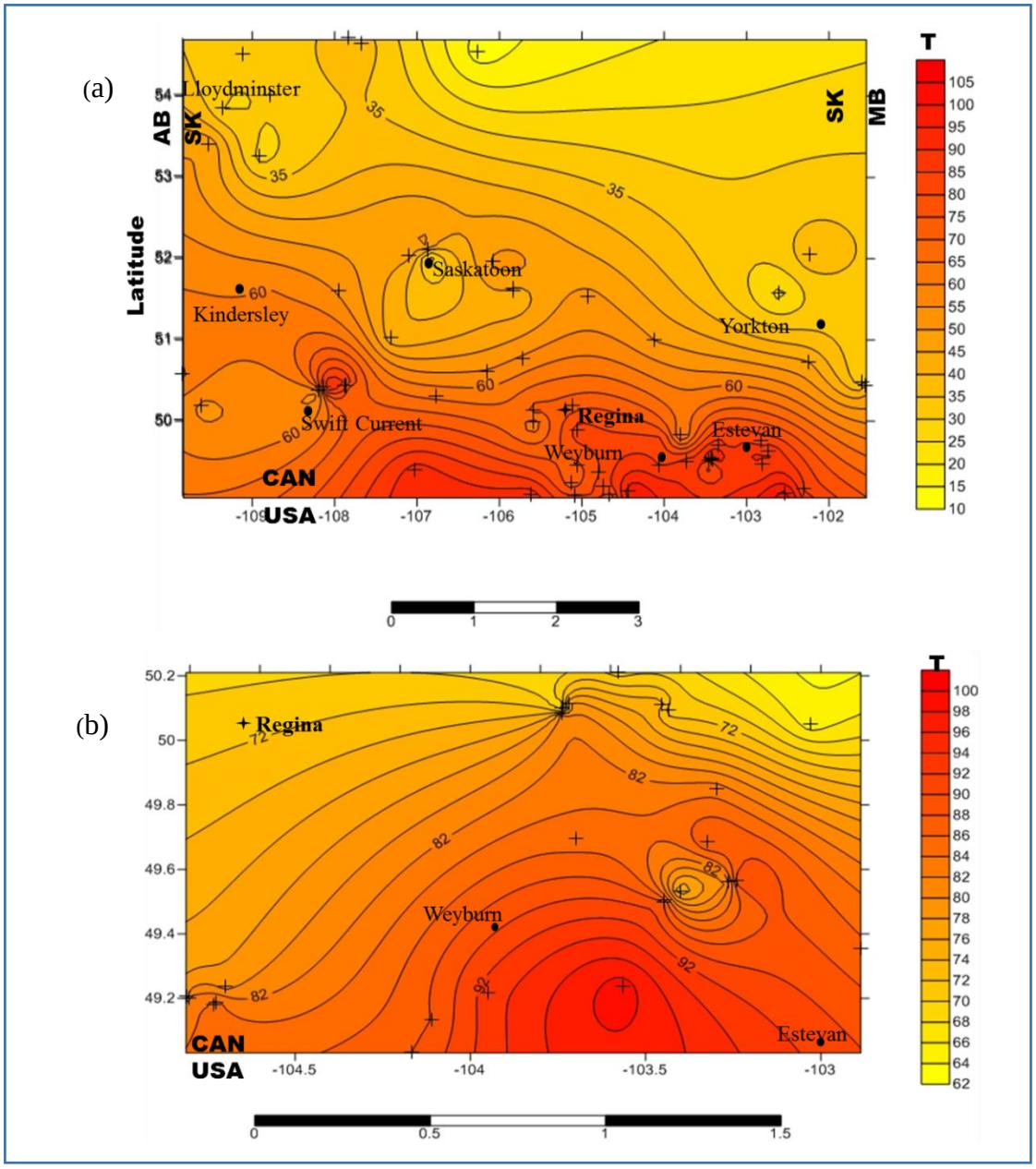

Figure 4.6 Bottom hole temperature (^{o}C) in southern Saskatchewan at depths ranging from 2-3 km within the (a) Deadwood-Winnipeg reservoirs and (b) Red River-Yeoman.

temperatures within the southernmost portion of Saskatchewan – within the Williston Basin.

This high temperature area includes: Regina, Swift Current, Weyburn and Estevan, with temperatures ranging from 60^{o}C to above 100^{o}C. The central and northern portion of the map, which contains Saskatoon, Kindersley, Yorkton, and Lloydminster, has temperatures below 50^{o}C.

4.2.2 Deadwood-Winnipeg reservoirs

The thermal power was calculated from the historical production rates using Equation 2.5. The sample calculation is shown below and in Appendix A.

Sample Calculations using Well 141/08-14-006-06W2/0

$Q = \text{Cum. Water Produced}/\text{Cum. Prod. hrs} = 106.3\text{m}/24\text{h} = 4.43\ (\text{m}^3/\text{h}) = 0.0012\ (\text{m}^3/\text{s})$

$P_T = Q^* \rho_w^* C_w^* \Delta T = 0.0012\ \text{m}^3/\text{s} * 1000\text{kg}/\text{m}^3 * 3770\ \text{J/kg}\ ^{o}\text{C} * 20^{o}\text{C} = 0.0927\ \text{MWt}$

$P_E = n_g^* P_T = 10\%^* 0.0927 = 0.01\ \text{MWe}$

The results displayed in Figure 4.7, show that just about 30% of the wells can produce thermal power of above 0.5 MWt.

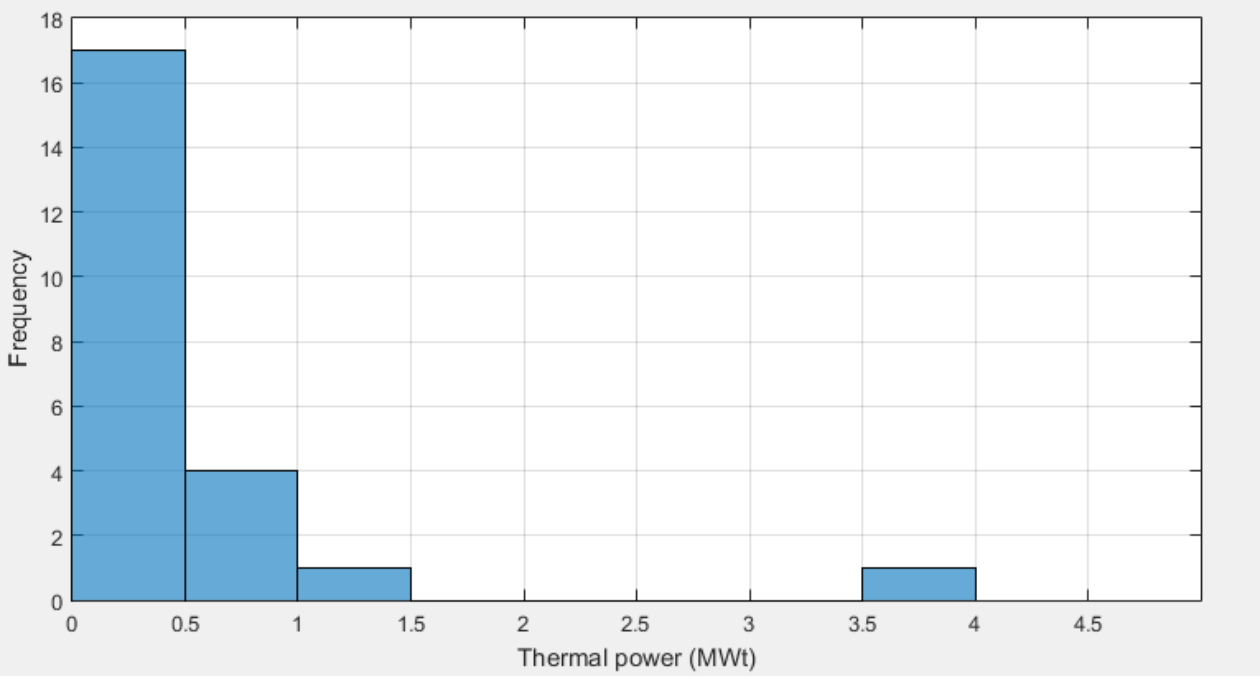

Figure 4.7 Histogram showing potential thermal power from Deadwood-Winnipeg wells

4.2.3 Red River-Yeoman reservoirs

The potential thermal power that can be generated from the wells within this reservoir is higher than that of the Deadwood-Winnipeg, with an average of 10 MWt and 10% of the wells capable of producing above 25 MWt of thermal power (Figure 4.8 and Appendix C).

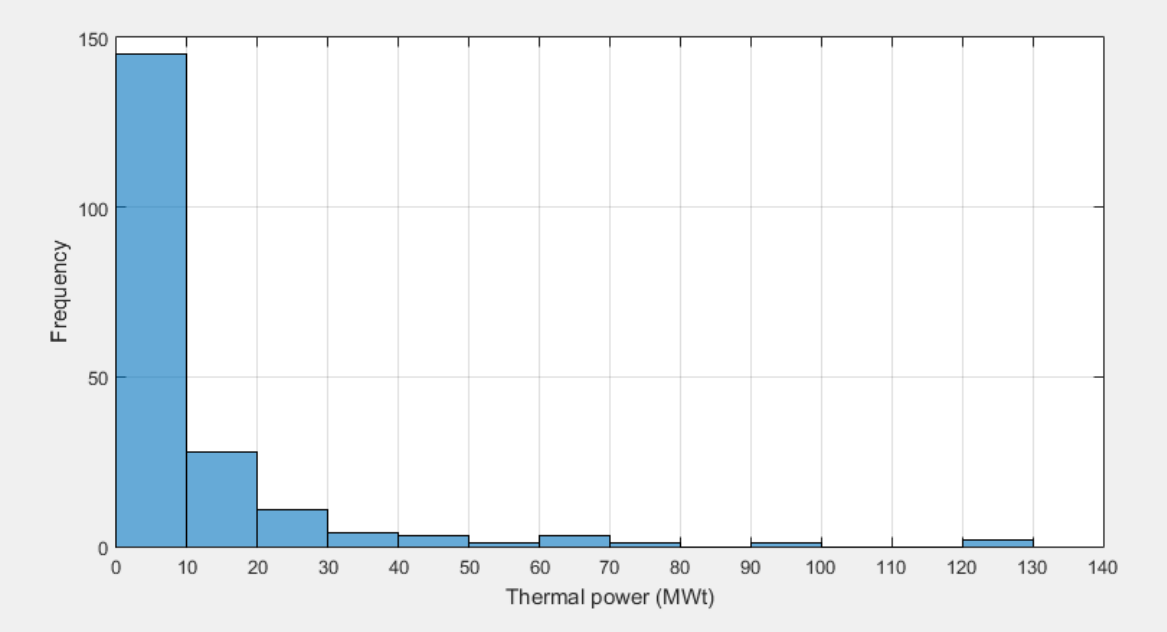

Figure 4.8 Histogram showing potential thermal power from Yeoman-Red River wells

4.3 Potential power produced based on hydraulic properties

The two reservoirs under study have similar and wide ranges of permeability and porosity values, and there seems to be a linear relationship between the porosity and the logarithm of permeability as generally expected, especially for Red River-Yeoman reservoirs (Figure 4.9). The horizontal permeability (kmax) was used to calculate the hydraulic conductivities (K) of these reservoirs and the storativity (S) of the reservoirs were estimated using Equation 2.12. Sample calculations are shown below; see the Appendix C & D for results. The theoretical production rates were calculated for each well. For the calculation of production rates, only wells with core permeability data were used.

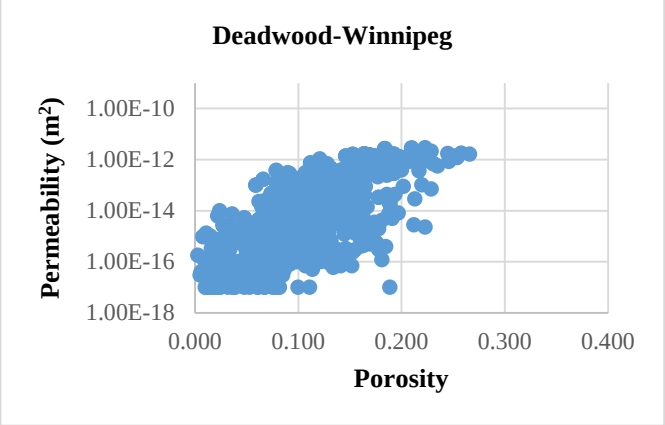

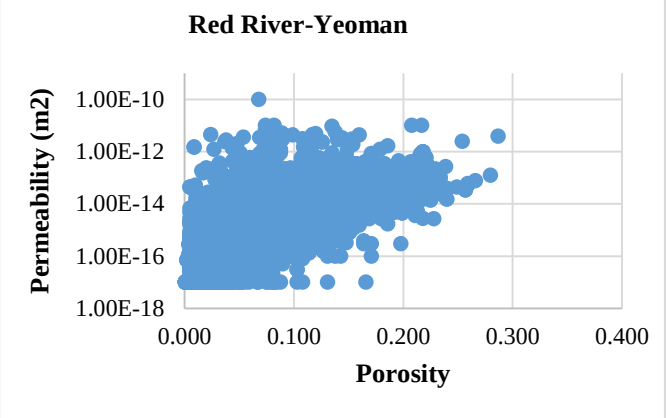

Figure 4.9 Permeability vs Porosity plot for Deadwood-Winnipeg and Yeoman-Red River reservoirs

Sample Calculations using Well 141/08-14-006-06W2/0

$K = (k * \rho_g * g)/\mu = 2.05E\text{-}14\ 9m^2 * 2700\ kg/m^3 * 9.8\ m/s^2/5.67E\text{-}4Pa.s = 9.587E\text{-}7\ m/s$

$T = K * h = 9.587E\text{-}7\ m/s * 53m = 5.08E\text{-}05\ m^2/s$

$S = \rho g(\alpha + ne\ \beta)h = 1000kg/m3 * 9.8m/s^2/ * (1.0E\text{-}8\ Pa^{-1} + (0.3 * 4.4E\text{-}10Pa^{-1})) * 53m = 5.26E\text{-}03$

$Q = \Delta sT/(0.183 \log(2.25Tt/(r^2 * S))) = 2662m * 5.08E\text{-}5\ m^2/s\ /(0.183 \log(2.25 * 5.08E\text{-}5\ m^2/s * 30 * 365.25 * 86400s/(1000^2 m * 5.26E\text{-}3))) = 2024.71\ m^3/h = 0.56\ m^3/s$

$P_T = Q * \rho w * Cw * \Delta T = 0.56\ m^3/s * 1000kg/m^3 * 3770\ J/kg\ ^oC * 20\ ^oC = 41.62\ MWt$

$P_E = ng * P_T = 10\% * 41.62 = 4.16\ MWe$

4.3.1 Comparison of potential from field data and hydraulic data within the Deadwood-Winnipeg reservoirs

The production rates estimated from hydraulic properties (maximum production rates) are generally higher than those of the field data (observed production rates) within the Deadwood-Winnipeg wells (Figure 4.10). Consequently, the estimated potential thermal power for the reservoir based on hydraulic properties and theoretical maximum production rates is higher. The question of "why?" will be answered in section 5.2. About 80% of the wells have pumping rates estimated from hydraulic properties between 1000 and 10000 m^3/h, with the capability of generating thermal power of above 10 MWt.

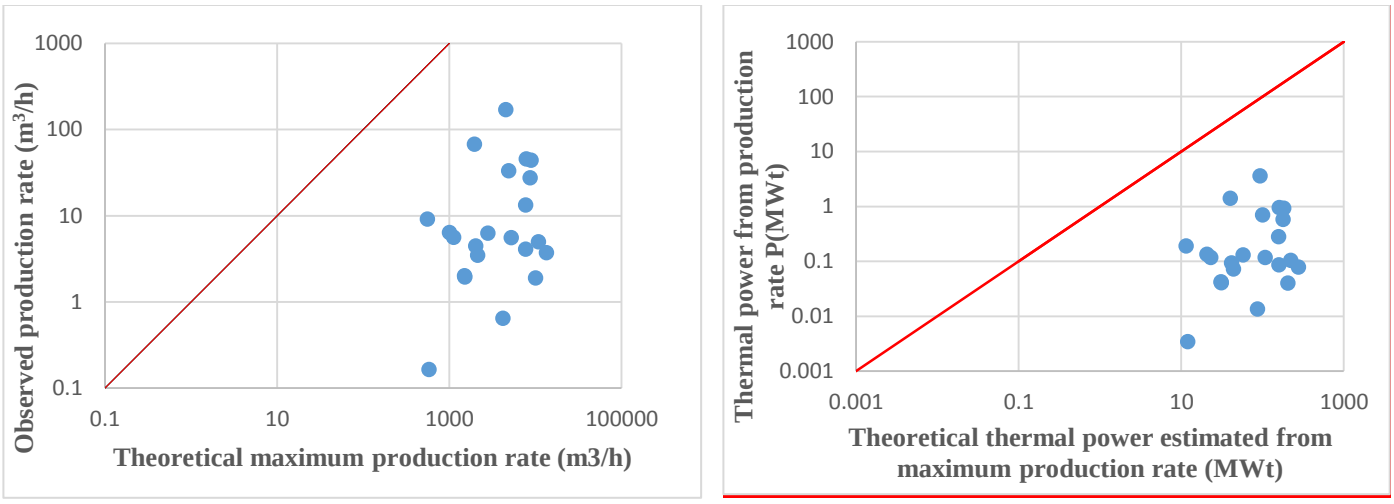

Figure 4.10 Comparison of observed and maximum production rate and thermal power values from field data and hydraulic data for Deadwood-Winnipeg reservoir

4.3.2 Comparison of calculated potential from field data and hydraulic data within the Red River-Yeoman reservoirs

The production rates and potential power derived from hydraulic properties of Red River-Yeoman reservoirs are also generally higher than those from field data, with more than half of the wells having theoretical production rates above 1000 m^3/h. The difference between the calculated and actual production rates is less than that observed for the Deadwood-Winnipeg reservoirs (Figure 4.11). Based on rates estimated from hydraulic properties about 85% of the wells can produce

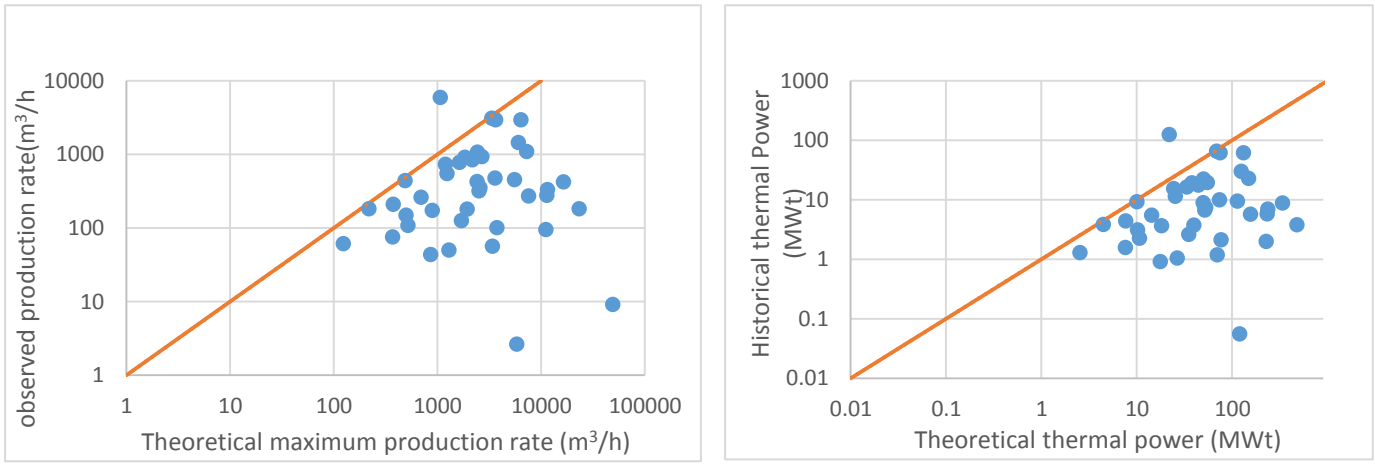

Figure 4.11 Comparison of observed and maximum production rate and thermal power values from field data and hydraulic data for Red River-Yeoman reservoir.

thermal power above 10 MWt, as shown in Figure 4.11. By comparison based on the field data about half of the wells can produce thermal power between 1 and 10 MWt.

4.4 Comparison of the pumping or production rates with Gringarten and Sauty Model

The properties of reservoirs under study are variable; therefore the effect of these variations was tested using the Gringarten & Sauty (1975) model. Various scenarios were considered by varying injection/production rate, reservoir thickness and porosity. Other parameters were kept constant. This provides a spacing constraint (1 km) used in the third method (rock thermal volume) to estimate the geothermal power within the block. The parameters used for this model are shown in Table 3.1.

The results from the analytical model discussed in section 2.1.2 show that the higher the injection/production rate the earlier the thermal cold front reaches the production well. In Figure 4.12 (a), for instance at the rate of 100 m^3/h (requiring a wellbore flowing pressure at least roughly 7 MPa) and constant thickness of 150 m, with a well separation distance of 500 m, the cold front will reach the production well at about 30 years. In comparison if the production/injection rate is as high as 350 m^3/h requiring a wellbore flowing pressure at least roughly 13 MPa), a separation distance of about 1 km is required for the reservoir lifetime of 30 years to be exceeded (Figure 4.12 (a)).

From the Gringarten and Sauty equation, the reservoir thickness affects the thermal breakthrough time as shown by Figure 4.12 (b). The thicker the reservoir the longer it takes for the cold front to arrive at the production well, therefore the lower the separation distance required for wells spacing. At an average thickness of 200 meters with a constant injection/production rate of 200 m^3/h (see Table 3.1), about 600 meters of separation distance is required between the wells for a sustainable reservoir life of up to 30 years.

The result of this analysis is consistent with the studies carried out by Gringarten and Sauty (1975), and Ferguson and Grasby (2014), which concluded that to achieve a reservoir with a lifetime of more than 30 years and produce at least 2 megawatts of electricity we need a reservoir with a thickness of 100 m, a temperature of 100^{o}C, an average injection/production rate of 80 m^3/h and a well separation distance of 900 – 1000 meters.

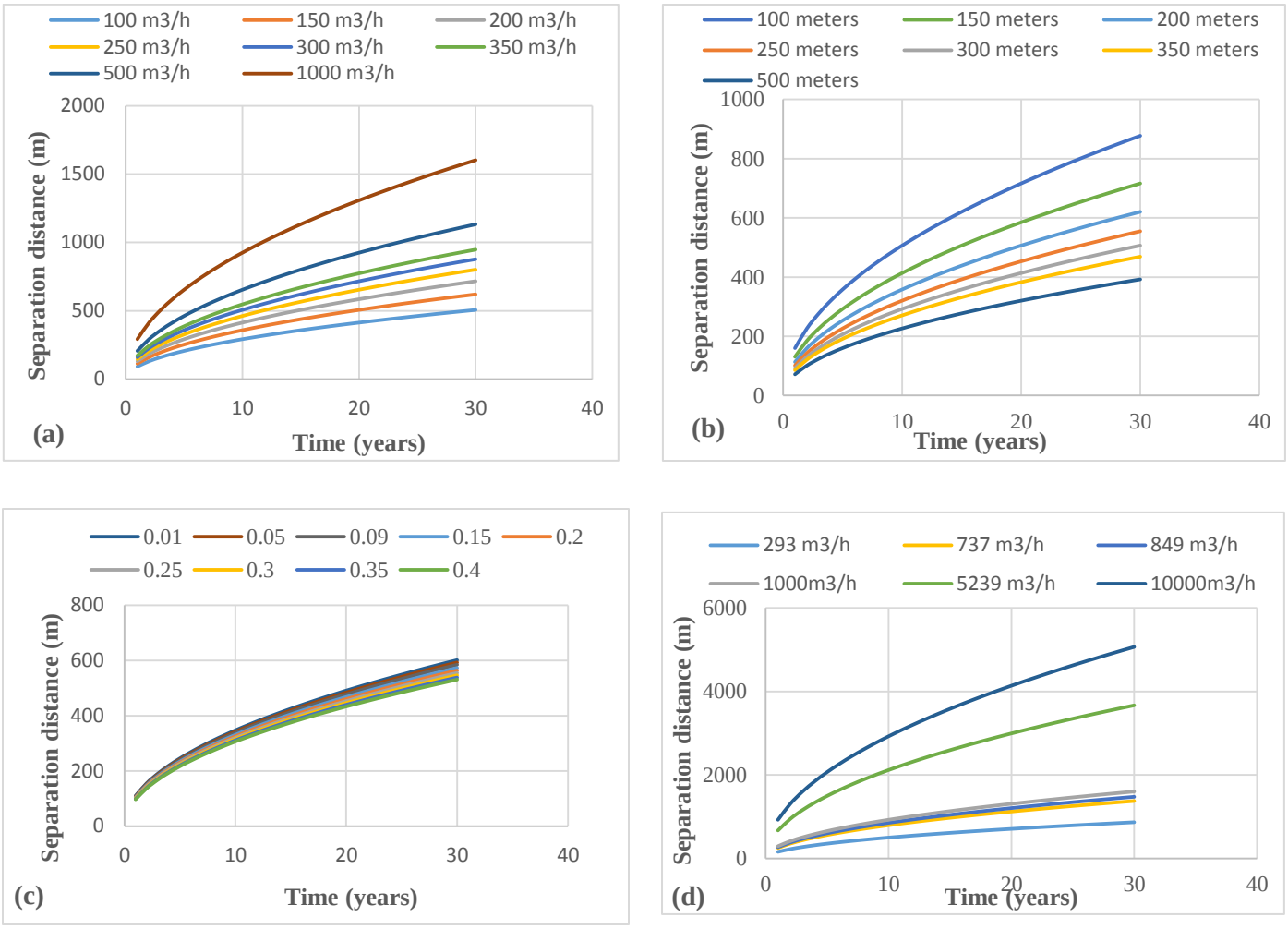

Figure 4.12 Effect of variation of (a) injection/production rates from Gringarten model, (b) reservoir thickness, (c) porosity, and (d) historical production/injection rates, on the relationship between well separation distance and the time at which breakthrough of the cold front occurs at the production well

The results also show that porosity has little to no effect in determining the sustainability of the doublet wells when all other parameters are held constant (Figure 4.12 (c)); i.e., by varying porosity from 1% – 40%, the well spacing remains within the range of 530 to 600 m. Petrophysical parameters such as permeability and porosity are important in determining the potential of a geothermal reservoir, even though porosity and permeability have little or no effect on the spacing of the wells they have significant effect on wellbore flowing pressure, therefore they cannot be neglected.

Using the results of the estimated production rates from production data, especially for Red River-Yeoman, it can be observed that the production rates up to about 1000 m^3/h (at least wellbore flowing pressure of about 23 MPa) will require well spacing in the range of 1-1.5 km to achieve a

reservoir lifetime of 30 years or more. With a very high and unusual production rate greater than 10000 m^3/h (at least wellbore flowing pressure of about 60 MPa), the injection well would need to be placed at large distance; i.e., greater than 5 km (Figure 4.12(d)).

This will not be economically viable and sustainable, because if placed at such distance, reservoir pressure would drop and so would the production rate and this can lead to a shorter reservoir lifetime. Also, an extraction of such magnitude can lead to subsidence and injection at such rate can result to hydraulic fracturing. Future research should therefore consider the effect of high production and injection rates on the reservoir. A high early production rate might result in rapid decline of production rate, especially if the injection well that recharges the reservoir is located at a great distance from the production well

4.5 Results from estimated pressure

As discussed in section 3.2.5, the wellbore flowing pressure (Pwf) required to sustain specified production/injection rate was estimated Table 4.2 shows the result of the estimate of selected wells based on the criteria discussed in section 3.2.5. The results show that the wellbore flowing pressure obtained for wells in Deadwood-Winnipeg and Red River-Yeoman reservoirs are sufficient to sustain the wells overtime. A sample calculation is shown below:

Sample Calculations for Injection Pressure using Well 131/08-16-006-11W2/0

$P = \rho g H$ = 1000 (kg/m^3) * 9.8 (m/s^2) * 2726 + (850-591.7) (m) = 29246140 Pa

$P_{wf} = P - \frac{Q\mu}{2\pi kh} \ln\frac{r/2}{r_w}$ = 29246140 (Pa) – ((0.0032 (m^3/s) * 6.81E-04(Pa.s))/2 *3.142 *8.12E-15 (m^2)*49(m))) * In (1000/2 (m)/0.15(m)) = 36315020Pa = 36.315 MPa

Table 4.2 Estimates of potential wellbore flowing pressures required to sustain the injection rates

Well ID	Reservoir Type	h (m)	k (m^2)	Q (m^3/s)	P (MPa)	Pwf (MPa)
131/08-16-006-11W2/0	Deadwood-Winnipeg	49	8.12E-15	0.0018	29.246	36.315
02/01-09-017-14W3/0	Deadwood-Winnipeg	173	1.00E-13	0.0037	20.406	20.409
141/08-22-008-13W2/0	Red River-Yeoman	18	6.35E-16	0.0171	26.052	21.132
101/03-20-002-16W2/0	Red River-Yeoman	381	8.78E-14	0.0025	31.556	31.558

However, when calculations were made using theoretical rates, some wells show unrealistically high pressures with values as high as 500 MPa for Deadwood-Winnipeg and values as high as1000 MPa for Red River-Yeoman. These kind of values could result to hydraulic fracturing because in this setting the in situ stress or minimum horizontal stress is 16-20 kPa/m Bell and Bachu (2003).

4.6 Potential power based on rock thermal properties of the reservoirs

The rock thermal properties are very important in determining the potential heat stored in the rock and the amount of geothermal electricity that can be generated from the reservoir. Though this might underestimate or overestimate the capacity of the reservoir, it gives an idea what might be achievable. Based on the kind of reservoir, in this study estimation was done with the available data and literature values for heat capacities. The Deadwood-Winnipeg reservoir is composed mainly of sandstone and bounded at the top by shale (caprock) and at the bottom by crystalline basement rock, while the Red River-Yeoman reservoir is dominantly carbonate rock overlain by Stony Mountain carbonate rocks and underlain by the shalely caprock as shown in Figure 4.13. These shalely units, with low thermal conductivity, can provide thermal insulation for both reservoirs, thereby maintaining high temperature at depth.

In this work, the assumed separation distance between the injection and production wells was 1 km (the same as that of Gringarten and Sauty, 1975), the width of influence was 2 km, and the maximum thicknesses for the reservoirs were 0.3 km for Deadwood-Winnipeg and 0.5 km for Red River-Yeoman. A rock density of 2700 Kg/m^3 was used for both reservoirs and an average heat capacity of 840 J/kg^{o}C for saturated porous sandstone was used for the Deadwood-Winnipeg and 851 J/kg^{o}C for limestone was used for the Red River-Yeoman in accordance with Eppelbaum et al. (2014). A reservoir temperature of 120^{o}C (maximum value from AccuMap) and ground surface temperature of 2^{o}C (Beltrami, 2003) were used. The potential thermal energy that can be extracted from reservoir of 0.3 km rock unit in a 2 km^2 area is calculated as follows:

$$Thermal\ Energy, H_G = \rho_s c_p V_B (T_A - T_0)$$

= (2700 kg/m^3) *(840 J/kg^{o}C) *(1km x 2km x 0.3km) *(120^{o}C-2^{o}C) = 1.61 10^{17} J

$$G_P = n_G \frac{H_G}{t_E}$$ = 0.1*1.62E+17/86400*365.25*30=16.96 MWe

As shown in Table 4.3, calculated potential thermal energies are about *161,000 TJ* for the Deadwood-Winnipeg reservoir and *271,000 TJ* for the Red River-Yeoman reservoir.

A sensitivity analysis was carried out to see how the width of influence affects the potential electric geothermal power using the Equations 2.13 and 2.15. The results are as shown in Figure 4.14, for scenarios where the well spacing of 1km and the reservoir thicknesses for Deadwood-Winnipeg and Red River-Yeoman, 0.3 and 0.5 km respectively were constant, but the width of influence changes using values of 2, 5, 7 and 10 km.

Table 4.3 Potential thermal energy that can be generated from the reservoirs based on rock thermal properties (*MWe – Megawatts electric – a measure of electric power generation. 1 equals 1 million watts or 1,000 kilowatts MWe).

Reservoir	**Reservoir thermal energy (J)**	**Potential Thermal Power (MWt)**	**Potential electric geothermal power (*MWe)**
Deadwood-Winnipeg	1.61×10^{17}	170	16.96
Red River-Yeoman	2.71×10^{17}	286	28.64

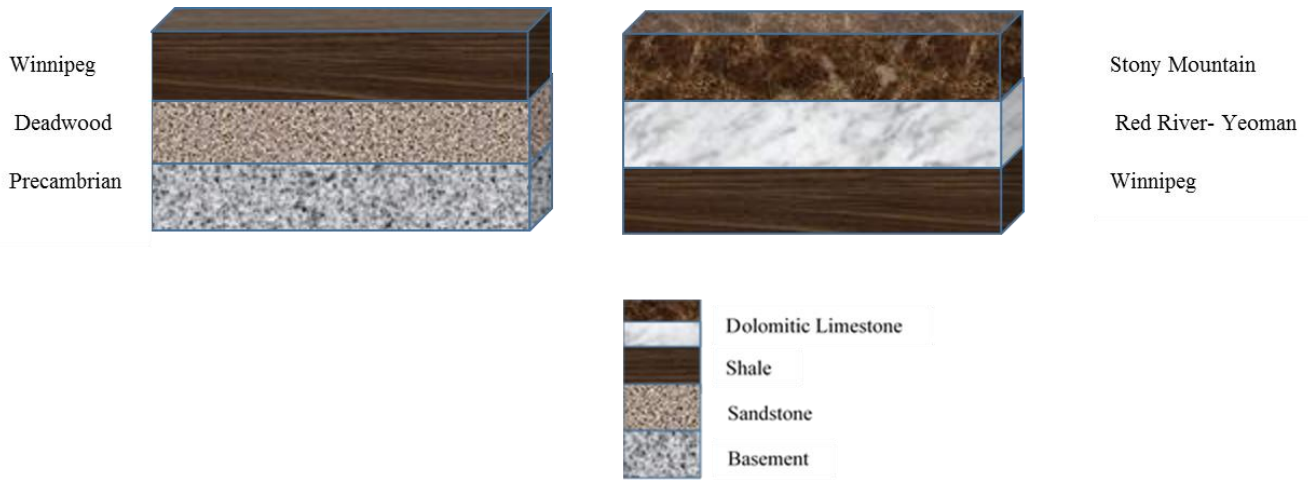

Figure 4.13 The lithology of Deadwood-Winnipeg and Red River-Yeoman reservoirs

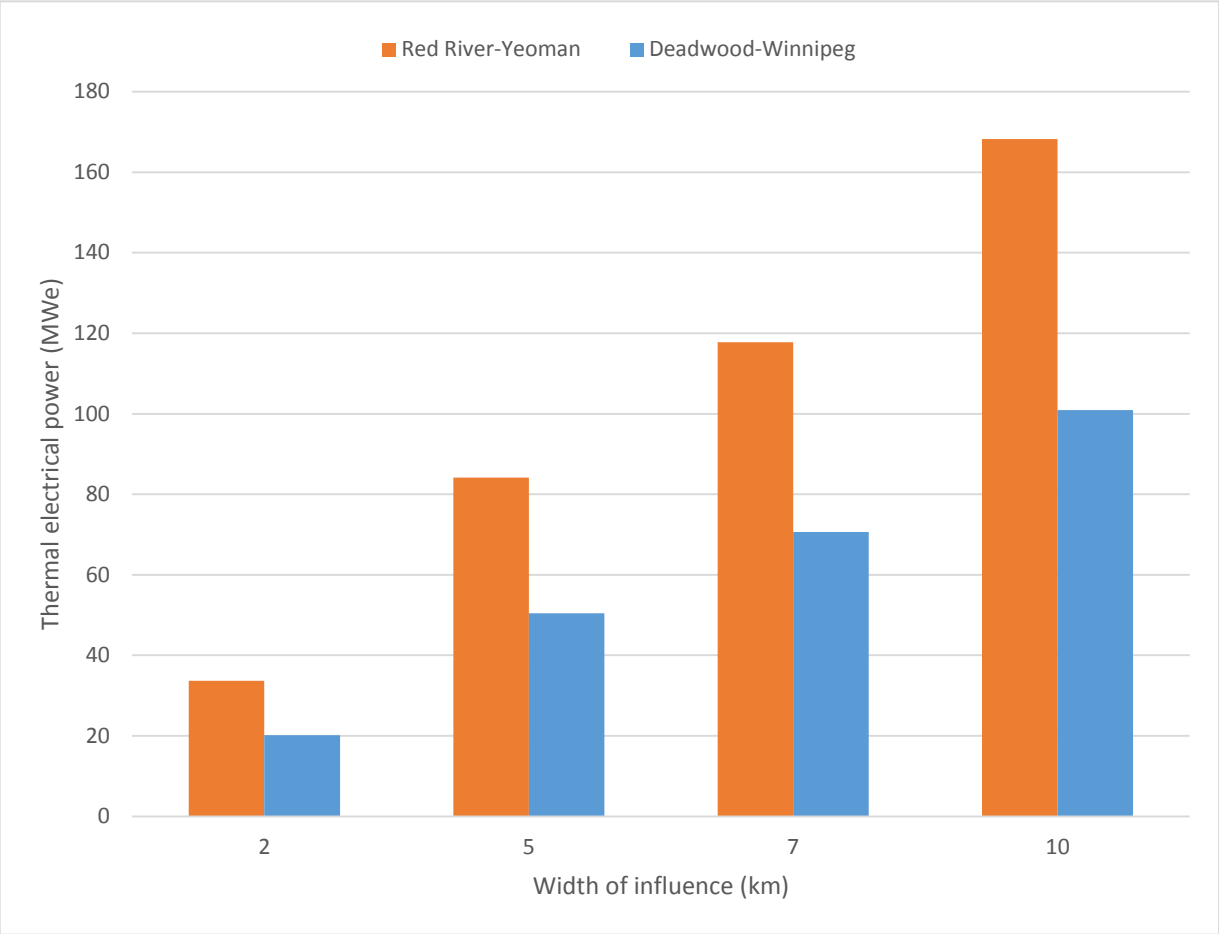

Figure 4.14 Sensitivity analysis for width influence on the reservoirs

As expected, the potential electric geothermal power is linearly dependent on width of influence.

4.7 Comparison of the results from three different methods

The average thermal power that can be generated from the reservoirs under study are shown in Table 4.4. For 10% conversion efficiency from thermal power to electrical power, the potential electrical power estimated from rock thermal volume (thermal properties) gives high values for both reservoirs; 17 MWe for Deadwood-Winnipeg and 29 MWe for Red River-Yeoman.

Provided the right temperature condition (80-150^{o}C) that can support a binary thermal power system exist, these thermal power values, irrespective of the method used, are sufficient to generate the required energy for direct purpose and/or electrical power generation (Table 4.4).

The implications of these results will be discussed in the Chapter 5.

Table 4.4 Average potential thermal energy per well that can be generated from the reservoirs based on observed production and injection rates, theoretical production rates and per block reservoir based on well spacing

Reservoirs	**Thermal power from production rates (MWt)**	**Thermal power from hydraulic properties (MWt)**	**Thermal power from rock thermal properties (MWt)**
Deadwood-Winnipeg	0.41(0.041 MWe)	101 (10.1 MWe)	170 (17.0 MWe)
Red River-Yeoman	10.07 (1.007 MWe)	105.4 (10.5 MWe)	286 (28.6 MWe)

5 DISCUSSION

The previous chapter presented and described the estimates of geothermal power within the deep reservoirs of the Williston Basin using three methods: estimation of geothermal power from observed pumping rates; from theoretical pumping rates; and from rock thermal volume.

This chapter attempts to interpret, analyze and explain the findings from this study. The first section compares the values from the sandstone and carbonates reservoirs and examines the geologic factors responsible for the differences of values obtained from the reservoirs. The second section compares the values from the three methods, examine possible factors responsible for the differences in the values obtained and critically evaluate the applicability of geothermal development within the Williston Basin. The final section discusses the potential within Saskatchewan with respect to temperature variations.

5.1 Geologic factors controlling production and injection rates

A feasible convectional geothermal system requires water, heat and permeability. Each of these factors should be considered while analyzing the geothermal potentials of the two reservoirs under study. The production rates are the major factor in this study that determines the geothermal power to be produced based on the first method. There are several factors affecting the rate of production and injection, the most important of these factors is rock type which controls rock properties such as permeability and porosity and further affects production and injection rates.

The reservoirs considered in this research are dominantly sandstone (Deadwood-Winnipeg) and carbonate (Red River-Yeoman) rocks. Based on the average results for the different methods shown in Table 4.4, the Red River-Yeoman reservoir shows higher estimated potential compared to Deadwood-Winnipeg due to its higher permeability, production rate and thickness.

The Red River-Yeoman pumping rates were generally high, which can be attributed to reservoir characteristics. For example, the core analysis summary report for the well with the maximum pumping rate within the Red River clearly noted that core from 2150 m depth is dolomitic limestone (about 70% dolomite) with vertical fracturing, intercrystalline porosity and vuggy porosity. As suggested by Murray (1960), dolomites typically have good reservoir quality. A 13% increment in porosity can occur due to dolomitization (Moore, 1989). Many studies within the

Williston basin also identified where dolomitization played a very important role in the good reservoir quality of the Red River-Yeoman (for example, Moore and Wade, 2013). There is also speculation that dolomite might have formed during burial at high temperature because of the hydrothermal fluids from Winnipeg or Deadwood sediments (Pak et al., 2001; Qing et al., 2001; Heinemann et al., 2005). This can be the reason for the high observed and theoretical production rates. A closer look at the core analysis summary reports of the low rate wells within Red River-Yeoman suggests that the rock units are intercalated dolomite and limestone, which are predominantly tight with poor matrix micro also known as porosity pinpoint porosity.

Similarly, the core analysis summary report for the highest rate production well within the Deadwood-Winnipeg reservoir shows that the core sample at the depth of about 2450 m is composed mainly of 50% sandstone with silica cement and glauconite grains, 40% sand, 5% of shale and 5% of pyrite with very good porosity and permeability. The presence of large amounts of shale is the predominant factor affecting low rate production wells, as shown by the core analysis summary reports from these wells, which show predominantly tight rock units with very poor pinpoint porosity. This shows that one of the main factors controlling production and injection rates are the reservoir characteristics (porosity and permeability). It is important to identify and concentrate on those areas with high productivity and avoid areas with low productivity in the exploration stage of geothermal energy. Alternatively, hydraulic fracturing can be used to enhance the hydraulic properties of areas with low porosity and permeability if the temperature of the reservoirs supports geothermal energy development.

It is also important to note that most of the wells in the Deadwood-Winnipeg were abandoned soon after drilling; therefore not much data was collected.

For the rock thermal volume method, the width of influence played a very important role in determining the geothermal heat that can be available; however, the width of influence may vary depending on the geologic condition of the reservoir. The volume of heat that can be extracted also depends on the porosity (primary, fracture and vuggy) and permeability, but these are not completely known, especially with theoretical production rate and rock thermal volume methods.

5.2 Differences in the estimation techniques

This research is focused on using three different techniques to estimate the potential geothermal electrical power that can be generated from the Deadwood-Winnipeg and Red River-Yeoman reservoirs of the Williston Basin. These include; estimation based on observed fluid rates, hydraulic properties, and rock thermal properties of the reservoirs (Table 5.1).

As summarized in Table 5.1, the major contributing factors for the differences in the results are; production rate for observed fluid rates, pressure change and permeability for hydraulic properties, and reservoir volume for the rock properties. Due to the limited data points available for the Deadwood-Winnipeg reservoir, conclusions cannot be made with respect to which reservoir has better prospects. However, the reasons for the variation with respect to different techniques can be examined. For instance, within the Deadwood-Winnipeg reservoir the average potential electrical power estimated from the observed fluid rates is 0.04 MWe, based on the theoretical production rates; 10.1 MWe and 34.2 MWe based on the rock thermal volume.

The first method gave the lowest set of values for the geothermal power that were generated per production well. The results are underestimated partly because the wells are not optimized for geothermal purposes since the interest is on hydrocarbon production and not coproduced fluids.

Table 5.1 Distinguishing factors of the different techniques used for this study

Techniques	**Influencing factors**	**Major contributing factors**
Observed production/injection rates (observed fluid rates)	Production rate, Pressure change, wellbore flowing pressure, formation pressure, temperature change, permeability, hydraulic conductivity, transmissivity, volumetric heat capacity, reservoir volume, operational factors (amount of water injected, water cut from oil wells, etc.)	Production rate
Theoretical production rate/Hydraulic properties	Heat capacity, pressure change, wellbore flowing pressure, formation pressure, temperature change, permeability, thickness, hydraulic conductivity, and transmissivity	Thickness and permeability
Rock thermal volume (thermal properties)	Volumetric heat capacity, reservoir volume and temperature change.	Reservoir volume

Conversely, the second method (using theoretical production rates) might be on a high side for some wells especially with the wide range of production/injection rates (100 to 40,000 m^3/h) and high wellbore flowing pressures. This appears favourable but is probably too high. Production/injection rates above 1000 m^3/h might not be sustainable if the injection well is placed at 1 Km as used for this study because this will lead to a faster thermal breakthrough and shorter reservoir lifetime of the geothermal plant. In this scenario, the well spacing would probably have to be much greater to avoid fast thermal breakthrough (Figure 4.12). Drawdown to the bottom of the well is also probably not a good idea due to subsidence issues, the potential to dewater overlying formations and logistical issues with setting equipment at the bottom of the well. Furthermore, wells do not really run for 24 hours; they are shut-down sometimes for maintenance or for recovery. When these constraints are factored-in, the predicted geothermal power values would be lower than projected. This can also account for the much lower values when compared to the first method. Therefore, the expected values might be somewhere between the higher values of the observed and the lower values per well for the theoretical production rates.

For the third method (using rock thermal volume), the sensitivity analysis conducted shows a much lower energy production value when the width of influence is 2 km and a much higher value when the width of influence is 10 km. The true width of influence is not really known but can be estimated using multiple-well tests such as interference and pulse tests. These tests can be used to determine reservoir properties between wells and establish links between the wells. Further, in accordance with MIT (2006), recovery factor ("percentage of heat recoverable from a stimulated volume of rock") should be considered. This parameter depends on the porosity (natural, fractured, and vuggy), permeability and heterogeneity of the reservoir. The MIT (2006) study used a recovery factor in the range of 2% - 20% for an enhanced geothermal system (EGS) reservoir; however, Satman and Türeyen (2012) applied a recovery factor of 32% for a doublet system within 30 years and 70% by the end of 72-year production period. When recovery factor is considered the geothermal electrical energy obtained from this study will be more reasonable. For instance, the Deadwood-Winnipeg geothermal electrical power of 17 MWe will be 5.44 MWe if a recovery factor of 32% (as used by Satman and Türeyen, 2012) for a doublet system within 30 years of production is applied. This result is comparable to the value obtained using the hydraulic

properties technique, but even if a recovery factor as low as 2% is applied, the value will still be higher than that obtained using observed production method.

It seem that the values of geothermal electrical power estimated using theoretical production rates and rock thermal volume are generally reasonable when these factors discussed above are considered, if other conditions of a good geothermal reservoir are favourable.

5.3 Potentials for direct use and electricity generation

Based on the factors considered in this study, there is a high potential for geothermal energy within the Williston Basin. However, one of the most important factors is temperature, and most of the wells within the Red River-Yeoman and Deadwood-Winnipeg reservoirs with high production rates have bottom-hole temperatures (BHTs) measurements below 100^{o}C (as shown in the previous chapter; see Figure 4.6). These BHT measurements may underestimate the actual temperature of the reservoir due to the interference of drilling mud. Therefore, based on this assumption the wells with high production rates located within the southern portion of Saskatchewan (including Regina, Swift Current, Weyburn and Estevan) are most probable for direct use purposes, which requires, temperatures above 50^{o}C (Milenić et al., 2010; Ferguson and Grasby 2014). Within the central and northern portion including (Saskatoon, Kindersley, Yorkton, Lloydminster) temperatures are below 50^{o}C and therefore direct use geothermal schemes might not be feasible.

Wells located within the southernmost portion of the map where BHTs range between 80^{o}C and greater than 100^{o}C, are most probable for geothermal electricity scheme, especially if the production rates and hydraulic properties of these wells are high.

6 CONCLUSION

6.1 Summary of findings and recommendation

Binary cycle geothermal plant technology capable of generating electricity from moderate temperature geothermal resources (80-150^{o}C) serves as the basis for this research was conducted. About 25 billion cubic meters of fluids of hot fluid have been produced and millions of cubic meters of fluids injected for several decades within the reservoirs of the Williston Basin. This thermal energy can be used for energy production purposes. This study sought to answer questions about the capability of this basin to generate sufficient thermal power for direct use and/or for electricity generation. Previous studies tended to focus on a more general approach in estimating the geothermal potential of the Williston Basin. However, this study focused on specific reservoirs (Deadwood-Winnipeg and Red River-Yeoman) within the Williston Basin, with the aim of estimating the thermal power that can be generated from these reservoirs using three different techniques as follow: observed production rates, theoretical production rates (hydraulic properties) and rock thermal volume (thermal properties) to answer the research question. The two reservoirs studied are sandstone (Deadwood-Winnipeg) and carbonate (Red River-Yeoman) reservoirs. The data used for this research were extracted from AccuMap and Geoscout database software. These data include summaries of production and injection histories, core analysis results, temperature, and pressure data.

The long-term production/injection rate for each hydrocarbon well studied within the afore-mentioned reservoirs was calculated from the water production/injection data reported in the hydrocarbon well's production/injection history data. These were entered into a simple thermal equation to estimate the thermal power that can be generated from each well within the reservoirs considered. The results show that, on average, each well within the Deadwood-Winnipeg reservoir and Red River-Yeoman reservoirs are capable of generating thermal power valued at 0.4 MWt and 10 MWt, respectively.

The hydraulic properties of the wells, which include transmissivity and storativity, were calculated from the core analysis data and literature values. The Cooper-Jacob empirical equation was then used to estimate the maximum possible values for production rates. The resulting production rates were compared to those used by the Gringarten and Sauty (1975) model.

Calculated production/injection rates above 1000 m^3/h might not be sustainable because the injection well would have to be placed at very large distance from the production well, otherwise faster thermal breakthrough will occur leading to shorter reservoir lifetime of the geothermal plant. These production values were used to estimate the potential power that can be generated from these reservoirs. The results show that, on average, the Deadwood-Winnipeg reservoir can generate thermal power of about 101 MWt and Red River-Yeoman can generate 105 MWt. These results may be overestimates considering the spacing constraint (1 km); however, if periods of shutdown for recovery and maintenance are factored into the equation, the result might be within a reasonable range. The factors that influenced these results are production rates, pressure and hydraulic conductivity values.

The final method estimated the geothermal power by calculating volumetric heat capacity of the geothermal reservoir with respect to the area of the reservoir between the production and injection wells, thermal properties and the thickness of the reservoir. The results show that, on average, the entire reservoir can generate higher geothermal power of about 170 MWt for Deadwood-Winnipeg and 286 MWt for the Red River-Yeoman reservoirs. The method overestimated the geothermal power that can be generated from the entire volume of the reservoir and the width of influence is not known; however, if a recovery factor is factored into the equation it gives values that are reasonable and comparable to those estimated from production/injection rates calculated using reservoir hydraulic properties.

Based on the findings of this research, there is potential thermal power for direct use purpose within the southern portion of Saskatchewan, especially at locations with temperatures above 50^{o}C. There is also potential for electricity generation purposes within the southern part which contains Swift Current, Estevan and Weyburn where temperatures are above 80^{o}C. Finally, the estimated potential power that can be generated from the deep Williston Basin reservoirs in Saskatchewan are between 0.4 MWt and 105 MWt per well. This energy capacity could be harnessed and used as we migrate from dependency on fossil fuel to clean energy technology. However, there are some challenges especially with the high start-up cost and transportation cost for getting power from dispersed remote locations to larger centers. More work needs to be done to demonstrate these findings.

6.2 Limitations of this research

This research has so far demonstrated that there is potential for geothermal power within the Saskatchewan portion of the Williston Basin for direct use (heating and cooling of buildings, agriculture, recreation etc.) and for electricity generation through different techniques. However, there are some major limitations to this study such as; the core data used for the estimating the theoretical production rates.

The average permeability values obtained from the well core data and used to estimate the hydraulic conductivity and transmissivity are sensitive to the production rate and may not be representative of the general reservoir characteristics and may not capture the heterogeneity of the reservoirs. Also, drawdown to the bottom of the well is probably not a good idea due to subsidence issues, the potential to dewater overlying formations, and logistical issues with setting equipment at the bottom of the well. Therefore, these might have impacted greatly on the very much high production rates obtained from hydraulic properties when compared to the field data.

6.3 Future research

The results from this research can form a base for future study. The maximum production rate calculated from the hydraulic properties might have been overestimated; therefore future research should look at ways to minimize this estimate by using direct analysis from DST data. More work needs to be done in terms of matching different permeability sources such as from laboratory core analysis, geophysical logs, and DST to see clearly if we are dealing with a homogenous or a heterogeneous reservoir and the effects this can have on the geothermal potential of the reservoirs studied. These can be achieved through a modelling approach or a pilot project.

To reduce the effect of these limitations, future research should consider a modelling approach to incorporate these measurements and simulate sustainability of the well over time based on different comparative analysis of hydraulic properties obtained. Furthermore, a pilot project for direct use application can be instituted and subsequently, components that can convert thermal power to electricity energy generation could be added. In-situ measurements can be carried out and operating data can be collected. These measurements and data can then be used to validate the model.

Future studies should also consider using those wells already identified as having high geothermal potential with temperatures above 80^{o}C, which are no longer producing hydrocarbon, for a pilot geothermal project for direct use and/or electricity generation to demonstrate the geothermal potential of Williston Basin. The data generated from the pilot project can be used to predict the reservoir lifetime of the scheme using a modelling approach, and at the same time serve as source of thermal power for direct use purpose or for electricity generation for the host community.

REFERENCES

Bachu, S. (1993). Basement Heat Flow in the Western Canada Sedimentary Basin. Tectonophysics, 222 (1993) 119-133, Elsevier Science Publishers B.V., Amsterdam

Bachu, S. and Hitchon, B. (1996). Regional-Scale Flow of Formation Waters in the Williston Basin. AAPG Bulletin, V. 80, No. 2 (February 1996), P. 248–264.

Bachu, S. (1995). Synthesis and model of formation-water flow in the Alberta Basin, Canada: AAPG Bulletin, v. 79, P. 1159–1178.

Bachu, S. and Burwash, R.A. (1994). Geothermal Regime in Western Canada Sedimentary Basin; *in* Geological Atlas of the Western Canada Sedimentary Basin, G.D. Mossop and I. Shetsen (comp.), Canadian Society of Petroleum Geologists and Alberta Research Council, Chapter 30 http://www.ags.gov.ab.ca/publications/wcsb_atlas/a_ch03/ch_03.html, [March, 2015]

Bear, J. (1972). *Dynamics of Fluids in Porous Media*. Dover Publications. ISBN 0-486-65675-6.

Bedre, M.G. and Anderson, B.J. (2012). Sensitivity Analysis of Low-Temperature Geothermal Reservoirs: Effect of Reservoir Parameters on the Direct Use of Geothermal Energy. GRC Transactions, Vol. 36, 2012.

Bekele, E.B., Person M.A., Rostron B.J., and Barnes R. (2002). Modeling secondary oil migration with core-scale data: Viking Formation, Alberta Basin. American Association of Petroleum Geologists. Manuscript received November 23, 1998; revised manuscript received October 3, 2000; final acceptance March 8, 2001.

Beltrami H., Gosselin C., and Mareschal, J. C. (2003). Ground sur face temperatures in Canada: Spatial and temporal variability. Geophysical Research Letters, Vol. 30, NO. 10, 1499, P. 3.

Benn, A.A. and Rostron, B.J. (1998). Regional hydrochemistry of Cambrian to Devonian aquifers in the Williston basin, Canada–U.S.A; in Christopher, J.E., Gilboy, C.F., Paterson, D.F., and Bend, S.L. (eds.), Eighth International Williston Basin Symposium, Sask. Geol. Soc., Spec. Publ. No. 13, p238-246.

Betcher, B., Grove, G., and Pupp, C. (1995). Groundwater in Manitoba: Hydrogeology, Quality Concerns, Management. Environment Canada, National Hydrology Research Institute, NHRI Contribution No. CS-93017.

Betcher, R.N. (1986). "Regional Hydrogeology of the Winnipeg Formation in Manitoba." Presented at Third Canadian Hydrogeology Conference, Saskatoon, SK.

Bredehoeft, J. D. (1965). The drillstem test: the petroleum industries deep well pump test. Ground Water, vol. 3, P. 31-36.

Bundschuh, J. and Suárez-Arriaga, M.C (2010). Introduction to the Numerical Modeling of Groundwater and Geothermal Systems - Fundamentals of Mass, Energy and Solute Transport in Poroelastic Rocks. Taylor & Francis Group, P.479.

CanGEA (2013). Canadian Geothermal Projects Overview 2013. CanGEA Calagary, www.cangea.ca.

Chevalier, S. and Banton, O. (1999). Modeling of heat transfer with the random walk method Part 1: application to thermal energy storage in porous aquifers, Journal of Hydrology, 222: 129-139.

Clark SP Jr (Ed.) (1966). Handbook of physical constants (revised edition). Geological Society of America. Memoir 97, Washington, DC.

Curtice, R. J. and E. D. Dalrymple. 2004. "Just the cost of doing business." World Oil pp. 7778.

Dake, L.P. (2001). Fundamentals of Reservoir Engineering. Elsevier, New York, P.443.

Dickson, Mary and Mario Fanelli. (2004). 'What is Geothermal Energy?' Prepared February 2004 for the International Geothermal Association. Accessed April 1, 2015. http://www.geothermal-energy.org/314,what_is_geothermal_energy.html

DiPippo, R. (2014). Second Law Assessment of Binary Plants for Power Generation from Low-Temperature Geothermal Fluids, Geothermics, V. 33, 2004, P. 565_586.

Duffield, W.A., and Sass, J.H., 2003. Geothermal Energy – Clean Power from the Earth's Heat. US department of the interior, USGS C1249. 36pp.

Eppelbaum L., Kutasov, I., and Pilchin, A. (2014). Applied Geothermics, Lecture Notes in Earth System Sciences, DOI: 10.1007/978-3-642-34023-9_2, Springer-Verlag Berlin Heidelberg. P. 106

ETB (2011). The engineering toolbox. Solids: specific heat capacities. http://www.engineeringtoolbox.com/

Ferguson, G. (2015). Deep Injection of Waste Water in the Western Canada Sedimentary Basin. Groundwater, 53: 187–194. doi: 10.1111/gwat.12198.

Ferguson, G. and Grasby S.E. (2014). The geothermal potential of the basal clastics of Saskatchewan, Canada. Hydrogeology J 22(1): P. 143–150

Ferguson, A.G., Betcher, R. N., and Grasby (2007). Hydrogeology of the Winnipeg Formation in Manitoba, Canada. Hydrogeology Journal 15: 573–587.

Fetter, C.W. (2001). Applied Hydrogeology (4th edn). Prentice-Hall, Engle-wood Cliffs, NJ, 598.

Freeze, R.A., and Cherry, J.A. (1979). Groundwater: Englewood Cliffs, NJ, Prentice-Hall, 604.

Fridleifsson, I.B., R. Bertani, E. Huenges, J. W. Lund, A. Ragnarsson, and L. Rybach (2008). The possible role and contribution of geothermal energy to the mitigation of climate change. In: O. Hohmeyer and T. Trittin (Eds.) IPCC Scoping Meeting on Renewable Energy Sources, Proceedings, Luebeck, Germany, 20-25 January 2008, 59-80.

Gong B., Liang H., Xin S. and Li K. (2011). Effect of Water Injection on Reservoir temperature during power generation in oil fields. PROCEEDINGS, Thirty-Sixth Workshop on Geothermal Reservoir Engineering Stanford University, Stanford, California, January 31 - February 2, 2011 SGP-TR-191.

Gosnold, W.D., McDonald, M.R., Klenner, R., and Merriam, D., 2012. Thermostratigraphy of the Williston Basin: GRC Transactions, v. 36, 663-670.

Gosnold, W., LeFever, R., Mann, M., Klenner, R., and Salehfar, H. (2010). EGS potential in the midcontinent of North America, GRC Transactions, V. 34.

Grasby, S.E., Allen, D.M., Bell, S., Chen, Z., Ferguson, G., Jessop, A., Kelman, M., Ko, M., Majorowicz, J., Moore, M., Raymond, J., and Therrien, R., (2012). Geothermal Energy Resource Potential of Canada, Geological Survey of Canada, Open File 6914 (revised).

Grasby, S.E., J. Majorowicz, & M. Ko. (2009). Geothermal maps of Canada. Natural Resources Canada, Geological Survey of Canada, Ottawa, Ont. Geological Survey of Canada Open File 6167.

Grasby SE and Chen Z (2005). Subglacial recharge into the Western Canada Sedimentary Basin—Impact of Pleistocene glaciation on basin hydrodynamics. *GSA Bulletin*; March/April 2005; V. 117; no. 3/4; P. 500–514;

Grasby, S.E., and Betcher, R. (2002). Regional hydrochemistry of the carbonate rock aquifer, southern Manitoba: Canadian Journal of Earth Sciences, V. 39, P. 1053–1063, doi: 10.1139/E02-021.

Gringarten A.C., Sauty J.P (1975). A theoretical study of heat extraction from aquifers with uniform regional flow. J Geophys Res 80(35):4956–4962.

Heinemann, K.A., Qing, H., and Bend, S. (2005). Preliminary results of organic matter analyses, Yeoman Formation (Red River), Saskatchewan: Implications for biozones and dolomitization patterns; in Summary of Investigations 2005, Volume 1, Saskatchewan Geological Survey, Sask. Industry and Resources, Misc. Rep. 2005-4.1, CD-ROM, Paper A-6, P.9.

Hitchon, B., Friedman, I. (1969). Geochemistry and origin of formation waters in the Western Canada Sedimentary Basin—I. Stable isotopes of hydrogen and oxygen. Geochim. Cosmochim. Acta 33, 1321–1349.

Hutchence K, Weston JH, Law AG, Vigrass LW and Jones FW (1986). Modeling of a liquid phase geothermal doublet system at Regina, Saskatchewan, Canada. Water Resour Res 22(10):1469. doi:10.1029/WR022i010p01469

Iampen, H.T. and Rostron B. J. (2000). Hydrogeochemistry of pre-Mississippian brines, Williston Basin, Canada–USA. Journal of Geochemical Exploration 69–70 (2000) 29–35 Elsevier Science B.V. P. 34

Jessop, A.M. and Vigrass, L.W. (1989). Geothermal measurements in a deep well in Regina, Saskatchewan; J. Volcanol. Geotherm. Resear. v37, no2, p151-166.

Jessop, A.M., Ghomeshei, M.M., and Drury, M. (1991). Geothermal Energy in Canada: Geothermics, v. 20, no. 5/6, P. 369-385.

Jones F. (2010). The Thermal State of the Williston Basin in Canada. Saskatchewan GS 2010 - Sixth International Symposium, P. 1-6.

Jones F. (1991). The thermal state of the Williston Basin in Canada. 6th Int. Williston Basin Symp. ed J E Christopher and F M Haidl (Saskatchewan Geological Society Special Publication no 11) (Regina: Saskatchewan Geological Society) P. 216–21

Kaplan, U (2007). Organic Rankine Cycle Configurations. Proceedings European Geothermal Congress Unterhaching, Germany.

Kent D.M and Christopher J.E (1994). Geological History of the Williston Basin & Sweetgrass Arch; *in* Geological Atlas of the Western Canada Sedimentary Basin, G.D. Mossop and I. Shetsen (comp.), Canadian Society of Petroleum Geologists and Alberta Research Council, http://www.ags.gov.ab.ca/publications/wcsb_atlas/atlas.html, Ch. 27 [2015].

Kestin, J., Ezzat Khalifa, H., Correia, R.J., 1981. Tables of the dynamics and kinematics viscosity of aqueous NaCl solutions in the temperature range 20–150 Celsius and the pressure range 0.1–35 MPa. Journal of Physical Chemistry 10 (1), P. 79–80.

Kreis L.K, Haidl F.M, Nimegeers A.R et al (2004). Lower Paleozoic map series: Saskatchewan. Saskatchewan Industry and Resources, Regina, SK, P.56.

Lengyel T (2013). Geothermics of the Phanerozoic strata of Saskatchewan. University of Alberta, Department of Earth and Atmospheric Sciences, M.Sc. Thesis.

Lippmann, M.J, and Tsang, C.F (1980). Ground-Water Use for Cooling: Associated Aquifer Temperature Changes. Ground Water, 18 (5) 452– 458.

Majorowicz, J. and Grasby, S.E. (2010). Heat flow, depth–temperature variations and stored thermal energy for enhanced geothermal systems in Canada. Journal of Geophysics and Engineering, Volume 7, Number 3, P. 233-242.

Majorowicz J.A., Garven G., Jessop A., Jessop C. (1999). Present heat flow along a profile across the western Canada Sedimentary Basin: the extent of hydrodynamic influence. Geothermics in basin analysis. Springer, Berlin, P. 61–79.

Majorowicz, J.A., Jones, F.W., and Jessop, A.M. (1986). Geothermics of the Williston Basin in Canada in relation to hydrodynamics and hydrocarbon occurrences. Geophysics, V. 51(3), P. 767-779.

Massachusetts Institute of Technology (2006). The Future of Geothermal Energy. Web. 23 August 2016. http://energy.mit.edu/wp-content/uploads/2006/11/MITEI-The-Future-of-Geothermal-Energy.pdf

McKenna, J., and Blackwell D. (2005). Geothermal electric power from Texas hydrocarbon fields: GRC Bulletin, v. 34/3, p. 121-128.

McKenna, J., Blackwell, D., and Moyes, C. (2005). "Geothermal Electric Power Supply Possible from Gulf Coast, Midcontinent Oil Field Waters", Oil and Gas Journal, September 5, 2005. P. 34-40.

Milenić D, Vasiljević P, Vranješ A (2010). Criteria for use of groundwater as renewable energy source in geothermal heat pump systems for building heating/cooling purposes. Energ Buildings 42(5):649–657. doi:10.1016/j.enbuild.2009.11.002.

Moore, C.H. (1989). Carbonate Diagenesis and Porosity: Elsevier Publ. Co., Developments in Sedimentology 46, P.338.

Moore, C. H., & Wade, W. J. (2013). Carbonate reservoirs: porosity and diagenesis in a sequence stratigraphic framework (Second edition). Amsterdam, Netherlands: Elsevier, 1-392.

Murray, R. C. (1960). Origin of porosity in carbonate rocks: Jour. Sed. Petrology, v. 30, p. 59-84.

Norford B.S., Haidl F.M., Besyz R.K., et al (1994). Middle Ordovician to Lower Devonian strata of the Western Canada Sedimentary Basin; *in* Geological Atlas of the Western Canada Sedimentary Basin, G.D. Mossop and I. Shetsen (comp.), CSPE and Alberta Research Council, chapter 9. http://www.ags.gov.ab.ca/publications/wcsb_atlas/atlas.html, [2015].

Okulitch, A.V. (2004). Geological Time Chart, 2004; Geological Survey of Canada, Open

File 3040 (National Earth Science Series, Geological Atlas) – REVISION http://www.er.gov.sk.ca/stratchart

Pak, R., Pemberton, S.G., and Gingras, M.K. (2001). Reservoir characterization of burrow-mottled carbonates: The Yeoman Formation of southern Saskatchewan – preliminary report; *in* Summary of Investigations 2001, Volume 1, Saskatchewan Geological Survey, Sask. Energy Mines, Misc. Rep. 2001-4.1, p10-13.

Palombi, D. and Rostron, B. (2010). Regional Hydrogeological Characterization in the Northeastern Margin of the Williston Basin, Saskatchewan-Manitoba, Canada. AAPG Search and Discovery Article #90172 © CSPG/CSEG/CWLS GeoConvention 2010, Calgary, Alberta, Canada, May 10-14, 2010.

Paterson, D.F. (1988). Review of regional stratigraphy relationships of the Winnipeg Group (Ordovician), the Deadwood Formation (Cambro-Ordovician) and underlying strata in Saskatchewan. In: L.P. Beck, ed., Summary of Investigations 1988, Saskatchewan Geological Survey, p.224-225.

Peterson, J. A. and MacCary, L. M. (1987): Regional stratigraphy and general petroleum geology of the U.S. Portion of the Williston Basin and adjacent areas. *In:* Peterson, J. A., Kent, D. M., Anderson, S. B., Pilatzke, R. H., and Longman, M. W. (eds.): Williston Basin: Anatomy of a Cratonic Oil Province. Rocky Mountain Association of Geologists, Denver, CO, P. 9-44.

Qing, H., Kent, D., and Bend, S. (2001). Preliminary results of isotopic geochemistry of Ordovician Red River carbonates, subsurface of southeastern Saskatchewan: Implication for process of dolomitization and diagenetic modification of dolomites: in Summary of Investigations 2001, Saskatchewan Geological Survey, Sask. Energy Mines, V.1, P. 1-9.

Satman A. and Türeyen O.I. (2012). Sustainability Factors for Doublets and Conventional Geothermal Systems. PROCEEDINGS, Thirty-Seventh Workshop on Geothermal Reservoir Engineering Stanford University, Stanford, California, January 30-February 1, 2012 SGP-TR-194

Singhal, B.B.S., and Gupta R.P. (2010). Applied Hydrogeology of Fractured Rocks Second Edition. DOI 10.1007/978-90-481-8799-7 Springer Dordrecht Heidelberg London New York. Chap. 8 and 18.

Slind O.L, Andrews G.D, Murray D.L et al (1994). Middle Cambrian to Lower Ordovician strata of the Western Canada Sedimentary Basin. In: Mossop GD, Shetsen I (eds) Geological atlas of the Western Canada Sedimentary Basin. Canadian Society of Petroleum Geologists/Alberta Research Council, Calgary, AB, P. 87–108

Tanguay, H.L. and Friedman, G.M. (2001). Petrophysical facies of the Ordovician red river formation, Williston Basin, U.S.A. Carbonates Evaporites 16, 71e92.

Tester, J.W, Blackwell D, Petty S, Richards M, Moore M.C, Anderson B, Livesay B, Augustine C, DiPippo R, Nichols K, Veatch R, Drake E, Toksoz N, Baria R, Batchelor A.S, Garnish J. (2006). The future of geothermal energy: impact of enhanced geothermal systems (EGS) on the United States in the 21st Century. Massachusetts Institute of Technology, Boston, MA, P.372.

Tobler, W (1979). A Transformational View of Cartography. The American Cartographer, 6, 101-106.

Vigrass L.W, Jessop A.M, Brunskill, B (2007). Regina geothermal project. In: Summary of investigations. Saskatchewan Geological Survey, Regina, SK, P. A–2

Vigrass L.W (1971). Depositional framework of the Winnipeg Formation in Manitoba and eastern Saskatchewan. In: Geological Association of Canada Special Paper no. 9, GAC, St. John's, NL, P. 225–234.

Weides, S., and Majorowicz, J. (2014). Implications of spatial variability in heat flow for geothermal resource evaluation in large foreland basins: the case of the Western Canada Sedimentary Basin. Energies 7(4), 2573-2594.

Wellmann, J.F., Horowitz, F.G., Schill, E. and Regenauer-Lieb, K. (2010). Towards incorporating uncertainty of structural data in 3D geological inversion. Tectonophysics 490 (3-4) 141–151.

Wright G.N., McMechan M.E., and Potter D.E.G. (1994). Structure and Architecture of the Western Canada Sedimentary Basin; *in* Geological Atlas of the Western Canada Sedimentary Basin, G.D. Mossop and I. Shetsen (comp.), Canadian Society of Petroleum Geologists and Alberta Research Council, http://www.ags.gov.ab.ca/publications/wcsb_atlas/a_ch03/ch_03.html, [March, 2015].

APPENDIX A. GEOTHERMAL POWER CALCULATION USING OBSERVED RATES FOR DEADWOOD-WINNIPEG WELLS

Sample Calculations using Well 141/08-14-006-06W2/0

Q = Cum. Water Produced/Cum. Prod. hrs = 106.3/24 =4.43 (m^3/h) = 0.0012 (m^3/s)
$P_T=Q^* \rho_w^* C_w^* \Delta T$ = 0.0012 (m^3/s) *1000(kg/m^3) *3770 (J/kg^{o}C) *(20^{o}C) = 0.0927 MWt
$P_E=n_g^* P_T$ =10%* 0.0927 = 0.01 MWe

UWI	Producing Zone	*Prod Hours*	*Cum Water (m3)*	X (m)	Q (m3/h)	P_T (MWt)	P_E (MWe)
141/08-14-006-06W2/0	WINNIPEG	24	106	2662	4.43	0.09	0.01
131/08-16-006-11W2/0	WINNIPEG	13218	84281	2738	6.38	0.13	0.01
192/09-20-006-11W2/2	WINNIPEG	456	20080	2708	44.04	0.92	0.09
111/16-20-006-11W2/0	WINNIPEG	674	1303	2719	1.93	0.04	0.00
142/04-35-006-11W2/2	WINNIPEG	238	1182	2715	4.97	0.10	0.01
111/11-16-007-07W2/0	WINNIPEG	152	949	2636	6.25	0.13	0.01
131/14-13-007-10W2/2	WINNIPEG	72	12	2672	0.16	0.00	0.00
131/11-14-007-10W2/0	WINNIPEG	624	2555	2673	4.09	0.09	0.01
113/04-02-007-11W2/0	WINNIPEG	72	46	2702	0.64	0.01	0.00
141/12-01-010-09W2/0	WINNIPEG	722	2500	2439	3.46	0.07	0.01
142/12-01-010-09W2/0	WINNIPEG	404	11107	2465	27.49	0.58	0.06
132/07-02-010-09W2/0	WINNIPEG	532	35764	2442	67.23	1.41	0.14
141/07-28-010-10W2/0	WINNIPEG	456	865	2435	1.90	0.04	0.00
191/08-06-010-15W2/0	WINNIPEG	33	5621	2474	170.34	3.57	0.36
141/14-32-009-09W2/3	WINNIPEG	672	22353	2520	33.26	0.70	0.07
111/11-03-017-14W3/0	DEADWOOD	264	528	2079	2.00	0.04	0.00
121/07-09-017-14W3/0	DEADWOOD	744	6763	2020	9.09	0.19	0.02
101/03-10-017-14W3/0	DEADWOOD	744	4141	2054	5.57	0.12	0.01
121/12-03-031-20W3/0	DEADWOOD	42049	1912024	2178	45.47	0.95	0.10
23/09-06-010-15W2/0	WINNIPEG	6320	23493	2497	3.72	0.08	0.01
02/01-09-017-14W3/0	DEADWOOD	81672	9870	2050	0.12	0.00	0.00
142/04-35-006-11W2/2	WINNIPEG	238	1182	2750	4.96	0.10	0.01
111/07-04-005-07W2/2	INTERLK	524	2939	2850	5.61	0.12	0.01

APPENDIX B. GEOTHERMAL POWER CALCULATION USING OBSERVED RATES FOR RED RIVER-YEOMAN WELLS

Sample Calculations using Well 101/01-14-001-17W2/0

Q = Cum. Water Produced/Cum. Prod. hrs = 78305/432 =181.26 (m3/hr) = 0.05(m3/s)
$P_T = Q^* \rho w^* Cw^* \Delta T =$ 0.05 (m3/s) *1000(kg/m3) *3770 (J/kg^{o}C) *(20^{o}C) = 3.80 MWt
$P_E = n_g * P_T$ =10%* 3.8 = 0.38 MWe

UWI	Producing Zone	*Prod Hours*	*Cum Water (m3)*	X (m)	Q (m3/h)	P_T (MWt)	P_E (MWe)
101/01-14-001-17W2/0	YEOMAN	432	78305	3112	181.26	3.80	0.38
101/03-20-002-16W2/0	REDRV	120	1096	3156	9.13	0.19	0.02
111/04-22-003-15W2/0	YEOMAN	48	4850	3073	101.03	2.12	0.21
131/06-02-003-21W2/0	YEOMAN	269	20203	2923	75.10	1.57	0.16
101/15-02-003-21W2/0	YEOMAN	96	281866	2862	2936.11	61.50	6.15
111/13-08-003-21W2/0	REDRV, YEOMAN	720	194789	2800	270.54	5.67	0.57
101/03-17-003-21W2/0	YEOMAN	744	813008	2858	1092.75	22.89	2.29
191/05-17-003-21W2/0	REDRV	316	932164	2790	2949.89	61.78	6.18
101/01-18-003-21W2/0	YEOMAN	120	39921	2791	332.67	6.97	0.70
192/05-25-003-21W2/0	REDRV	712	76832	2773	107.91	2.26	0.23
111/07-25-003-21W2/0	REDRV	72	4056	2787	56.34	1.18	0.12
131/08-14-004-07W2/2	REDRV, YEOMAN	202	179311	2895	887.68	18.59	1.86
121/08-22-004-07W2/0	YEOMAN	504	26186	2908	51.96	1.09	0.11
191/16-02-004-21W2/2	REDRV	711	267052	2800	375.60	7.87	0.79
141/10-30-004-21W2/2	YEOMAN	708	492893	2921	696.18	14.58	1.46
121/13-24-005-05W2/0	YEOMAN	498	4845	2786	9.73	0.20	0.02
111/07-04-005-07W2/0	REDRV	309	258834	2850	837.65	17.54	1.75
121/15-05-005-07W2/2	REDRV	24	50153	2838	2089.69	43.77	4.38
192/02-09-006-05W2/0	REDRV	128	20105	2658	157.07	3.29	0.33
101/09-02-006-06W2/0	REDRV	24	21865	2590	911.06	19.08	1.91
141/08-14-006-06W2/2	YEOMAN	514	4048	2662	7.87	0.16	0.02
191/16-29-006-06W2/0	YEOMAN	108	155309	2471	1438.04	30.12	3.01
101/09-01-006-11W2/0	YEOMAN	478	5728	2750	11.98	0.25	0.03
131/14-12-006-11W2/2	REDRV	600	7847	2761	13.08	0.27	0.03
131/03-14-006-11W2/0	REDRV	600	11641	2728	19.40	0.41	0.04
192/11-15-006-11W2/0	YEOMAN	720	198714	2616	275.99	5.78	0.58

192/08-16-006-11W2/0	YEOMAN	620	280406	2607	452.27	9.47	0.95
121/10-16-006-11W2/2	REDRV	241	22688	2747	94.14	1.97	0.20
191/09-20-006-11W2/2	REDRV	648	175830	2586	271.34	5.68	0.57
191/12-21-006-11W2/0	YEOMAN	504	250134	2898	496.30	10.39	1.04
111/14-26-006-11W2/0	YEOMAN	475	9609	2711	20.23	0.42	0.04
121/07-29-006-11W2/0	YEOMAN	646	1701	2809	2.63	0.06	0.01
141/10-29-006-11W2/0	YEOMAN	312	56017	2820	179.54	3.76	0.38
111/15-34-006-11W2/0	YEOMAN	449	37723	2747	84.02	1.76	0.18
191/16-34-006-11W2/0	REDRV	507	22122	2576	43.63	0.91	0.09
141/04-35-006-11W2/0	YEOMAN	142	298666	2750	2103.28	44.05	4.41
131/11-35-006-11W2/0	REDRV, YEOMAN	408	65150	2743	159.68	3.34	0.33
101/01-05-006-19W2/0	YEOMAN	72	43266	2953	600.91	12.59	1.26
141/06-05-006-19W2/0	REDRV	64	706	2841	11.03	0.23	0.02
111/15-04-007-10W2/0	REDRV	498	119992	2750	240.95	5.05	0.50
131/14-13-007-10W2/0	YEOMAN	48	35086	2552	730.95	15.31	1.53
131/11-14-007-10W2/2	YEOMAN	720	107277	2674	149.00	3.12	0.31
191/05-02-007-11W2/0	YEOMAN	720	189798	2568	263.61	5.52	0.55
101/12-02-007-11W2/0	YEOMAN	720	303633	2752	421.71	8.83	0.88
121/16-03-007-11W2/0	YEOMAN	288	564376	2709	1959.64	41.04	4.10
141/02-10-007-11W2/0	YEOMAN	720	15761	2744	21.89	0.46	0.05
131/08-18-007-11W2/0	REDRV	240	760	2627	3.17	0.07	0.01
111/15-20-007-11W2/0	YEOMAN	588	142700	2757	242.69	5.08	0.51
141/07-24-008-09W2/2	REDRV, YEOMAN	336	19017	2578	56.60	1.19	0.12
131/02-32-008-10W2/0	YEOMAN	660	282125	2588	427.46	8.95	0.90
191/03-32-008-10W2/0	YEOMAN	720	561740	2394	780.19	16.34	1.63
141/08-22-008-13W2/0	YEOMAN	720	44182	2475	61.36	1.29	0.13
121/05-23-008-13W2/0	YEOMAN	720	131826	2615	183.09	3.83	0.38
111/01-33-008-13W2/0	YEOMAN	720	396687	2553	550.95	11.54	1.15
111/16-33-008-13W2/0	YEOMAN	720	90031	2580	125.04	2.62	0.26
141/13-34-008-13W2/0	YEOMAN	720	131474	2490	182.60	3.82	0.38
101/14-36-008-13W2/2	YEOMAN	24	17577	2581	732.38	15.34	1.53
121/04-05-009-08W2/2	YEOMAN	134	2166	2514	16.17	0.34	0.03
141/14-32-009-09W2/0	YEOMAN	324	298326	2520	920.76	19.28	1.93
132/13-36-009-09W2/3	REDRV	718	192333	2461	267.87	5.61	0.56
191/05-16-009-10W2/0	YEOMAN	144	57140	2524	396.81	8.31	0.83
111/11-02-009-13W2/0	REDRV	288	1284	2593	4.46	0.09	0.01
111/03-03-009-13W2/0	YEOMAN	720	150627	2485	209.20	4.38	0.44
191/08-03-009-13W2/0	YEOMAN	720	187605	2424	260.56	5.46	0.55

141/12-01-010-09W2/2	YEOMAN	508	303119	2439	596.69	12.50	1.25
191/07-02-010-09W2/0	REDRV, YEOMAN	624	510583	2462	818.24	17.14	1.71
141/07-28-010-10W2/2	YEOMAN	72	223430	2435	3103.19	64.99	6.50
192/08-06-010-15W2/0	YEOMAN	528	154687	2349	292.97	6.14	0.61
131/14-33-011-08W2/0	YEOMAN	258	16216	2224	62.85	1.32	0.13
121/16-32-011-10W2/0	REDRV	720	141422	2413	196.42	4.11	0.41
121/05-11-011-14W2/2	YEOMAN	24	147002	2436	6125.08	128.29	12.83
111/04-04-012-08W2/2	YEOMAN	667	273269	2345	409.70	8.58	0.86
131/05-34-012-08W2/0	REDRV	24	41184	2212	1715.99	35.94	3.59
141/05-34-012-08W2/0	REDRV	687	477	2275	0.69	0.01	0.00
131/12-11-012-09W2/0	YEOMAN	720	145593	2383	202.21	4.24	0.42
121/01-19-012-10W2/0	REDRV	456	800	2408	1.75	0.04	0.00
111/08-12-012-11W2/0	YEOMAN	308	518	2440	1.68	0.04	0.00
141/11-29-012-13W2/0	YEOMAN	720	480890	2257	667.90	13.99	1.40
121/06-36-012-15W2/0	YEOMAN	96	10873	2326	113.26	2.37	0.24
111/01-04-013-08W2/0	YEOMAN	1	5931	2145	5931.10	124.22	12.42
131/11-34-013-08W2/0	YEOMAN	720	67387	2233	93.59	1.96	0.20
111/06-10-013-11W2/0	YEOMAN	720	100589	2326	139.71	2.93	0.29
121/08-21-013-11W2/0	REDRV	720	207111	2312	287.65	6.02	0.60
101/10-21-013-11W2/0	REDRV	720	3607	2237	5.01	0.10	0.01
121/04-22-013-11W2/0	YEOMAN	720	670049	2313	930.62	19.49	1.95
121/06-28-013-11W2/0	REDRV	688	325662	2294	473.35	9.91	0.99
191/06-28-013-11W2/0	YEOMAN	720	316721	2156	439.89	9.21	0.92
121/15-10-013-12W2/0	REDRV, YEOMAN	720	62029	2296	86.15	1.80	0.18
101/01-15-013-12W2/0	REDRV, YEOMAN	720	157719	2326	219.05	4.59	0.46
111/01-05-013-13W2/0	YEOMAN	481	571062	2255	1187.24	24.87	2.49
131/15-05-013-13W2/0	YEOMAN	720	149165	2241	207.17	4.34	0.43
141/02-08-013-13W2/0	YEOMAN	696	160824	2313	231.07	4.84	0.48
131/10-08-013-13W2/0	YEOMAN	720	130526	2304	181.29	3.80	0.38
111/11-08-013-13W2/0	REDRV, YEOMAN	240	184791	2300	769.96	16.13	1.61
121/15-08-013-13W2/0	YEOMAN	537	145066	2246	270.14	5.66	0.57
191/02-17-013-13W2/0	YEOMAN	720	253147	2153	351.59	7.36	0.74
101/03-17-013-13W2/2	YEOMAN	720	19762	2315	27.45	0.57	0.06
141/07-17-013-13W2/0	YEOMAN	104	9845	2239	94.66	1.98	0.20
121/08-17-013-13W2/0	YEOMAN	720	120557	2282	167.44	3.51	0.35
111/09-17-013-13W2/0	YEOMAN	720	136437	2237	189.50	3.97	0.40
111/10-17-013-13W2/0	YEOMAN	672	177167	2312	263.64	5.52	0.55
141/14-17-013-13W2/0	YEOMAN	720	29392	2295	40.82	0.85	0.09

141/02-20-013-13W2/0	YEOMAN	720	80706	2284	112.09	2.35	0.23
101/04-20-013-13W2/0	YEOMAN	720	22392	2233	31.10	0.65	0.07
131/06-20-013-13W2/0	YEOMAN	48	2660	2293	55.42	1.16	0.12
131/08-20-013-13W2/0	YEOMAN	679	127576	2246	187.89	3.94	0.39
131/09-20-013-13W2/0	REDRV, YEOMAN	720	229872	2300	319.27	6.69	0.67
101/11-20-013-13W2/0	YEOMAN	720	7970	2254	11.07	0.23	0.02
141/15-20-013-13W2/0	YEOMAN	720	211382	2232	293.59	6.15	0.61
121/12-21-013-13W2/0	REDRV, YEOMAN	480	201	2353	0.42	0.01	0.00
131/07-28-013-13W2/0	REDRV, YEOMAN	720	125054	2220	173.69	3.64	0.36
101/10-28-013-13W2/0	YEOMAN	720	710735	2336	987.13	20.67	2.07
121/16-28-013-13W2/0	REDRV	552	126932	2249	229.95	4.82	0.48
111/02-29-013-13W2/0	REDRV, YEOMAN	720	91126	2300	126.56	2.65	0.27
101/06-33-013-20W2/0	REDRV, YEOMAN	350	660	2322	1.89	0.04	0.00
191/08-14-014-12W2/0	YEOMAN	692	376959	2109	544.74	11.41	1.14
131/16-14-014-12W2/0	YEOMAN	452	26446	2280	58.51	1.23	0.12
121/02-23-014-12W2/0	YEOMAN	720	25062	2185	34.81	0.73	0.07
141/01-27-014-12W2/0	YEOMAN	556	267785	2268	481.63	10.09	1.01
141/11-27-014-12W2/0	YEOMAN	708	127988	2192	180.77	3.79	0.38
131/01-33-014-12W2/0	REDRV	720	35823	2258	49.75	1.04	0.10
111/06-34-014-12W2/0	YEOMAN	720	195318	2253	271.27	5.68	0.57
191/03-33-006-11W2/2	REDRV	720	52104	3003	72.37	1.52	0.15
191/10-18-007-11W2/2	REDRV	219	82231	2990	375.48	7.86	0.79
141/03-32-008-10W2/0	REDRV	460	96488	2450	209.76	4.39	0.44
191/10-16-006-11W2/2	REDRV	120	58129	2820	484.41	10.15	1.01
191/08-16-006-11W2/2	REDRV	288	339481	2900	1178.75	24.69	2.47
191/13-12-006-11W2/2	REDRV	168	754681	3080	4492.15	94.09	9.41
121/10-03-008-05W2/0	REDRV	636	27934	2475	43.92	0.92	0.09
111/04-02-007-11W2/0	REDRV	384	403672	2709	1051.23	22.02	2.20
141/14-26-006-11W2/3	REDRV	495	2971	2719	6.00	0.13	0.01
131/07-15-006-11W2/0	REDRV	720	108984	2855	151.37	3.17	0.32
191/07-30-004-21W2/0	REDRV	456	62286	3111	136.59	2.86	0.29
191/05-20-004-21W2/0	REDRV	242	96678	3374	399.50	8.37	0.84
121/12-04-004-21W2/0	REDRV	708	139859	3018	197.54	4.14	0.41
191/05-25-003-21W2/0	REDRV	717	57447	3975	80.12	1.68	0.17
191/10-33-014-12W2/0	REDRV	720	31197	2802	43.33	0.91	0.09
121/12-21-013-13W2/0	REDRV, YEOMAN	480	201	2353	0.42	0.01	0.00

192/01-02-009-13W2/0	REDRV	698	18229	3555	26.12	0.55	0.05
191/01-02-009-13W2/2	REDRV	10	24626	2878	2462.64	51.58	5.16
132/13-36-009-09W2/3	REDRV	718	192333	2462	267.87	5.61	0.56
191/13-14-007-11W2/2	REDRV	192	11401	2916	59.38	1.24	0.12
191/01-03-007-11W2/2	REDRV	720	69492	2925	96.52	2.02	0.20
111/15-04-007-10W2/0	REDRV	498	119992	2750	240.95	5.05	0.50
141/06-05-006-19W2/0	REDRV	64	706	2843	11.03	0.23	0.02
131/11-35-006-11W2/0	REDRV, YEOMAN	408	65150	2743	159.68	3.34	0.33
142/04-35-006-11W2/3	REDRV	720	85661	2715	118.97	2.49	0.25
192/14-14-006-11W2/2	REDRV	144	156	2615	1.08	0.02	0.00
191/12-10-006-11W2/0	REDRV	24	39045	2619	1626.88	34.07	3.41
191/12-28-006-06W2/2	REDRV	48	35236	3070	734.09	15.38	1.54
191/06-33-005-19W2/0	REDRV	24	3489	2710	145.37	3.04	0.30
191/03-11-004-21W2/2	REDRV	711	464671	2813	653.55	13.69	1.37
191/11-09-004-21W2/0	REDRV	1	310	2768	309.70	6.49	0.65
191/02-08-004-21W2/0	REDRV	362	372217	2791	1028.22	21.54	2.15
121/04-09-004-12W2/0	REDRV	96	419	2885	4.36	0.09	0.01
131/06-07-004-12W2/2	REDRV	737	71852	2955	97.49	2.04	0.20
191/10-14-004-07W2/0	REDRV	661	133424	2712	201.85	4.23	0.42
101/01-10-003-21W2/2	REDRV	140	54889	2945	392.06	8.21	0.82
191/02-04-003-20W2/2	REDRV	720	89176	2852	123.86	2.59	0.26
191/14-28-003-12W2/2	REDRV	336	42871	2850	127.59	2.67	0.27
101/06-28-003-12W2/0	REDRV	24	25570	2996	1065.40	22.31	2.23
191/15-23-001-17W2/0	REDRV	720	31376	3075	43.58	0.91	0.09
121/07-23-001-17W2/0	YEOMAN	130	4841	3194	37.24	0.78	0.08
191/11-28-003-12W2/0	YEOMAN	720	978853	2852	1359.52	28.47	2.85
191/11-03-003-20W2/0	YEOMAN	720	47152	2866	65.49	1.37	0.14
101/11-02-003-21W2/0	YEOMAN	24	44603	2960	1858.47	38.92	3.89
191/10-30-004-21W2/0	YEOMAN	168	36287	2734	215.99	4.52	0.45
141/08-14-006-06W2/0	WINNIPEG	24	106	2662	4.43	0.09	0.01
111/09-29-006-06W2/0	YEOMAN	28	27609	2655	986.05	20.65	2.07
191/01-15-006-11W2/0	YEOMAN	456	13753	2619	30.16	0.63	0.06
191/12-21-006-11W2/0	YEOMAN	504	250134	2594	496.30	10.39	1.04
192/12-21-006-11W2/0	YEOMAN	720	46050	2580	63.96	1.34	0.13
101/01-26-006-11W2/2	MIDALE	673	42451	1414	63.08	1.32	0.13
122/07-29-006-11W2/2	YEOMAN	240	2487	2635	10.36	0.22	0.02
191/01-05-006-19W2/2	YEOMAN	144	1362	2739	9.46	0.20	0.02
131/11-14-007-10W2/0	WINNIPEG	624	2555	2674	4.09	0.09	0.01
111/07-03-007-11W2/0	YEOMAN	134	128013	2744	955.32	20.01	2.00

191/09-03-007-11W2/0	YEOMAN	408	211727	2566	518.94	10.87	1.09
191/12-34-008-13W2/0	YEOMAN	680	708176	2420	1041.44	21.81	2.18
191/06-03-009-13W2/0	YEOMAN	720	7254	2421	10.08	0.21	0.02
191/08-06-010-15W2/2	YEOMAN	528	70251	2474	133.05	2.79	0.28
191/01-04-013-08W2/2	YEOMAN	48	171723	2123	3577.56	74.93	7.49
191/14-28-005-10W2/0	YEOMAN	27	13368	2701	495.13	10.37	1.04
121/04-28-006-11W2/0	YEOMAN	364	36827	2619	101.17	2.12	0.21
141/04-35-007-05W2/0	YEOMAN	432	20080	2505	46.48	0.97	0.10
121/03-24-007-07W2/0	YEOMAN	354	835	2610	2.36	0.05	0.00
141/08-03-009-13W2/2	YEOMAN	360	67041	2558	186.23	3.90	0.39
121/04-15-012-08W2/0	YEOMAN	24	20115	2315	838.13	17.55	1.76
121/03-13-006-11W2/0	YEOMAN	96	625	2739	6.51	0.14	0.01
191/11-15-006-11W2/2	YEOMAN	264	4981	2612	18.87	0.40	0.04
193/01-27-006-11W2/2	YEOMAN	720	156879	2586	217.89	4.56	0.46
111/01-29-006-11W2/2	YEOMAN	528	274758	2583	520.37	10.90	1.09
192/16-34-006-11W2/2	YEOMAN	720	136445	2569	189.51	3.97	0.40
121/14-14-007-11W2/0	YEOMAN	247	469	2663	1.90	0.04	0.00
191/04-28-013-11W2/0	YEOMAN	720	130406	2139	181.12	3.79	0.38
111/08-05-013-13W2/0	YEOMAN	720	588874	2313	817.88	17.13	1.71
191/14-14-014-12W2/0	YEOMAN	720	25589	2107	35.54	0.74	0.07
191/07-23-014-12W2/0	YEOMAN	720	126631	2126	175.88	3.68	0.37
111/07-04-005-07W2/0	REDRV	309	258834	2850	837.65	17.54	1.75

APPENDIX C. GEOTHERMAL POWER CALCULATION USING HYDRAULIC PROPERTIES FOR DEADWOOD-WINNIPEG WELLS

Sample Calculations using Well 141/08-14-006-06W2/0

K = (k * ρg* g)/μ = 2.05E-14 * 2700 * 9.8)/5.67E-4 = 9.587E-7

T = K * h = 9.587E-7 * 53 = 5.08E-05 m2/s

S = ρwg(α+ne β)h = 1000 * 9.8 * (1.0E-8 + (0.3 * 4.4E-10)) * 53 = 5.26E-03

Q = ΔsT/(0.183 log(2.25Tt/(r2 S))) = 2662 * 5.08E-5/(0.183 log(2.25 * 5.08E-5 * 30 * 365.25 * 86400/(10002 * 5.26E-3))) = 2024.71 (m3/hr) = 0.56 (m3/s)

PT=Q* ρw*Cw*ΔT = 0.56 (m3/s) *1000(kg/m3) *3770 (J/KgoC) *(20oC) = 41.62 MWt

PE=ng*PT =10%* 41.62 = 4.16 MWe

UWI	Producing Zone	X (m)	Avg. k (m^2)	*K* (m/s)	*h* (m)	ρ (Kg/m^3)	*T* (°C)	*μ* (Pa.s)	*α* (Pa-1)	*β* (Pa-1)	*T=K*h* (m^2/s)	*S*	$\log\left(\frac{2.25Tt}{r^2S}\right)$	*Q* (m3/h)	P_T (MWt)	P_E (MWe)
141/08-14-006-06W2/0	WINNIPEG	2662	2.05E-14	9.58E-07	53	1000	88	5.67E-04	1.00E-08	4.40E-10	5.08E-05	5.26E-03	1.31	2024.71	41.62	4.16
131/08-16-006-11W2/0	WINNIPEG	2738	8.12E-15	3.15E-07	49	1000	70	6.81E-04	1.00E-08	4.40E-10	1.55E-05	4.87E-03	0.83	1002.55	20.61	2.06
192/09-20-006-11W2/2	WINNIPEG	2708	3.89E-14	1.92E-06	48	1000	90	5.36E-04	1.00E-08	4.40E-10	2.69E-04	1.39E-02	1.61	8865.44	182.23	18.22
111/16-20-006-11W2/0	WINNIPEG	2719	1.56E-14	6.06E-07	52	1000	70	6.81E-04	1.00E-08	4.40E-10	3.15E-05	5.16E-03	1.11	1513.53	31.11	3.11
142/04-35-006-11W2/2	WINNIPEG	2715	1.62E-13	7.58E-06	59	1000	87	5.67E-04	1.00E-08	4.40E-10	4.47E-04	5.86E-03	2.21	10799.72	221.99	22.20
111/11-16-007-07W2/0	WINNIPEG	2636	8.67E-14	1.59E-06	52	1000	91	5.35E-04	1.00E-08	4.40E-10	8.26E-05	5.16E-03	1.53	2795.28	57.46	5.75
131/14-13-007-10W2/2	WINNIPEG	2672	1.89E-15	3.27E-08	7	1000	87	5.67E-04	1.00E-08	4.40E-10	1.70E-06	5.16E-03	0.15	583.13	11.99	1.20
131/11-14-007-10W2/0	WINNIPEG	2673	3.12E-13	5.72E-06	54	1000	92	5.35E-04	1.00E-08	4.40E-10	3.06E-04	5.31E-03	2.09	7702.71	158.33	15.83
113/04-02-007-11W2/0	WINNIPEG	2702	6.57E-14	1.27E-06	90	1000	95	5.07E-04	1.00E-08	4.40E-10	1.14E-04	8.89E-03	1.44	4207.21	86.48	8.65
141/12-01-010-09W2/0	WINNIPEG	2439	1.06E-14	1.83E-07	145	1000	84	5.66E-04	1.00E-08	4.40E-10	2.65E-05	1.44E-02	0.59	2138.05	43.95	4.39
142/12-01-010-09W2/0	WINNIPEG	2465	3.09E-13	5.34E-06	69	1000	87	5.67E-04	1.00E-08	4.40E-10	3.68E-04	6.85E-03	2.06	8678.05	178.38	17.84
132/07-02-010-09W2/0	WINNIPEG	2442	8.39E-14	1.45E-06	42	1000	87	5.67E-04	1.00E-08	4.40E-10	6.09E-05	4.17E-03	1.49	1959.07	40.27	4.03
141/07-28-010-10W2/0	WINNIPEG	2435	5.45E-13	9.44E-06	51	1000	84	5.66E-04	1.00E-08	4.40E-10	4.82E-04	5.06E-03	2.31	10002.31	205.60	20.56
191/08-06-010-15W2/0	WINNIPEG	2474	1.54E-13	2.51E-06	64	1000	81	6.01E-04	1.00E-08	4.40E-10	1.60E-04	6.35E-03	1.73	4511.81	92.74	9.27
141/14-32-009-09W2/3	WINNIPEG	2520	1.54E-13	2.51E-06	68	1000	80	6.01E-04	1.00E-08	4.40E-10	1.70E-04	6.75E-03	1.73	4881.57	100.34	10.03
111/11-03-017-14W3/0	DEADWOOD	2079	6.65E-14	1.02E-06	48	1000	73	6.39E-04	1.00E-08	4.40E-10	4.91E-05	4.78E-03	1.34	1497.28	30.78	3.08
121/07-09-017-14W3/0	DEADWOOD	2020	2.06E-15	3.57E-08	46	1000	84	5.66E-04	1.00E-08	4.40E-10	1.63E-06	4.54E-03	0.12	557.06	11.45	1.15
101/03-10-017-14W3/0	DEADWOOD	2017	9.85E-14	1.61E-06	127	1000	82	6.01E-04	1.00E-08	4.40E-10	2.04E-04	1.26E-02	1.54	5256.43	108.05	10.80
121/12-03-031-20W3/0	DEADWOOD	2178	3.47E-14	4.34E-07	407	1000	60	7.82E-04	1.00E-08	4.40E-10	1.77E-04	4.04E-02	0.97	7812.90	160.60	16.06
23/09-06-010-15W2/0	WINNIPEG	2497	9.11E-13	1.58E-05	44	1000	84	5.66E-04	1.00E-08	4.40E-10	6.94E-04	4.37E-03	2.53	13476.42	277.02	27.70
02/01-09-017-14W3/0	DEADWOOD	2050	1.00E-13	1.73E-06	173	1000	83	5.66E-04	1.00E-08	4.40E-10	3.00E-04	1.72E-02	1.57	7694.10	158.16	15.82
111/07-04-005-07W2/2	INTERLK	2850	7.75E-15	1.50E-07	68	1000	87	5.07E-04	1.00E-08	4.40E-10	1.02E-05	6.75E-03	0.51	1126.49	23.16	2.32

APPENDIX D. GEOTHERMAL POWER CALCULATION USING HYDRAULIC PROPERTIES FOR RED RIVER-YEOMAN WELLS

Sample Calculations using Well 131/06-02-003-21W2/0

$K = (k * \rho_g * g)/\mu = 4.79E\text{-}16 * 2650 * 9.8)/5.67E\text{-}4 = 2.20E\text{-}8$

$T = K * h = 2.20E\text{-}7 * 95 = 2.08E\text{-}06\ m^2/s$

$S = \rho_w g(\alpha + n_e \beta)h = 1000 * 9.8 * (1.0E\text{-}8 + (0.3 * 4.40E\text{-}10)) * 95 = 9.35E\text{-}03$

$Q = \Delta sT/(0.183 \log(2.25Tt/(r^2 S))) = 2923 * 2.08E\text{-}06/(0.183 \log(2.25 * 2.08E\text{-}06 * 30 * 365.25 * 86400/(1000^2 * 9.35E\text{-}3))) = 369.62\ (m^3/hr) = 0.10\ (m^3/s)$

$P_T = Q * \rho_w * C_w * \Delta T = 0.10\ (m^3/s) * 1000(kg/m^3) * 3770\ (J/Kg^oC) * (20^oC) = 7.63\ MWt$

$P_E = n_g * P_T = 10\% * 7.63 = 0.76\ MWe$

UWI	Producing Zone	X (m)	Avg. k (m^2)	K (m/s)	h (m)	ρ (Kg/m^3)	T (°C)	μ (Pa.s)	α (Pa-1)	β (Pa-1)	T=K*h	S	$\log\left(\frac{2.25Tt}{r^2 S}\right)$	Q (m3/h)	P_T (MWt)	P_E (MWe)
131/06-02-003-21W2/0	YEOMAN	2923	4.79E-16	2.20E-08	95	1000	84	5.66E-04	1.00E-08	4.40E-10	2.08E-06	9.35E-03	0.32	369.62	7.60	0.76
101/03-17-003-21W2/0	YEOMAN	2858	2.13E-13	9.79E-06	31	1000	84	5.66E-04	1.00E-08	4.40E-10	2.99E-04	3.01E-03	2.33	7221.68	148.45	14.84
191/05-17-003-21W2/0	REDRV	2790	6.02E-14	2.60E-06	45	1000	82	6.01E-04	1.00E-08	4.40E-10	1.16E-04	4.41E-03	1.75	3645.57	74.94	7.49
192/05-25-003-21W2/0	REDRV	2773	6.36E-16	2.42E-08	110	1000	72	6.81E-04	1.00E-08	4.40E-10	2.67E-06	1.09E-02	0.28	517.95	10.65	1.06
101/09-02-006-06W2/0	REDRV	2590	2.73E-14	1.25E-06	41	1000	88	5.67E-04	1.00E-08	4.40E-10	5.17E-05	4.07E-03	1.43	1838.53	37.79	3.78
191/16-29-006-06W2/0	YEOMAN	2471	1.81E-14	6.91E-07	211	1000	72	6.81E-04	1.00E-08	4.40E-10	1.46E-04	2.08E-02	1.17	6039.46	124.14	12.41
192/11-15-006-11W2/0	YEOMAN	2616	1.74E-14	6.64E-07	382	1000	72	6.81E-04	1.00E-08	4.40E-10	2.54E-04	3.77E-02	1.16	11289.29	232.06	23.21
192/08-16-006-11W2/0	YEOMAN	2607	2.37E-14	9.04E-07	154	1000	73	6.81E-04	1.00E-08	4.40E-10	1.39E-04	1.52E-02	1.29	5531.88	113.71	11.37
191/16-34-006-11W2/0	REDRV	2576	6.23E-16	2.38E-08	207	1000	72	6.81E-04	1.00E-08	4.40E-10	4.92E-06	2.04E-02	0.29	860.24	17.68	1.77
13+9:91/11-14-007-10W2/	YEOMAN	2674	5.86E-16	2.53E-08	98	1000	80	6.01E-04	1.00E-08	4.40E-10	2.47E-06	9.62E-03	0.26	495.78	10.19	1.02
191/03-32-008-10W2/0	YEOMAN	2394	6.19E-16	2.36E-08	428	1000	69	6.81E-04	1.00E-08	4.40E-10	1.01E-05	4.22E-02	0.29	1626.19	33.43	3.34
141/08-22-008-13W2/0	YEOMAN	2475	6.35E-16	2.91E-08	18	1000	85	5.66E-04	1.00E-08	4.40E-10	5.10E-07	1.73E-03	0.20	123.14	2.53	0.25
141/13-34-008-13W2/0	YEOMAN	2490	9.00E-16	3.21E-08	22	1000	63	7.28E-04	1.00E-08	4.40E-10	7.06E-07	2.17E-03	0.16	217.30	4.47	0.45
111/03-03-009-13W2/0	YEOMAN	2485	8.00E-16	3.05E-08	45	1000	73	6.81E-04	1.00E-08	4.40E-10	1.38E-06	4.47E-03	0.18	372.65	7.66	0.77
191/08-03-009-13W2/0	YEOMAN	2424	3.07E-14	1.33E-06	16	1000	82	6.01E-04	1.00E-08	4.40E-10	2.12E-05	1.58E-03	1.46	694.52	14.28	1.43
141/07-28-010-10W2/2	YEOMAN	2435	1.64E-14	7.54E-07	112	1000	83	5.66E-04	1.00E-08	4.40E-10	8.45E-05	1.10E-02	1.21	3338.74	68.63	6.86
191/06-28-013-11W2/0	YEOMAN	2156	4.81E-14	1.83E-06	10	1000	72	6.81E-04	1.00E-08	4.40E-10	1.83E-05	9.86E-04	1.60	486.82	10.01	1.00
191/02-17-013-13W2/0	YEOMAN	2153	9.47E-15	3.38E-07	155	1000	67	7.28E-04	1.00E-08	4.40E-10	5.24E-05	1.53E-02	0.86	2569.91	52.83	5.28
191/08-14-014-12W2/0	YEOMAN	2109	9.57E-16	3.41E-08	115	1000	65	7.28E-04	1.00E-08	4.40E-10	3.93E-06	1.13E-02	0.13	1230.31	25.29	2.53
101/01-14-001-17W2/0	YEOMAN	3112	1.89E-13	8.64E-06	100	1000	88	5.67E-04	1.00E-08	4.40E-10	8.64E-04	9.86E-03	2.27	23289.47	478.73	47.87
101/03-20-002-16W2/0	REDRV	3156	8.78E-14	4.02E-06	381	1000	88	5.67E-04	1.00E-08	4.40E-10	1.53E-03	3.75E-02	1.94	48995.62	1007.13	100.71
111/04-22-003-15W2/0	YEOMAN	2938	1.16E-14	5.33E-07	128	1000	93	5.67E-04	1.00E-08	4.40E-10	6.84E-05	1.27E-02	1.06	3726.50	76.60	7.66
101/15-02-003-21W2/0	YEOMAN	2862	4.09E-14	1.88E-06	97	1000	85	5.66E-04	1.00E-08	4.40E-10	1.82E-04	9.57E-03	1.61	6373.25	131.01	13.10
111/13-08-003-21W2/0	REDRV,YEON	2800	5.39E-14	2.47E-06	96	1000	83	5.66E-04	1.00E-08	4.40E-10	2.37E-04	9.47E-03	1.73	7570.31	155.61	15.56
101/01-18-003-21W2/0	YEOMAN	2791	9.99E-14	4.31E-06	96	1000	79	6.01E-04	1.00E-08	4.40E-10	4.12E-04	9.42E-03	1.97	11488.63	236.16	23.62
111/07-25-003-21W2/0	REDRV	2787	3.20E-14	1.38E-06	66	1000	79	6.01E-04	1.00E-08	4.40E-10	9.11E-05	6.49E-03	1.48	3385.10	69.58	6.96
141/10-29-006-11W2/0	YEOMAN	2820	7.59E-16	3.47E-08	125	1000	87	5.67E-04	1.00E-08	4.40E-10	4.35E-06	1.24E-02	0.12	1935.15	39.78	3.98
131/14-13-007-10W2/0	YEOMAN	2552	4.18E-14	1.91E-06	20	1000	90	5.67E-04	1.00E-08	4.40E-10	3.83E-05	1.97E-03	1.62	1189.23	24.45	2.44
101/12-02-007-11W2/0	YEOMAN	2752	1.79E-13	6.83E-06	96	1000	74	6.81E-04	1.00E-08	4.40E-10	6.56E-04	9.47E-03	2.17	16370.82	336.51	33.65
111/16-33-008-13W2/0	YEOMAN	2580	6.66E-15	3.06E-07	90	1000	85	5.66E-04	1.00E-08	4.40E-10	2.75E-05	8.86E-03	0.82	1699.93	34.94	3.49
111/01-04-013-08W2/0	YEOMAN	2145	2.36E-14	8.41E-07	38	1000	65	7.28E-04	1.00E-08	4.40E-10	3.18E-05	3.73E-03	1.26	1065.17	21.90	2.19
121/04-22-013-11W2/0	YEOMAN	2313	1.20E-13	4.59E-06	26	1000	71	6.81E-04	1.00E-08	4.40E-10	1.17E-04	2.52E-03	2.00	2667.35	54.83	5.48
121/06-28-013-11W2/0	REDRV	2294	5.59E-14	2.13E-06	62	1000	75	6.81E-04	1.00E-08	4.40E-10	1.32E-04	6.12E-03	1.66	3584.50	73.68	7.37
141/07-17-013-13W2/0	YEOMAN	2239	1.03E-13	4.47E-06	112	1000	80	6.01E-04	1.00E-08	4.40E-10	5.00E-04	1.10E-02	1.98	11105.92	228.29	22.83
131/09-20-013-13W2/0	REDRV,YEON	2300	1.58E-14	5.65E-07	107	1000	65	7.28E-04	1.00E-08	4.40E-10	6.01E-05	1.05E-02	1.09	2505.68	51.51	5.15
131/07-28-013-13W2/0	REDRV,YEON	2220	2.81E-14	1.22E-06	24	1000	78	6.01E-04	1.00E-08	4.40E-10	2.88E-05	2.34E-03	1.42	886.66	18.23	1.82
131/01-33-014-12W2/0	REDRV	2258	4.07E-15	1.55E-07	98	1000	69	6.81E-04	1.00E-08	4.40E-10	1.52E-05	9.67E-03	0.53	1286.56	26.45	2.64
101/06-28-003-12W2/0	REDRV	2996	6.82E-16	3.67E-08	113	1000	99	4.82E-04	1.00E-08	4.40E-10	4.15E-06	1.11E-02	0.10	2427.02	49.89	4.99
131/02-32-008-10W2/0	YEOMAN	2588	1.05E-14	4.82E-07	100	1000	88	5.67E-04	1.00E-08	4.40E-10	4.82E-05	9.86E-03	1.02	2411.57	49.57	4.96
121/07-29-006-11W2/0	YEOMAN	2809	4.11E-14	1.88E-06	90	1000	89	5.67E-04	1.00E-08	4.40E-10	1.69E-04	8.88E-03	1.61	5817.48	119.58	11.96
111/07-04-005-07W2/0	REDRV	2850	1.01E-14	4.64E-07	83	1000	87	5.67E-04	1.00E-08	4.40E-10	3.85E-05	8.19E-03	1.00	2157.51	44.35	4.43

APPENDIX E. MAP SHOWING DEADWOOD-WINNIPEG WELLS

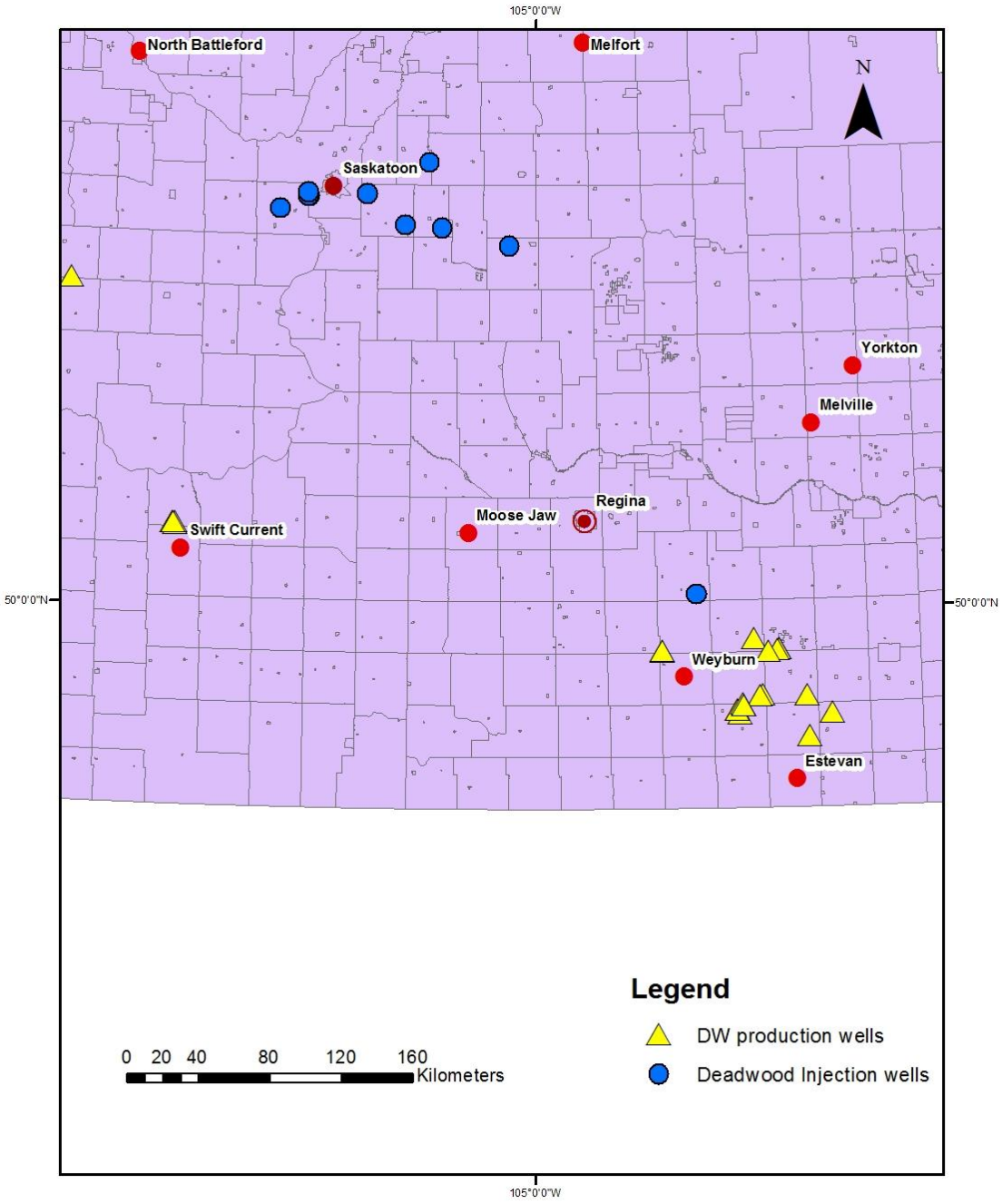

APPENDIX F. MAP SHOWING RED RIVER-YEOMAN WELLS